FINAL REPORT
NASA GRANT: NSG-1181 (Suppl. 1)

PART B

HOWARD UNIVERSITY
SCHOOL OF ENGINEERING
DEPARTMENT OF MECHANICAL ENGINEERING
WASHINGTON, D.C. 20059

FINAL REPORT
NASA GRANT: NSG-1181 (Suppl-1)

THE DYNAMICS AND OPTIMAL CONTROL OF SPINNING SPACECRAFT WITH MOVABLE TELESCOPING APPENDAGES
Part B

EFFECT OF GRAVITY-GRADIENT TORQUES ON THE DYNAMICS OF A SPINNING SPACECRAFT WITH TELESCOPING APPENDAGES

by

Peter M. Bainum
Professor of Aerospace Engineering
Principal Investigator

and

Mahesh Rajan
Graduate Research Assistant

May 1977

ABSTRACT

The effects of gravity-gradient torques during boom deployment maneuvers of a spinning spacecraft are examined. Two different configurations are considered:

(1) where the booms extend only along the hub principal axes.

(2) where one or two booms are offset from the principal axes.

For the special case of symmetric deployment (principal axes booms) the stability boundaries are determined and a stability chart is used to study the system behavior. Possible cases of instability during this type of maneuver are identified. In the second configuration an expression for gravity torque about the hub center of mass has been developed. The non-linear equations of motion are solved numerically and the substantial influence of the gravity torque during asymmetric deployment maneuvers is indicated.

TABLE OF CONTENTS

LIST OF ILLUSTRATIONS

LIST OF ILLUSTRATIONS (cont)

LIST OF ILLUSTRATIONS (cont)

NOMENCLATURE

A_1, A_2	=	Time varying coefficients in the equations of motion for small out of plane Euler angles
a	=	Offset of the control boom with end mass m_1 from the d_2, d_3 plane
$\hat{a}_1, \hat{a}_2, \hat{a}_3$	=	Unit vectors in the orbiting reference frame
$\hat{a}_1$	=	Unit vector along the geocentric position vector to the hub center of mass for asymmetric deployment
B	=	Coefficient in the system characteristic equation for a rigid spinning spacecraft
b	=	Offset of control boom with end mass m_1 from the d_3, d_1 plane
$b(t)$	=	Time varying coefficients in the equation for h_1, h_2 for symmetric deployment
$\hat{b}_1, \hat{b}_2, \hat{b}_3$	=	Vector basis defined after the first Euler angle (Θ_1) rotation
C	=	Coefficient in the system characteristic equation for a rigid spinning spacecraft
$\underline{C}$	=	$\begin{bmatrix} C_1 \\ C_2 \end{bmatrix}$ = Constant vector appearing in the analytical solution for the Euler angles without gravity-gradient for symmetric deployment
$\hat{c}_1, \hat{c}_2, \hat{c}_3$	=	Vector basis defined after the second Euler angle (Θ_2) rotation
c_1, c_2, c_3	=	Extension rates along 1,2,3 principal axes, respectively
c	=	Extension rate along 1,2 axes when inertia symmetry about spin axis is maintained and extension rate along all the three axes when they are equal
d_1, d_2, d_3	=	Principal axes of the spacecraft
$\hat{d}_1, \hat{d}_2, \hat{d}_3$	=	Unit vectors along the body principal axes

dm	=	Elemental mass
F_1	=	$B/2\Omega^2$
F_2	=	C/Ω^4
$f(t)$	=	$\dot{I}(t)/I(t)$
g_0	=	Gravitational acceleration at the earths surface
h_1, h_2, h_3	=	Angular momentum components in the body axes
I_1, I_2, I_3	=	Instantanious values of principal moments of inertia
I_1^*, I_2^*, I_3^*	=	Hub principal moments of inertia
I	=	$I_1(t) = I_2(t)$ for symmetric deployment
K	=	$(I_3-I)/I$ = constant for rigid spinning spacecraft
k	=	Gravitational constant for earth
$\bar{L}$	=	Angular momentum of hub about point Q
$\bar{L}_{m_i/Q}$	=	Angular momentum of control mass with respect to point Q
ℓ_1, ℓ_2, ℓ_3	=	Boom lengths along the principal axes 1,2,3 respectively
M	=	Mass of main part of spacecraft
m	=	Boom end mass
m_1, m_2, m_3	=	Boom end masses along 1,2,3 principal axes respectively
m_1, m_2	=	Control masses for asymmetric deployment
$\bar{N}$	=	Gravity torque
N_1, N_2, N_3	=	Gravity-Gradient torque components
p	=	$2mc^2+2m_3c_3^2$
p_1	=	$2mc^2$

q_0^* = Constant appearing in the solution for angular momentum for torque free system

$\overline{R}$ = Geocentric position vector to hub center of mass

R = $|\overline{R}|$ = Radius of orbit for symmetric deployment

$\overline{R}_c$ = Geocentric position vector of composite center of mass

$\overline{r}_1$ = Position vector of control mass m_1 referenced to point Q

$\overline{r}_2$ = Position vector of control mass m_2 referenced to point Q

$\overline{r}_c$ = Position vector of composite center of mass referenced to point Q

$\overline{r}$ = Position vector to elemental mass dm referenced to point Q

s = Laplace Transform variable

t = Time

x = Coordinate of the control boom end mass m_2 along the d_1 axis

z = Coordinate of the control boom end mass m_1 along the d_3 axis

α = $(\omega_3-\Omega)/\Omega$ (spin factor)

γ = Nutation angle

ω_i = Angular velocities about 1,2,3 axes respectively ($i = 1,2,3$)

Ω = Orbital angular rate

ψ_0^* = Constant appearing in the solution for angular momentum for torque free system

ϕ = $\psi_0^*+\theta_3(0)$

$\Theta_1, \Theta_2, \Theta_3$ = Euler angles

μ = $4mc^2$

μ_1 = $m_1(M+m_2)/M+\Sigma m)$

μ_2 = $m_2(M+m_1)/(M+\Sigma M)$

μ_3 = $-m_1 m_2/(M+\Sigma m)$

$\underline{\underline{I}}$ = Moment of inertia dyadic of satellite for symmetric deployment

$\underline{\underline{I}}_m$ = Moment of inertia dyadic of hub for asymmetric deployment

$\cdot$ = Indicates differentiation with respect to t

(0) = Indicates initial conditions

Subscripts

Q = reference point taken at hub center of mass

I. INTRODUCTION

A number of spacecraft have long telescoping appendages. These appendages might be on-board antennas which must be extended in orbit after the initial injection sequence. The dynamics of such spacecraft has been discussed in the recent literature in the absence of external disturbance torques.[1] The purpose of this study is to determine the effects of gravity-gradient torques during the boom deployment maneuver.

The first part of the current study will examine the effect of the gravity-gradient torque when the telescoping booms are deployed in pairs along the spacecraft principal axes. Possible use of such a deployment maneuver for detumbling a spacecraft has been examined in a recent paper.[2] From an application of Lyapunov's second method (using modified forms of the rotational kinetic energy as a Lyapunov function) sequences of boom extension maneuvers can be determined so that the spacecraft will approach either of the two desired final states: close to a zero inertial angular velocity state, or a final spin rate about only one of the principal axes. This study did not consider the effects of external torques.

For the special case of a gravitationally stabilized satellite librating in the orbit plane, the effect of gravity-gradient during the deployment maneuver has been studied previously.[3] An approximate series solution has been obtained to simulate the dynamics and the results compared with those of numerical integration.

In the current study the non-linear equations of motion for a spinning spacecraft including the effects of gravity-gradient torques are developed and these are solved numerically. For the special case of a symmetric spinning rigid spacecraft the stability chart previously developed can be used to study the system behavior.[4,5]

In the second configuration studied here, the system is assumed to consist of a central hub and one or two control masses offset from the principal axes. The dynamics of such spacecraft, in torque free space, has been discussed in the recent literature.[6-7] Reference 6 has examined the feasibility of a movable mass control device, for detumbling a large space station where a single internal mass is constrained to move along a linear track. In Ref. 7 a control law for the boom mass position is obtained such that a quadratic cost functional involving the weighted components of the angular velocity plus the control is minimized when the final time is unspecified. In order to evaluate the gravity torque effects an expression for the torque based on asimilar procedure adopted in Ref. 8 is developed. The complete non-linear equations of motion with the gravity torque are obtained and the influence of the gravity torque due to asymmetry is illustrated.

II. SYMMETRIC DEPLOYMENT

A. Eulers Equations

In the first configuration the booms extend along the principal axes of the spacecraft as shown in Fig. 1. It is assumed that the booms are massless and perfectly rigid. Using vector components in the d_1,d_2,d_3 reference frame the Euler's moment equations with time varying moments of inertia are

$$\begin{aligned} \dot{h}_1 - \omega_3\omega_2 (I_2 - I_3) &= N_1 \\ \dot{h}_2 - \omega_1\omega_3 (I_3 - I_1) &= N_2 \\ \dot{h}_3 - \omega_2\omega_1 (I_1 - I_2) &= N_3 \end{aligned} \tag{1}$$

where $h_i = I_i\omega_i$ $(i = 1,2,3)$. $I_i = I_i(t)$ are the principal moments of inertia, ω_i are the components of the inertial angular velocity in the d_1,d_2,d_3 frame and N_i are the external torque components about the center of mass. In this analysis all the external torques of the system except the gravity-gradient torque are neglected so that N_i represent the gravity-gradient torque components.

B. Reference Frames

Equations (1) will be expanded here in terms of the coordinates and unit vectors defined by Figs. 2. and 3., which together establish an orbiting reference frame and three attitude angles Θ_1, Θ_2, Θ_3 relating body-fixed unit vectors $\hat{d}_1,\hat{d}_2,\hat{d}_3$ to the unit vectors fixed in the orbiting reference frame $\hat{a}_1,\hat{a}_2,\hat{a}_3$. Θ_1, Θ_2, Θ_3

correspond to three successive positive rotations about the vectors: $\hat{a}_1$, $\hat{b}_2$, $\hat{c}_3$, respectively. Specifically, unit vector $\hat{a}_1$ is directed along the radial line from the earth to the satellite mass center O (local vertical), unit vector $\hat{a}_3$ is directed along the trajectory binormal (normal to the plane of orbit) and $\hat{a}_2$ is defined to make $\hat{a}_1$, $\hat{a}_2$, $\hat{a}_3$ a right-handed orthogonal triad. We further assume that the center of mass of the system moves in a circular orbit, so that $\hat{a}_2$ is along the path of the trajectory.

The transformation from the principal body axes reference frame to the orbiting reference frame with the chosen Θ_1, Θ_2, Θ_3 Euler angle sequence, becomes, after combining the three rotational matrices,

$$\begin{bmatrix} \hat{a}_1 \\ \hat{a}_2 \\ \hat{a}_3 \end{bmatrix} = \left[\begin{array}{c|c|c} c\Theta_2 c\Theta_3 & -c\Theta_2 s\Theta_3 & s\Theta_2 \\ c\Theta_1 s\Theta_3 + s\Theta_1 s\Theta_2 c\Theta_3 & c\Theta_1 c\Theta_3 - s\Theta_1 s\Theta_2 s\Theta_3 & -s\Theta_1 c\Theta_2 \\ s\Theta_1 s\Theta_3 - c\Theta_1 s\Theta_2 c\Theta_3 & s\Theta_1 c\Theta_3 + c\Theta_1 s\Theta_2 s\Theta_3 & c\Theta_1 c\Theta_2 \end{array}\right] \begin{bmatrix} \hat{d}_1 \\ \hat{d}_2 \\ \hat{d}_3 \end{bmatrix} \tag{2}$$

where positive angles correspond to rotations in the positive right-hand sense as illustrated in Fig. 3. "s" represents the sine function and "c" represents the cosine function.

By examination of Fig. 3, the expression for the inertial angular velocity, $\bar{\omega}$, of the satellite in a circular orbit, can be written down as

$$\bar{\omega} = \dot{\Theta}_3 \hat{c}_3 + \dot{\Theta}_2 \hat{b}_2 + \dot{\Theta}_1 \hat{a}_1 + \Omega \hat{a}_3 \tag{3}$$

where Ω is the orbital angular rate. From consideration of the

individual Euler angle rotations and Eq. (2) the following relationships between the various unit vectors can be developed:

$$\hat{c}_3 = \hat{d}_3$$

$$\hat{b}_2 = s\theta_3\hat{d}_1 + c\theta_3\hat{d}_2$$

$$\hat{a}_1 = c\theta_2 c\theta_3\hat{d}_1 - c\theta_2 s\theta_3\hat{d}_2 + s\theta_2\hat{d}_3$$

$$\hat{a}_3 = (s\theta_1 s\theta_3 - c\theta_1 s\theta_2 c\theta_3)\hat{d}_1 + (s\theta_1 c\theta_3 + c\theta_1 s\theta_2 s\theta_3)\hat{d}_2 + c\theta_1 c\theta_2\hat{d}_3 \qquad (4)$$

After substitution of Eqs. (4) into Eq. (3) the inertial angular velocity components in the body axes can be expressed as follows:

$$\omega_1 = \dot{\theta}_2 s\theta_3 + \Omega(s\theta_1 s\theta_3 - c\theta_1 s\theta_2 c\theta_3) + \dot{\theta}_1 c\theta_2 c\theta_3$$

$$\omega_2 = \dot{\theta}_2 c\theta_3 + \Omega(s\theta_1 c\theta_3 + c\theta_1 s\theta_2 s\theta_3) - \dot{\theta}_1 c\theta_2 s\theta_3$$

$$\omega_3 = \dot{\theta}_3 + \Omega c\theta_1 c\theta_2 - \dot{\theta}_1 s\theta_2 \qquad (5)$$

C. Gravity-Gradient Torque

The gravity-gradient torque $\bar{N}$ about the satellite mass center O is given by[8]

$$\bar{N} = \frac{3k}{R^3}\,\hat{a}_1 \times \square \cdot \hat{a}_1 \qquad (6)$$

where

$$k = g_0 R_0^2$$

with g_0 the gravitational acceleration at the earth's surface and R_0 the radius of the earth. $\hat{a}_1$ is the unit vector along the local vertical, $\square$ is the inertia dyadic about the satellite mass center and R is the orbit radius. For a satellite in a circular orbit,

$$\frac{k}{R^3} = \Omega^2 \tag{7}$$

The expression for $\hat{a}_1$ from Eq. (4) is substituted into Eq. (6) and the body reference frame is chosen as a set of principal axes so that $\square$ is diagonal. Then the components of the gravity-gradient torque in the body frame are:

$$N_1 = \frac{3k}{R^3}(I_2-I_3)\, c\theta_2 s\theta_2 s\theta_3$$

$$N_2 = \frac{3k}{R^3}(I_1-I_3)\, c\theta_2 s\theta_2 c\theta_3$$

$$N_3 = \frac{3k}{R^3}(I_1-I_2)(c\theta_2)^2 c\theta_3 s\theta_3 \tag{8}$$

D. Non-Linear Equations of Motion

Equations(5) can be solved as a set of three simultaneous equations for $\dot{\theta}_1$, $\dot{\theta}_2$ and $\dot{\theta}_3$ to yield:

$$\dot{\theta}_1 = (\omega_1 c\theta_3 - \omega_2 s\theta_3 + \Omega c\theta_1 s\theta_2)/c\theta_2$$

$$\dot{\theta}_2 = (\omega_1 s\theta_3 + \omega_2 c\theta_3 - \Omega s\theta_1)$$

$$\dot{\theta}_3 = (\omega_3 c\theta_2 + \omega_2 s\theta_2 s\theta_3 - \omega_1 c\theta_3 s\theta_2 - \Omega c\theta_1)/c\theta_2 \tag{9}$$

After substitution of Eq. (8) into Eq. (1) the following non-linear equations of motion result.

$$\dot{\omega}_1 = \{\omega_3\omega_2(I_2-I_3) - \dot{I}_1\omega_1 + \frac{3k}{R^3}(I_2-I_3)c\theta_2 s\theta_2 s\theta_3\}/I_1$$

$$\dot{\omega}_2 = \{\omega_1\omega_3(I_3-I_1) - \dot{I}_2\omega_2 + \frac{3k}{R^3}(I_1-I_3)c\theta_2 s\theta_2 c\theta_3\}/I_2$$

$$\dot{\omega}_3 = \{\omega_2\omega_1(I_1-I_2) - \dot{I}_3\omega_3 + \frac{3k}{R^3}(I_1-I_2)(c\theta_2)^2 c\theta_3 s\theta_3\}/I_3 \qquad (10)$$

Equations (9) and (10) are the complete non-linear equations of motion for the system. These are solved numerically as a system of six first order differential equations.

E. Motion for Small Out of Plane Euler Angles

For an initially symmetric satellite, if the mass symmetry (about the spin axis) is maintained during deployment, the equations of motion reduce to:

$$\dot{h}_1 + b(t)h_2 = -\frac{3\Omega^2}{h_0} b(t) I\ I_3 c\theta_2 s\theta_2 s\theta_3$$

$$\dot{h}_2 - b(t)h_1 = -\frac{3\Omega^2}{h_0} b(t) I\ I_3 c\theta_2 s\theta_2 c\theta_3 \qquad (11)$$

$$h_3 = h_0 = \text{constant}$$

where

$$I_1(t) = I_2(t) = I(t)$$

$$b(t) = \frac{I_3 - I}{I_3 I} h_0 \qquad (12)$$

To study the stability of the system for small perturbations about the spin axis we examine the equations of motion assuming that $|\theta_1|$, $|\theta_2|$ are small (but not θ_3 which reflects the spin). It

should be noted that the angle between the normal to the orbit plane and the body 3 axis is a function of θ_1 and θ_2 (see Fig. 3). Under these assumptions, the expressions for the inertial angular velocity components, Eqs. (5), become:

$$\omega_1 = (\ddot{\theta}_2+\Omega\theta_1)s\theta_3+(\dot{\theta}_1-\Omega\theta_2)c\theta_3$$

$$\omega_2 = (\ddot{\theta}_2+\Omega\theta_1)c\theta_3-(\dot{\theta}_1-\Omega\theta_2)s\theta_3$$

$$\omega_3 = \dot{\theta}_3+\Omega \tag{13}$$

and the corresponding components of inertial angular acceleration:

$$\dot{\omega}_1 = (\dddot{\theta}_2+\Omega\dot{\theta}_1-\dot{\theta}_3\dot{\theta}_1+\Omega\theta_2\dot{\theta}_3)s\theta_3+(\ddot{\theta}_1-\Omega\dot{\theta}_2+\dot{\theta}_3\dot{\theta}_2+\Omega\theta_1\dot{\theta}_3)c\theta_3$$

$$\dot{\omega}_2 = (\dddot{\theta}_2+\Omega\dot{\theta}_1-\dot{\theta}_3\dot{\theta}_1+\Omega\theta_2\dot{\theta}_3)c\theta_3-(\ddot{\theta}_1-\Omega\dot{\theta}_2+\dot{\theta}_3\dot{\theta}_2+\Omega\theta_1\dot{\theta}_3)s\theta_3$$

$$\dot{\omega}_3 = \ddot{\theta}_3 \tag{14}$$

Substitution of Eqs. (12), (13), (14) into Eq. (11) yields the equations governing the motion in which $|\theta_1|$, $|\theta_2|$ remain small as:

$$A_1 \cos\theta_3 + A_2 \sin\theta_3 = 0$$

$$A_1 \sin\theta_3 - A_2 \cos\theta_3 = 0 \tag{15}$$

where

$$A_1 = \dddot{\theta}_1 - \{\Omega-\dot{\theta}_3-b(t)\}\dot{\theta}_2 + f(t)(\dot{\theta}_1-\Omega\theta_2) + \Omega\theta_1\{\dot{\theta}_3+b(t)\}$$

$$A_2 = \ddot{\theta}_2 + \{\Omega-\dot{\theta}_3-b(t)\}\dot{\theta}_1 + f(t)(\dot{\theta}_2+\Omega\theta_1) + \Omega\theta_2\{\dot{\theta}_3+b(t)\}$$

$$+ \frac{3\Omega^2}{\omega_3} b(t)\theta_2 \tag{16}$$

and

$$f(t) = \dot{I}(t)/I(t)$$

In general these coupled equations cannot be solved in closed form. However the system behavior can be studied with the aid of the stability chart previously developed for a symmetrical spinning satellite.[4,5]

F. Stability Chart

Since Eqs. (15) and (16) represent the equations of motion for a spinning spacecraft for which the principal moments of inertias are functions of time, these equations would also represent the equations of motion for a spinning spacecraft when the principal inertias are not functions of time, provided the terms due to time varying moments of inertia are modified so that:

$$f(t) = 0,\ b(t) = b = \frac{I_3 - I}{I_3 I}\, h_0 = \text{constant}$$

The modified equations are (under the requirement that $A_1 = A_2 = 0$):

$$\ddot{\theta}_1 + (b+\dot{\theta}_3-\Omega)\dot{\theta}_2 + \Omega(b+\dot{\theta}_3)\theta_1 = 0$$

$$\ddot{\theta}_2 - (b+\dot{\theta}_3-\Omega)\dot{\theta}_1 + \Omega(b+\dot{\theta}_3)\theta_2 + \frac{3\Omega^2}{\omega_3}\, b\theta_2 = 0 \qquad (17)$$

Observe that $\dot{\theta}_3$ is also a constant. We now define two important parameters, K, an inertia ratio and , α, a spin factor as follows:

$$K = (I_3 - I)/I$$

$$\alpha = \dot{\theta}_3/\Omega = (\omega_3 - \Omega)/\Omega \qquad (18)$$

With the aid of Eqs. (18), the parameter b can be written as

$$b = K\omega_3 = K\Omega(\alpha+1)$$

After introduction of these parameters Eqs. (17) become

$$\ddot{\theta}_1+\Omega\{K(\alpha+1)+(\alpha-1)\}\dot{\theta}_2+\Omega^2\{K(\alpha+1)+\alpha\}\theta_1 = 0$$

$$\ddot{\theta}_2-\Omega\{K(\alpha+1)+(\alpha-1)\}\dot{\theta}_1+\Omega^2\{K(\alpha+1)+\alpha\}\theta_2+3K\Omega^2\theta_2 = 0 \qquad (19)$$

If we take the Laplace Transforms of these two equations, the subsidiary equation can be arranged as follows:

$$\begin{bmatrix} s^2+\Omega^2\{K(\alpha+1)+\alpha\} & \Omega\{K(\alpha+1)+(\alpha-1)\}s \\ -\Omega\{K(\alpha+1)+(\alpha-1)\}s & s^2+\Omega^2\{K(\alpha+1)+\alpha\}+3K\Omega^2 \end{bmatrix} \begin{bmatrix} \bar{\theta}_1(s) \\ \bar{\theta}_2(s) \end{bmatrix}$$

$$= \begin{bmatrix} s\theta_1(0)+\dot{\theta}_1(0)+\Omega\{K(\alpha+1)+(\alpha-1)\}\theta_2(0) \\ s\theta_2(0)+\dot{\theta}_2(0)-\Omega\{K(\alpha+1)+(\alpha-1)\}\theta_1(0) \end{bmatrix} \qquad (20)$$

where $\bar{\theta}_1(s)$, $\bar{\theta}_2(s)$ represent the Laplace Transforms of θ_1 and θ_2, respectively, and $\theta_1(0)$, $\theta_2(0)$, $\dot{\theta}_1(0)$, $\dot{\theta}_2(0)$ are the initial conditions.

The stability of the system can be established by examining the characteristic equation associated with Eq. (20) which is of the form:

$$s^4 - Bs^2 + C = 0$$

where

$$\frac{B}{2\Omega^2} = -[\{K(\alpha+1)+\alpha\} + \frac{1}{2}\{K(\alpha+1) + (\alpha-1)\}^2 + \frac{3}{2}K]$$

$$\frac{C}{\Omega^4} = \{K(\alpha+1)+\alpha\}^2 + 3K\{K(\alpha+1) + \alpha\}$$

For stability, the roots of the characteristic equation

$$s = \pm\sqrt{\frac{B}{2} \pm \sqrt{\left(\frac{B}{2}\right)^2 - C}}\ , \tag{21}$$

must not have a positive real part. Two symbols F_1 and F_2 are defined as:

$$F_1 = \frac{B}{2\Omega^2} \tag{22}$$

$$F_2 = \frac{C}{\Omega^4}$$

A brief study of Eq. (21) indicates that the condition under which there will be no positive real parts are:

(1) $F_1 < 0$

(2) $F_2 > 0$

(3) $(F_1)^2 - F_2 > 0$

To obtain numerical results, the variation of the quantities F_1, F_2, $(F_1)^2 - F_2$ were plotted in the α, K plane. The boundary of the stable and unstable regions is established and the results are illustrated in Fig. 4. The unstable regions are indicated by the cross-hatch marks. This stability chart has been previously

obtained by Thomson (Ref. 4) and Kane (Ref. 5).

G. Analytical Solution for Euler Angles for Symmetric Extension Without Gravity-Gradient Torques

The equations of motion for a spinning symmetric satellite with telescoping appendages in torque free space under the assumption that $|\theta_1|$, $|\theta_2|$ are small are obtained from Eqs. (9) and (11) as:

$$\dot{h}_1 + b(t)h_2 = 0 \tag{23.a}$$

$$\dot{h}_2 - b(t)h_1 = 0 \tag{23.b}$$

$$\dot{\theta}_1 - \Omega\theta_2 = \frac{h_1}{I(t)} \cos\theta_3 - \frac{h_2}{I(t)} \sin\theta_3 \tag{23.c}$$

$$\dot{\theta}_2 + \Omega\theta_1 = \frac{h_1}{I(t)} \sin\theta_3 + \frac{h_2}{I(t)} \cos\theta_3 \tag{23.d}$$

$$\dot{\theta}_3 = \omega_3 - \Omega \tag{23.e}$$

The solution to the first two of the above equations has been previously obtained as:[1]

$$\begin{aligned} h_1 &= q_0^* \cos\left(\int_0^t b(t)dt + \psi_0^*\right) \\ h_2 &= q_0^* \sin\left(\int_0^t b(t)dt + \psi_0^*\right) \end{aligned} \tag{24}$$

where q_0^* and ψ_0^* are constants depending on the initial conditions. For linear extension rates and under the assumption that the masses

emanate from the center of mass of the spacecraft, the instantanious moments of inertia for symmetrical deployment become (see Fig. 1):

$$I_1 = I_2 = I(t) = I^* + 2mc^2t^2 + 2m_3c_3^2\,t^2$$
$$I_3(t) = I_3^* + 4mc^2t^2 \tag{25}$$

where

$$\ell_1 = \ell_2 = ct,\ m_1 = m_2 = m$$
$$\ell_3 = c_3t \tag{26}$$

ℓ_1, ℓ_2, ℓ_3 are the distances of the end masses m_1, m_2, m_3 from the satellite mass center 0, respectively, c the extension rate along the 1, 2 symmetry axes, and c_3 the extension rate along the 3 axis. Let

$$\mu = 4mc^2$$
$$p = 2mc^2 + 2m_3c_3^2 \tag{27}$$

so that

$$I(t) = I^* + pt^2$$
$$I_3(t) = I_3^* + \mu t^2 \tag{28}$$

$$\int_0^t b(t)dt = \int_0^t \frac{I_3(t)-I(t)}{I_3(t)I(t)}\,h_0\,dt$$

Equation (24) can be written:

$$h_1(t) = q_0^* \cos\left[\frac{h_0}{\sqrt{I^*p}}\tan^{-1}\left(\frac{t}{\sqrt{I^*/p}}\right) - \frac{h_0}{\sqrt{I_3^*\mu}}\tan^{-1}\left(\frac{t}{\sqrt{I_3^*/\mu}}\right) + \psi_0^*\right]$$

$$h_2(t) = q_0^* \sin\left[\frac{h_0}{\sqrt{I^*p}}\tan^{-1}\left(\frac{t}{\sqrt{I^*/p}}\right) - \frac{h_0}{\sqrt{I_3^*\mu}}\tan^{-1}\left(\frac{t}{\sqrt{I_3/\mu}}\right) + \psi_0^*\right] \quad (29)$$

where the constants q_0^* and ψ_0^* are related to the initial conditions as follows:

$$q_0^* = \sqrt{h_1^2(0) + h_2^2(0)}$$

$$\psi_0^* = \tan^{-1}\frac{h_2(0)}{h_1(0)} \quad (30)$$

After integration of Eq. (23.c),

$$\theta_3(t) = \frac{h_0}{\sqrt{I_3^*\mu}}\tan^{-1}\left(\frac{t}{\sqrt{I_3^*/\mu}}\right) - \Omega t + \theta_3(0) \quad (31)$$

where $\theta_3(0)$ is the initial condition at $t = 0$. Equations (31) and (29) are then substituted into Eqs. (23.c) and (23.d) with the result:

$$\dot{\theta}_1 - \Omega\theta_2 = \frac{q_0^*}{I^* + pt^2}\left[\cos\left\{\frac{h_0}{\sqrt{I^*p}}\tan^{-1}\left(\frac{t}{\sqrt{I^*/p}}\right) - \Omega t + \psi_0^* + \theta_3(0)\right\}\right]$$

$$\dot{\theta}_2 + \Omega\theta_1 = \frac{q_0^*}{I^* + pt^2}\left[\sin\left\{\frac{h_0}{\sqrt{I^*p}}\tan^{-1}\left(\frac{t}{\sqrt{I^*/p}}\right) - \Omega t + \psi_0^* + \theta_3(0)\right\}\right] \quad (32)$$

The variation of parameter technique for solving a system of

first order differential equations is now applied to solve Eqs. (32). We seek a solution of the form

$$\underline{\Theta}(t) = \underline{\psi}(t)\underline{u}(t) \tag{33}$$

where the fundamental matrix, $\underline{\psi}(t)$, is given by:

$$\underline{\psi}(t) = \begin{bmatrix} \cos \Omega t & \sin \Omega t \\ -\sin \Omega t & \cos \Omega t \end{bmatrix} \tag{34}$$

and the vectors $\underline{u}(t)$ and $\underline{\Theta}(t)$ are

$$\underline{u}(t) = \int_0^t \underline{\psi}^{-1}(s)\, \underline{g}(s)\, ds + \underline{C} \tag{35}$$

$$\underline{\Theta}(t) = \begin{bmatrix} \Theta_1 \\ \Theta_2 \end{bmatrix}$$

In Eq. (35), $\underline{g}(t)$ represents the right-hand side of Eq. (32) and $\underline{C}$ is a constant vector.

$$\underline{u}(t) = \int_0^t \begin{bmatrix} \cos \Omega s & -\sin \Omega s \\ \sin \Omega s & \cos \Omega s \end{bmatrix} \begin{bmatrix} \dfrac{q_0^*}{I^* + ps^2} \cos\left\{ \dfrac{h_0}{\sqrt{I^* p}} \tan^{-1}\left(\dfrac{s}{\sqrt{I^*/p}} \right) \right. \\ \dfrac{q_0^*}{I^* + ps^2} \sin\left\{ \dfrac{h_0}{\sqrt{I^* p}} \tan^{-1}\left(\dfrac{s}{\sqrt{I^*/p}} \right) \right. \end{bmatrix}$$

$$\left. \begin{bmatrix} -\Omega s + \phi \\ -\Omega s + \phi \end{bmatrix} \right\} ds + \underline{C} \tag{36}$$

where

$$\phi = \psi_0^* + \theta_3(0) \tag{37}$$

The solution for θ_1, θ_2 can be obtained by first evaluating the integral in Eq. (36) and then substituting this result into Eq. (33).

$$\begin{bmatrix} \theta_1 \\ \theta_2 \end{bmatrix} = \begin{bmatrix} \cos\Omega t & \sin\Omega t \\ -\sin\Omega t & \cos\Omega t \end{bmatrix} \begin{bmatrix} \frac{q_0^*}{h_0} \left[\sin\left\{ \frac{h_0}{\sqrt{I^* p}} \tan^{-1}\left(\frac{t}{\sqrt{I^*/p}} \right) + \phi \right\} \right] \\ \frac{q_0^*}{h_0} \left[\cos\left\{ \frac{h_0}{\sqrt{I^* p}} \tan^{-1}\left(\frac{t}{\sqrt{I^*/p}} \right) + \phi \right\} \right] \end{bmatrix}$$

$$\begin{bmatrix} -\sin\phi \\ -\cos\phi \end{bmatrix} + \begin{bmatrix} C_1 \\ C_2 \end{bmatrix} \tag{38}$$

C_1, C_2 are constants which can be related to the initial conditions by

$$C_1 = \theta_1(0)$$
$$C_2 = \theta_2(0) \tag{39}$$

From consideration of Eq. (38), the following conclusions can be drawn:

(1) For small $t/\sqrt{I^*/p}$, $\tan^{-1}\ (t/\sqrt{I^*/p})$ can be approximated by: $t/\sqrt{I^*/p}$, so that the frequency of oscillation is given by $h_0/I^* = I_3^*\omega_3(0)/I^*$. This indicates that for high initial spin rates oscillations will be characterized by a high frequency mode.

(2) For t sufficiently large, $\frac{h_0}{\sqrt{I^*p}} \tan^{-1} \frac{t}{\sqrt{I^*/p}}$ can be approximated by a constant: $\frac{h_0}{\sqrt{I^*p}} \frac{\pi}{2}$. θ_1 and θ_2 are then periodic with a frequency of Ω (the orbital frequency).

The analytical solution developed is plotted in Fig. 5.a and is compared with numerical integration including the effect of gravity-gradient, for an initial spin rate of 3 rad/sec. The behavior observed is a confirmation of the above two conclusions. As time increases the analytical solution becomes less valid due to the accumulated effects of the gravity-gradient torques.

H. Numerical Results

The non-linear equations of motion (9), (10) are solved numerically. The numerical integration is carried out using a NOVA-840 computer, with RKGS subroutine.[9] The subroutine RKGS solves the initial-value problem by means of a fourth-order Runge-Kutta formula using the modification due to Gill. The integration procedure is stable and self-starting; that is, only the functional value at a single previous point is required to obtain the functional values ahead. For this reason it is easy to change the step size at any step in the calculation. The entire input of the procedure is: (1) lower and upper bound of the integration interval, initial increment of the independent variable, upper bound for the local truncation error; (2) initial values for the dependent variable and weights for local truncation

errors in each component of the dependent variables; (3) the number of differential equations in the system; (4) as external subroutine sub-programs, the computation of the right-hand side of the system of differential equations; for flexibility in output an output subroutine.

To study the system for which $|\theta_1|$, $|\theta_2|$ remain small the stability chart developed (Fig. 4) can be employed to analyze the following cases of interest:

(1) Extension only along the '3' principal axis: A previous study[2] in the application of telescoping booms for detumbling a spacecraft, to achieve a desired spin about one of the principal axes has suggested (based on a modified form of kinetic energy as a Lyapunov function) extension of booms along all three principal axes until the final desired spin rate is reached and then continuing the extension of the set of booms along the nominal spin axis until the transverse components of the angular velocity reach an acceptably small amplitude.[2] For extension of booms along the spin axis only and for a symmetrical spacecraft it is clear that in the stability chart the spin parameter, α, will remain constant during deployment, while the moment of inertia ratio, K, decreases. The value of K at any instant of time for this case is given by

$$K = \frac{(I_3^* - I^* - p_1 t^2)}{I^* + p_1 t^2} \tag{40}$$

where starred quantities represent the initial values and

$p_1 = 2mc^2$

m = end mass

c = extension rate

From consideration of Eq. (40) as t becomes large, K, tends towards -1. In the upper-half of the stability chart, the stability boundary, $F_2 = 0$, tends toward K = -1·0 asymptotically. This implies that for a wide range of spin rates commonly used, extension only along the '3' axis could result in the system eventually being driven to an unstable state. Typical examples of such deployment maneuvers have been simulated and the responses shown in Figs. 5.b,c; 6.a,b; 7.a,b; 9.a,b; and 10.a,b.

In Fig. 5.b the response of the ω_1 and ω_2 components of the angular velocity with and without the gravity-gradient torque are compared. The initial conditions, end masses, extension rate and initial principal inertias are indicated in the figure. For this case an initial (high) spin rate of 3.0 rad/sec is assumed. Clearly, the envelope of ω_1 and ω_2 with gravity-gradient torque present shows the growth in amplitude after 250 secs. For this case the response of the nutation angle (Fig. 5.c) indicates the potential instability during extension after 250 seconds. Since $\alpha = 2.9 \times 10^3$ here, this case can not be indicated in the regions of the stability chart as plotted. However use of Eq. (40) shows that for t > 12 secs, the value of K becomes less than -0.8.

Figures 6.a,b and 7.a,b illustrate the responses of ω_1, ω_2 and nutation angle for two different extension rates: c_3 = 4.0 ft/sec and c_3 = 0.5 ft/sec, respectively, both with the same initial conditions. In either case, α = 1.0, and is a constant during the extension maneuver. Initially K = 1.0. Figs. 6.a and 7.a show that with the gravitational torque included, the ω_2 component increases in amplitude after an initial tendency to decrease. After 60 secs for the first case (Fig. 6.b) and 250 secs for the second case (Fig. 7.b), the nutation angle increases and almost doubles its initial value within 280 secs and 500 secs, respectively. The time history of the slower extension case (0.5 ft/sec) is indicated on a redrawn version of the stability chart in Fig. 8. In this chart the horizontal dotted line parallel to the K axis passing through α = 1.0 corresponds to the 0.5 ft/sec extension rate discussed earlier in Figs. 7.a,b. The system crossed the stability boundary at t = 39 secs, which corresponds to approximately 20 feet of boom extension. It can be concluded from Fig. 7.b that although the system crosses the stability boundary at t = 39 secs, the instability is not exhibited in the form of the growth of the nutation angle during the extension maneuver, until about 250 secs, when the nutation angle begins to grow in an exponential fashion.

Two more cases of extension only along the '3' axis were simulated, beginning in the unstable region in the right-half of

the stability chart, that is the unstable region for positive K. The responses for the two cases with extension rates of 4 ft/sec and 0.5 ft/sec are shown in Figs. 9.a,b and Figs. 10.a,b respectively. The responses are similar to the cases of Figs. 6 and 7. Even for the slower extension rate of 0.5 ft/sec, no appreciable increase in the nutation angle was observed as the system passes through the unstable region for $K > 0$.

(2) Extension maneuver along all three axes

A previous study[2] on detumbling a randomly spinning spacecraft using telescoping appendages had considered zero inertial angular velocity as a final desired state of the system. The authors using the rotational kinetic energy as a Lyapunov function had concluded that the necessary conditions for asymptotic stability in torque free space are satisfied for positive constant boom extension rates. When the dynamics for symmetric extension with the gravity-gradient torque is considered, it is observed that the parameter $\alpha = (\omega_3 - \Omega)/\Omega$ eventually tends towards -1.0 for sufficiently large time. If the same end masses and extension rates were employed along all three principal axes, the inertia ratio K at any instant of time would be given by

$$K = \frac{I_3^* - I^*}{I^* + \mu t^2} \tag{41}$$

where

$\mu = 4m\,c^2$; m = end mass; c = extension rate

Equation (41) suggests that for sufficiently large time, K tends towards 0. Although the point (0, -1) in the stability chart is a boundary point, in practice, extension along all three axes with the same end masses and extension rates could never result in the system actually reaching this point.

Typical examples of such deployment maneuvers have been simulated and the responses shown in Figs. 11 and 12.a,b. In Fig. 11 the system is initially in the stable region with $\alpha(0) = 5.0$ and $K(0) = 0.6$. The initial conditions are indicated in the figure. For this case the responses of the components of the angular velocity and the nutation angle show negligible difference with gravity-gradient present or absent. The nutation angle is observed to be a constant. The time history for this case has been indicated in Fig. 8. by the dash-double dot curve beginning at the point (0.6,5). With the assumed extension rate of 4 ft/sec and end mass of 0.01 slugs, the system moves rapidly down the stability chart. It enters the unstable region for positive K, at about 8 secs which corresponds to 32 feet of boom length. However it stays only very briefly in this unstable region reentering the stable region again in about 10 seconds. Clearly any such deployment strategy should ensure that the extension of booms is not terminated in this unstable region.

Figs. 12.a,b show the response of a system initially in the unstable region with $\alpha(0) = 5.0$ and $K(0) = -0.6$. Here a small

difference in the response of ω_1, ω_2, ω_3 was observed with gravity-gradient present and then absent. Within 630 secs of response time this difference is not noticeable within the scale shown in the figure. However the response of the nutation angle (Fig. 12.b) shows a slight growth for the case with gravity-gradient present after about 430 seconds. The time history for this case is indicated by the dash-dot curve beginning at the point (-0.6,5) in Fig. 8. It is observed that the system tends to the point (0,-1) from the left. The system briefly passes through the narrow strip of the stable region close to the K axis in the left-half of the stability chart, although never entering the stable region elsewhere even for the slow extension rate of 0.1 ft/sec used.

(3) Extension along the 1,2 principal axes

A number of spin-stabilized satellites have long appendages in the plane of rotation. Hughes[10] has studied the dynamics of the satellite during the deployment maneuver assuming torque free conditions. For symmetric extension along the 1,2 principal axis only the spin parameter, $\alpha = (\omega_3-\Omega)/\Omega$, tends towards -1.0 for sufficiently large time. The inertia factor K at any instant of time during the deployment maneuver is given by

$$K = \frac{I_3^* + \mu t^2 - I^* - \frac{\mu}{2} t^2}{I^* + \frac{\mu}{2} t^2} \qquad (42)$$

where

$\mu = 4\ mc^2$; m = end mass; c = extension rate.

From Eq. (42) it can be concluded that, given sufficiently large time the factor K tends towards 1.0. So one can expect that under suitable conditions extension only along the 1,2 principal axes would eventually drive the system to the point (1,-1), which lies in the unstable region for positive K in the stability chart (see Fig. 4).

Two typical extension maneuvers for this case have been simulated and the responses presented in Figs. 13.a,b and 14.a,b. Fig 13.a shows the response of the transverse components of the angular velocity, for a system initially in the stable region; $K(0) = 0.4$ and $\alpha(0) = 5.0$. The initial conditions are indicated in the figure. It is seen that the ω_2 component for the case with gravity-gradient torque, begins to increase after about 270 secs. The nutation angle (Fig. 13.b) likewise begins an exponential type growth at about the same time. The spin, ω_3, is not affected since the gravity-gradient torque about the spin axis vanishes for symmetric deployment and the responses with or without the gravity-gradient torque are identical. The time history trajectory for this case has been indicated in Fig. 15 by the dash-double cross curve beginning at the point (0.4,5). For the assumed extension rate of 0.5 ft/sec and an end mass of 0.01 slugs the system crosses into the unstable region for positive K after 87 secs which corresponds to about 44 feet of extended boom. Although the

system enters the unstable region after 87 secs, instability is not exhibited in the form of growth in the nutation angle until about 270 seconds.

Another case of deployment along the 1,2 axes beginning in the unstable region ($\alpha(0) = 5.0$, $K(0) = -0.6$) has been simulated and the results presented in Figs. 14.a,b. A slow extension rate of 0.1 ft/sec has been assumed for this case. Fig. 14.a shows that with the gravity-gradient present the ω_2 component becomes positive at about 500 secs and continues to grow further, whereas the response without gravity-gradient torque shows that ω_2 tends towards zero. Fig. 14.b shows that with the gravity-gradient torque the nutation angle begins to grow after 360 seconds. The time history for this case is indicated in Fig. 15. by the dash-cross curve beginning at the point (-0.6,5). The system enters the stable region at $t = 74$ secs, leaves it again and reenters the unstable region for positive K at $t = 179$ secs. Although the system is moving through the unstable region for $t > 179$ secs, it takes about 360 secs before the instability is indicated as a pronounced growth in the nutation angle.

III. ASYMMETRIC DEPLOYMENT

A. Configuration

The system is assumed to consist of a rigid central hub (Fig. 16.a) with center of mass at point Q and one or two extendible telescoping booms with end masses m_1 and m_2, respectively. The mass along the boom lengths is assumed negligible in comparison with the end masses. It is assumed that, in general, the two booms will be offset from the hub principal axes with the coordinates a, b, c, d indicating the amount of offset. Previous studies have considered this type of configuration for detumbling a spacecraft.[6,7] It has been pointed out that for three axis optimal control more than one offset boom (orthogonal to each other) is required and that for two axis optimal control a single offset boom is sufficient.[7]

B. Development of Gravity Torque Components

The general configuration of the two mass offset system is shown in Fig. 16.b. Whenever there is an asymmetric (internal) mass motion in a spacecraft system, the position of the composite center of mass and the orientation of the system principal axes will vary with time. The choice of the composite center of mass of the system as the reference point in the body, leads to time varying moments of inertia in the rotational equations of motion. This problem can be circumvented by choosing the vehicle (hub) center of mass as the reference point and the hub principal axes as the body reference frame. In Fig. 16.b, d_1, d_2, d_3 represent the

hub principal axes; Q, the hub center of mass; $\bar{R}$, the geocentric position vector of the hub center of mass; $\bar{R}_c$ the geocentric position vector of the composite center of mass, C; m_1 and m_2 are the control masses whose position vectors relative to point Q are indicated by $\bar{r}_1$ and $\bar{r}_2$, respectively. $\bar{r}_c$ is the position vector of the composite center of mass referenced to point Q.

If $\bar{r}$ represents the vector from point Q to an elemental mass dm, then the torque applied by gravity about the hub center of mass is[8]

$$\bar{N}_Q = \int \bar{r} \times \left[- \frac{k(\bar{R} + \bar{r})}{|\bar{R} + \bar{r}|^3} \right] dm \tag{43}$$

where $k = g_0 R_0^2$ with g_0 the gravitational acceleration at the earth's surface and R_0 the radius of the earth. Eq. (43) can be expressed as:

$$\bar{N}_Q = \frac{k\bar{R}}{R^3} \times \int \frac{\bar{r}\, dm}{\left[1 + \frac{\bar{r} \cdot \bar{R}}{R^2} \right]^3} \tag{44}$$

where $R = |\bar{R}|$ and the integration is taken over the total mass. Expanding the denominator of the integrand in a binomial series provides the approximation[8]

$$\bar{N}_Q = \frac{k\bar{R}}{R^3} \times \int_{\bar{r}} \left[1 - \frac{3\,\bar{r}\cdot\bar{R}}{R^2}\right] dm \qquad (45)$$

in which terms above the first degree in $(\bar{R}\cdot\bar{r}/R^2)$ have been neglected in comparison with first degree terms. This approximation is justified by the observation that the satellite dimensions are small in comparison with the orbital radius. The main body can be treated as a continuum and the offset masses treated as discrete particles so that the integral in Eq. (45) can be divided into an integral over the main body and a summation for the end masses. Equation (45) can then be written as:

$$\bar{N}_Q = \frac{k\bar{R}}{R^3} \times \int_{\text{main body}} \bar{r} \left[1 - \frac{3\,\bar{r}\cdot\bar{R}}{R^2}\right] dm + \frac{k\bar{R}}{R^3} \times \sum_{i=1}^{2} \bar{r}_i \left[1 - \frac{3\,\bar{r}_i\cdot\bar{R}}{R^2}\right] m_i \qquad (46)$$

By definition of the center of mass of the hub $\int \bar{r}\,dm$ is zero. Eq. (46) then becomes

$$\bar{N}_Q = \frac{3k}{R^3}\,\hat{a}_1' \times \square_m \cdot \hat{a}_1' + \frac{k}{R^2}\,\hat{a}_1' \times \sum_{i=1}^{2} m_i \bar{r}_i \left[1 - \frac{3}{R}\,\bar{r}_i \cdot \hat{a}_1'\right] \qquad (47)$$

where

$\hat{a}_1'$ - unit vector along the geocentric position vector of the main body center of mass.

R - distance of the main body center of mass from the center of the earth.

$\underline{\underline{I}}_m$ - moment of inertia dyadic of the main body.

Here it is important to observe that in general the factor $\sum_i m_i \bar{r}_i$ does not vanish. Equation (47) is an expression for the gravity torque about the hub center of mass for a system with two offset control masses. Here it will be expanded to yield the gravity torque components in the hub reference frame for the specific configuration shown in Fig. 16.a.

We now make the assumptions that the unit vector $\hat{a}_1'$ defined above can be considered equivalent to the unit vector along the composite system local vertical and that the distance, R, as defined above is equivalent to the orbital radius. These assumptions are justified by the fact that for the choice of control masses as one percent of the satellite mass,[6] the displacement between the hub center of mass and the composite center of mass would be extremely small in comparison with the orbit radius. It is then possible to make use of the same set of Euler angles (Fig. 3) as defined for the symmetric deployment in Section II, now relating the orbiting reference frame (Fig. 2) to the hub principal axes reference frame, d_1, d_2, d_3. The transformation between these two reference frames is given by Eq. (2) and the vector $\hat{a}_1'$ is obtained from Eq. (4) and is given as follows:

$$\hat{a}_1' = c\theta_2 c\theta_3 \hat{d}_1 - c\theta_2 s\theta_3 \hat{d}_2 + s\theta_2 \hat{d}_3 \qquad (48)$$

For the two mass system shown in Fig. 15 the control mass position vectors are given by:

$$\bar{r}_1 = a\,\hat{d}_1 + b\,\hat{d}_2 + z\,\hat{d}_3$$
$$\bar{r}_2 = x\,\hat{d}_1 + c\,\hat{d}_2 + d\,\hat{d}_3 \qquad (49)$$

Equations (48) and (49) are substituted into Eq. (47), resulting in the following gravity torque components

$$N_1 = \frac{3k}{R^3}(I_2-I_3)\,c\theta_2 s\theta_2 s\theta_3 + \frac{k}{R^2}[m_1\{-zc\theta_2 s\theta_3 - bs\theta_2\} + m_2\{-dc\theta_2 s\theta_3 - cs\theta_2\}] - \frac{3k}{R^3}[m_1(ac\theta_2 c\theta_3 - bc\theta_2 s\theta_3 + zs\theta_2)(-zc\theta_2 s\theta_3 - bs\theta_2) + m_2(xc\theta_2 c\theta_3 - cc\theta_2 s\theta_3 + ds\theta_2)(-dc\theta_2 s\theta_3 - cs\theta_2)] \qquad (50.a)$$

$$N_2 = \frac{3k}{R^3}(I_1-I_3)\,c\theta_2 s\theta_2 c\theta_3 + \frac{k}{R^2}[m_1\{-zc\theta_2 c\theta_3 + as\theta_2\} + m_2\{-dc\theta_2 c\theta_3 + xs\theta_2\}] - \frac{3k}{R^3}[m_1(ac\theta_2 c\theta_3 - bc\theta_2 s\theta_3 + zs\theta_2)(as\theta_2 - zc\theta_2 c\theta_3) + m_2(xc\theta_2 c\theta_3 - cc\theta_2 s\theta_3 + ds\theta_2)(xs\theta_2 - dc\theta_2 c\theta_3)] \qquad (50.b)$$

$$N_3 = \frac{3k}{R^3}(I_1-I_2)(c\theta_2)^2 c\theta_3 s\theta_3 + \frac{k}{R^2}[m_1\{bc\theta_2 c\theta_3+ac\theta_2 s\theta_3\}$$

$$+m_2\{cc\theta_2 c\theta_3+xc\theta_2 s\theta_3\}] - \frac{3k}{R^3}[m_1(ac\theta_2 c\theta_3-bc\theta_2 s\theta_3$$

$$+zs\theta_2)(bc\theta_2 c\theta_3+ac\theta_2 s\theta_3)+m_2(xc\theta_2 c\theta_3-cc\theta_2 s\theta_3$$

$$+ds\theta_2)(cc\theta_2 c\theta_3+xc\theta_2 s\theta_3)] \qquad (50.c)$$

C. Equations of Motion

The complete equations of motion with telescoping type control booms in the presence of gravity torque are developed. The torque free equations of motion for the system have been previously developed[7] and this development is briefly reproduced here, after modification to include the gravity torque.

The generalized vector equation of motion for such a system containing a central hub and moving connected masses can be written:[11]

$$\bar{N}_Q = \dot{\bar{L}}_Q + \sum_{i=1}^{n} m_i (\bar{r}_{i/Q}) \times \ddot{\bar{R}} \qquad (51)$$

where $\bar{N}_Q$ refers to the gravity torque, Q refers to the reference point which is assumed to be at the center of mass of the hub, $\ddot{\bar{R}}$ is the inertial acceleration of the reference point and $\bar{r}_{i/Q}$ is the position vector of mass, m_i, with respect to point Q (Fig. 16.b.) It should also be noted that $\bar{R}_c$ is the position vector of the composite system center of mass whose position will change with the movement of m_1 and m_2. The composite c.m. is assumed to move

in a circular orbit, and it is assumed that coupling between orbital (translational) motion and the attitude dynamics is a higher order effect.

The angular momentum of the system measured with respect to point, Q, has three components,

$$\bar{L}_Q = \bar{L}_{b/Q} + \bar{L}_{m_1/Q} + \bar{L}_{m_2/Q} \tag{52}$$

where $\bar{L}_{b/Q}$ describes the momentum of the hub, and $\bar{L}_{m_i/Q}$ describes the momentum of mass m_i. The hub momentum may be expressed in terms of the hub principal moments of inertia and angular velocity components as:

$$\bar{L}_{b/Q} = I_1\omega_1\hat{d}_1 + I_2\omega_2\hat{d}_2 + I_3\omega_3\hat{d}_3 \tag{53}$$

where $\hat{d}_1$, $\hat{d}_2$, $\hat{d}_3$ are unit vectors along the hub principal axes, and

$$\bar{L}_{m_i/Q} = m_i\,(\bar{r}_i \times \dot{\bar{r}}_i) \;; \quad i = 1,2 \tag{54}$$

where $\bar{r}_i$ describes the position of m_i relative to $Q(\bar{r}_{i/Q})$.

We will now consider the inertial acceleration of the reference point (Fig. 16).

$$\ddot{\bar{R}} = \ddot{\bar{R}}_c - \ddot{\bar{r}}_c \tag{55}$$

Under the assumption that coupling between translational and rotational motion can be neglected, $\ddot{\bar{R}}_c = 0$, and

$$\ddot{\bar{R}} = -\ddot{\bar{r}}_c \tag{56}$$

From the definition of the system center of mass we can relate

$$\ddot{\bar{R}} = - \frac{m_1 \ddot{\bar{r}}_1 + m_2 \ddot{\bar{r}}_2}{M + \Sigma m} \tag{57}$$

where M represents the hub mass and

$$\Sigma m = m_1 + m_2$$

After substituting Eqs. (53), (54) and (57) into Eq. (51) the following rotational equation results:[7]

$$\dot{\bar{L}}_{b/Q} + \mu_1 \, (\bar{r}_1 \times \ddot{\bar{r}}_1) + \mu_2 \, (\bar{r}_2 \times \ddot{\bar{r}}_2) + \mu_3 \, (\bar{r}_1 \times \ddot{\bar{r}}_2 + \bar{r}_2 \times \ddot{\bar{r}}_1) = \bar{N}_Q \tag{58}$$

where

$$\mu_1 = m_1 \, (M + m_2)/(M + \Sigma m)$$

$$\mu_2 = m_2 \, (M + m_1)/(M + \Sigma m)$$

$$\mu_3 = - m_1 m_2/(M + \Sigma m)$$

Eq. (58) is then expanded using the familiar relationship,

$$\dot{\bar{L}}_{b/Q} = \left. \frac{d\bar{L}_b}{dt} \right|_{body} + \bar{\omega} \times \bar{L}_{b/Q} \tag{59}$$

and for the specific geometry of Fig. 16.a,

$$\bar{r}_1 = a \, \hat{d}_1 + b \, \hat{d}_2 + z \, \hat{d}_3 \tag{60}$$

$$\bar{r}_2 = x \, \hat{d}_1 + c \, \hat{d}_2 + d \, \hat{d}_3 \tag{61}$$

The acceleration terms $\ddot{\bar{r}}_i$ (i = 1,2) may be calculated by using

$$\ddot{\bar{r}}_i = \bar{\omega} \times (\bar{\omega} \times \bar{r}_i) + \dot{\bar{\omega}} \times \bar{r}_i + 2\bar{\omega} \times [\dot{\bar{r}}_i]_{body}$$

$$+ [\ddot{\bar{r}}_i]_{body}$$

together with Eqs. (60) and (61).

The complete nonlinear equations of motion are obtained by expansion of Eq. (58) and substitution for the gravity torque components from Eqs. (50.a), (50.b), and (50.c).

$$I_1\dot{\omega}_1 + (I_3-I_2)\,\omega_2\omega_3 + \mu_1\,[(b^2+z^2)\,\dot{\omega}_1 - ab\dot{\omega}_2 - az\dot{\omega}_3 - az\omega_1\omega_2$$

$$+(b^2-z^2)\,\omega_2\omega_3 + ab\omega_1\omega_3 + 2z\dot{z}\,\omega_1 + bz\,(\omega_3^2 - \omega_2^2) + b\ddot{z}]$$

$$+\mu_2\,[c^2+d^2)\,\dot{\omega}_1 - cx\dot{\omega}_2 - dx\dot{\omega}_3 - dx\omega_1\omega_2 + (c^2-d^2)\,\omega_2\omega_3$$

$$+cx\omega_1\omega_3 - 2c\dot{x}\omega_2 - 2d\dot{x}\omega_3 + cd\,(\omega_3^2-\omega_2^2)] + \mu_3[2(bc+dz)\,\dot{\omega}_1$$

$$-(ac+bx)\,\dot{\omega}_2 - (ad+xz)\,\dot{\omega}_3 - (ad+zx)\,\omega_1\omega_2 + 2(bc-dz)\,\omega_2\omega_3$$

$$+(ac+bx)\,\omega_1\omega_3 + 2d\dot{z}\omega_1 - 2b\dot{x}\omega_2 - 2\dot{x}z\omega_3 + (bd+cz)\,(\omega_3^2-\omega_2^2)$$

$$+ c\ddot{z}] = \frac{3k}{R^3}\,(I_2-I_3)c\theta_2 s\theta_2 s\theta_3 + \frac{k}{R^2}\,[m_1\,\{-zc\theta_2 s\theta_3 - bs\theta_2\}$$

$$+m_2\,\{-dc\theta_2 s\theta_3 - cs\theta_2\}] - \frac{3k}{R^3}\,[m_1\,(ac\theta_2 c\theta_3 - bc\theta_2 s\theta_3$$

$$+zs\theta_2)\,(-zc\theta_2 s\theta_3 - bs\theta_2) + m_2\,(xc\theta_2 c\theta_3 - cc\theta_2 s\theta_3$$

$$+ds\theta_2)\,(-dc\theta_2 s\theta_3 - cs\theta_2)] \qquad (63.a)$$

$$I_2\dot{\omega}_2 + (I_1-I_3)\,\omega_3\omega_1 - \mu_1\,[ab\dot{\omega}_1 - (a^2+z^2)\,\dot{\omega}_2 + bz\dot{\omega}_3 - bz\omega_1\omega_2$$

$$+ab\omega_2\omega_3 + (a^2-z^2)\,\omega_3\omega_1 - 2z\dot{z}\omega_2 + az(\omega_3^2-\omega_1^2) + a\ddot{z}] - \mu_2[cx\dot{\omega}_1$$

$$-(d^2+x^2)\dot{\omega}_2 + cd\dot{\omega}_3 - cd\omega_1\omega_2 + cx\omega_2\omega_3 + (x^2-d^2)\omega_3\omega_1$$

$$-2x\dot{x}\omega_2 + dx(\omega_3^2-\omega_1^2) - d\ddot{x}] - \mu_3[ac+bx)\dot{\omega}_1 - 2(ax+dz)\dot{\omega}_2$$

$$+ (bd+cz)\dot{\omega}_3 - (bd+cz)\omega_1\omega_2 + (ac+bx)\omega_2\omega_3 + 2(ax-dz)\omega_3\omega_1$$

$$-2(a\dot{x}+d\dot{z})\omega_2 + (ad+xz)\,(\omega_3^2-\omega_1^2) + x\ddot{z}-z\ddot{x}]$$

$$= \frac{3k}{R^3}\,(I_1-I_3)c\theta_2 s\theta_2 c\theta_3 + \frac{k}{R^2}\,[m_1\{-zc\theta_2 c\theta_3 + as\theta_2\}$$

$$+m_2\{-dc\theta_2 c\theta_3 + xs\theta_2\}] - \frac{3k}{R^3}\,[m_1(ac\theta_2 c\theta_3 - bc\theta_2 s\theta_3$$

$$+zs\theta_2)\,(as\theta_2 - zc\theta_2 c\theta_3) + m_2(xc\theta_2 c\theta_3 - cc\theta_2 s\theta_3$$

$$+ds\theta_2)\,(xs\theta_2 - dc\theta_2 c\theta_3)] \qquad (63.b)$$

$$I_3\dot{\omega}_3 + (I_2-I_1)\omega_1\omega_2 - \mu_1[az\dot{\omega}_1 + bz\dot{\omega}_2 - (a^2+b^2)\dot{\omega}_3$$

$$+(b^2-a^2)\omega_1\omega_2 - az\omega_2\omega_3 + bz\omega_3\omega_1 + 2a\dot{z}\omega_1 + 2b\dot{z}\omega_2 + ab(\omega_1^2-\omega_2^2)]$$

$$-\mu_2[dx\dot{\omega}_1 + cd\dot{\omega}_2 - (c^2+x^2)\dot{\omega}_3 + (c^2-x^2)\omega_1\omega_2 - dx\omega_2\omega_3$$

$$+cd\omega_3\omega_1 - 2x\dot{x}\omega_3 + cx(\omega_1^2 - \omega_2^2) + c\ddot{x}] - \mu_3[(ad+xz)\dot{\omega}_1$$

$$+(bd+cz)\dot{\omega}_2 - 2(bc+ax)\dot{\omega}_3 + 2\,(bc-ax)\omega_1\omega_2 - (ad+xz)\omega_2\omega_3$$

$$+ (bd+cz)\omega_3\omega_1 + 2x\dot{z}\omega_1 + 2c\dot{z}\omega_2 - 2a\dot{x}\omega_3 + (ac+bx)\,(\omega_1^2-\omega_2^2)$$

$$+ b\ddot{x}] = \frac{3k}{R^3}\,(I_1-I_2)\,(c\theta_2)^2 c\theta_3 s\theta_3 + \frac{k}{R^2}\,[m_1\{bc\theta_2 c\theta_3$$

$$+ ac\theta_2 s\theta_3\} + m_2\{cc\theta_2 c\theta_3 + xc\theta_2 s\theta_3\}] - \frac{3k}{R^3}\,[m_1(ac\theta_2 c\theta_3$$

$$- bc\theta_2 s\theta_3 + zs\theta_2)\,(bc\theta_2 c\theta_3 + ac\theta_2 s\theta_3) + m_2(xc\theta_2 c\theta_3$$

$$- cc\theta_2 s\theta_3 + ds\theta_2)\,(cc\theta_2 c\theta_3 + xc\theta_2 s\theta_3)] \qquad (63.c)$$

Equations (9), which relate the Euler angular rates to the angular velocity components, together with the above Eqs. (63.a), (63.b) and (63.c) are the complete non-linear equations of motion for the two mass asymmetric system. Due to their complexity, no attempt has been made to obtain an analytical solution.

D. Numerical Results

The equations of motion developed are solved numerically using the RKGS subroutine outlined earlier in section II. In Ref. 7 a control law has been obtained for the boom end mass position such that a quadratic cost functional involving the weighted components of angular velocity plus the control is minimized when the final time is unspecified, assuming torque free conditions.

As an illustrative example the system parameters and initial conditions are selected from Ref. 7 for a large space station. It is to be noted that the satellite mass and the control mass here are 32 times larger when compared with those used in Ref. 6.

$I_1 = I_2 = I = 10.5 \times 10^6$ slug-ft^2 $(1.42 \times 10^7$kg-m$^2)$

$I_3 = 15 \times 10^6$ slug-ft^2 $(2.03 \times 10^7$kg-m$^2)$

$M = 1.37 \times 10^5$ slugs $(6.21 \times 10^4$ kg)

$m_3 = 1800$ slugs (26112 lbm)

$a = 65$ ft (19.8m), $b = 0$ ft (0m)

$\omega_1(0) = 0.391$ rad/sec, $\omega_2(0) = 0.0$ rad/sec, $\omega_3(0) = 0.314$ rad/sec.

In all the cases in this study only a single boom (Z boom) offset from the spin axis has been considered. A specific example has been chosen from Ref. 7 for which the Z boom control law is stated as follows:

$$\ddot{z} + (0.314)^2 z = - 0.314 \times 17.72 \{kc_1\omega_1 + kc_2\omega_2\} \tag{64}$$

where kc_1 and kc_2 are constants chosen based on optimal control theory.[7] In this case:

$$kc_1 = - 3.92, \; kc_2 = 9.56.$$

The solution to Eq. (64) with the initial conditions $z(0) = 0$, $\dot{z}(0) = 0$ for the torque free case is given in Ref. 7 as:

$$z(t) = 17.72 \{0.655 \sin 0.314t + 0.417 \cos 0.314t - e^{-0.54 \times 0.314t}(0.417 \cos 0.428 \times 0.314t + 2.056 \sin 0.428 \times 0.314t)\} \tag{65}$$

In the first part of the numerical study the effectiveness of the above control law in the presence of gravity torque is determined. Two cases of interest have been identified and the system behavior for these two cases are compared with the behavior for the torque free system.

Case.1: where the control law as given by Eq. (64) employs the actual components of the angular velocity ω_1, ω_2, ω_3, in the presence of gravity torque.

Case.2: where the Z boom motion is according to the idealized control, the controller using the angular velocity components for

the torque free system. For this hypothetical case the Z boom motion is input into the program as given by Eq. (65).

Figure 17.a shows the Z boom motion for Case.1 by the dash-cross curve, and for Case.2 by the solid line. It is seen from Eq. (65) that the boom will experience a steady state oscillation after the initial transient for Case.2. Observe that for this case within 10-15 seconds the transient part of this motion is removed leaving a remaining steady state oscillation. For Case.1 the Z boom motion amplitude increases after 40 secs and would reach displacements of nearly 300 feet in 60 seconds (assuming that much boom length could be extended).

Fig. 17.b shows the response of the ω_1 component of the angular velocity. When gravity torque is neglected the amplitude of ω_1 decreases with time and becomes close to zero in about 20 seconds of response time, whereas for Case.1. and 2. the response shows a markedly different variation with ω_1 becoming as high as -0.12 rad/sec and -1.5 rad/sec respectively within 60 seconds of response. Figs. 17.c shows a similar behavior for the ω_2 component. For the case without the gravity torque $|\omega_2|$ becomes close to zero as opposed to the large amplitude motion for Case.1 and Case.2. Figure 17.d indicates that ω_3 is constant when gravity torque is neglected, whereas for Case.2 the motion is periodic over a mean value of 0.6 rad/sec. For Case.1, corresponding to the actual Z boom motion, the ω_3 response is somewhat

similar to Case.2 until about 40 seconds after which it suddenly increases rapidly. This sudden increase corresponds to the high amplitudes of the Z boom motion. Fig. 17.e. shows the response of the nutation angle. For all cases there is an initial tendency to reduce this angle. However after 8 secs, with gravity-gradient present there is a definite tendency to exceed the initial value.

For a single boom offset system in Eq. (58) the term $\mu_1(\bar{r}_1 \times \ddot{\bar{r}}_1)$ can be identified as the reaction torque due to the control, while $\bar{N}_Q$ is the gravity torque. The magnitude of the reaction torque for the actual Z boom motion in the presence of gravity torque is compared with the magnitude of the gravity torque in Fig. 17.f.

From these responses it can be concluded that the gravity torque has a profound influence on the system behavior. If the controller senses the actual angular velocities with the gravity torque present the very high amplitudes of the Z boom motion would force the spacecraft to a larger amplitude nutational state. If the idealized control is used even though the response is a little better than the previous case the results are clearly undesirable. These results indicate that with gravity-gradient present this method of control could be used for only a very limited time period, after which the Z boom motion would have to be terminated.

It was thought that the presence of a counter mass, such that the composite center of mass would coincide with the hub center of mass for the zero position of the Z boom, might improve the system response. To study this configuration the X boom mass, m_2, was chosen equivalent to the Z boom mass and placed so as to maintain the symmetry of the spacecraft initially when $z = 0$ (see Fig. 16.a).

Identical initial conditions and satellite parameters as used in Fig. 17 were employed. The Z boom motion was assumed to be the ideal motion based on the control law for the torque free system.

The Z boom motion and the nutation angle response are shown in Fig. 18.a. It is observed that with gravity torque even in the presence of a counter mass the satellite would achieve a very large nutation angle reaching as high as 80 degrees after 39 seconds. When the gravity torque is neglected the nucation angle decreases initially and has almost a constant value of 2 degrees after 20 seconds. Fig. 18.b shows the response of the components of angular velocity. The decrease in the magnitude of the ω_3 component and increases in the magnitudes of the ω_1 and ω_2 components explain the high value of nutation angle at 39 seconds observed with the gravity torque. The responses without the gravity torque show a periodic motion for ω_1 and ω_2 after the initial transient, while ω_3 remains nearly constant. This example with a counter mass points out the undesirable response in the presence of gravity gradient for the choice of parameters and initial conditions used.

It has been pointed out in Ref. 7 that there is a residual oscillation in the Z boom after the spacecraft has been detumbled using the control sequence. To study the response of the system in the presence of gravity torque, when the Z boom executes a sinusoidal motion the following equation is chosen to represent the

motion of the Z boom:

$$z = 4 \sin 0.314t$$

The responses with and without the gravity torque are shown in Fig. 19.a,b. In Fig. 19.a we see the Z boom motion and the corresponding nutation angle response. The initial conditions are indicated. The nutation angle response with the gravity torque shows periodic peaks reaching a maximum value of 9 degrees, while intermittently reaching a minimum value of about 2 degrees. When the gravity torque is absent the nutation angle is periodic over a mean value of 5.5 degrees. The corresponding responses of the angular velocity components are shown in Fig. 19.b. In the presence of the gravity torque ω_1 and ω_2 have intermittent peaks and troughs while ω_3 is oscillatory over a mean value of 0.55 rad/sec. The responses without the gravity torque show that ω_1 and ω_2 are sinusoidal while ω_3 remains a constant. The adverse effect of the gravity torque during the boom motion is clearly seen.

A close study of Eq. (47) explains the substantial effect of the gravity torque observed in all the cases described above. The presence of the term $\Sigma m_i \bar{r}_i$ results in the gravity force on each control mass exerting a torque about the hub mass center. Clearly the torque resulting from this is an order of magnitude in r/R larger, than that which would result if the torque were taken about the composite center of mass. Here it would be inappropriate to call the torque as gravity-gradient torque since it is usually

understood to mean the torque about the satellite composite mass center due to differential gravity force acting on each element of the body.

In Eq. (47) if we isolate the term

$$\frac{m_1 k}{R^2} \hat{a}_1' \times \bar{r}_1 + \frac{m_2 k}{R^2} \hat{a}_1' \times \bar{r}_2$$

we see that even in the presence of the counter mass the vector addition of $\bar{r}_1$ and $\bar{r}_2$ (if $\bar{r}_1$ represents the position of the Z boom mass and $\bar{r}_2$ the position of the counter mass) for the maximum z displacement would be such as to make the above mentioned term quite appreciable. This explains the undesirable response in the presence of the counter mass.

From the previous cases studied it was concluded that to improve the performance of the system in the environment of the earths' gravity either the control mass and/or the amplitude of the Z boom oscillations have to be smaller. Further, the initial tendency of the nutation angle to decrease even in the presence of the gravity torque suggests that the presence of suitable damping in the boom mechanism would serve to diminish the undesirable large amplitude residual oscillations of the Z boom, while maintaining the initial beneficial effect of the control. Consequently two changes were made in the satellite parameters listed on page 36; the new mass of the satellite M = 4258 slugs (6.21×10^4 kg) and the new Z boom control mass m = 55.95 slugs (816 kg). Introduction of damping in the boom motion would result in the control Equation (64) being modified as:

$\ddot{z} + c\ (0.314)\ \dot{z} + (0.314)^2\ z = -0.314 \times 17.72\ \{kc_1\omega_1 + kc_2\omega_2\}$ where c is the damping constant. The constants kc_1 and kc_2 can be determined for the modified satellite parameters as suggested in Ref. 7. They were calculated to be:

$$kc_1 = -3.3188,\ kc_2 = 31.366.$$

The response of the system for this case has been plotted in Figs. 20.a and 20.b under the same set of initial conditions and boom offset coordinates as used in Figs. 17. Figure 20.a shows Z boom motion for three different cases. The Z boom motion is indicated by the solid line in the absence of gravity torque and damping; by the dash-dot line in the presence of the gravity torque but no damping; by the dash-cross line in the presence of the gravity torque and in the presence of boom damping. The damping constant for this example was chosen to be, c = 0.4, which represents less than critical damping in the absence of control. The corresponding response of the nutation angle is shown in Fig. 20.b. In the absence of gravity torque and damping the nutation angle approaches zero within 175 sec. With damping in the boom motion the improvement in the response of the system in the presence of gravity torque is clearly seen. It should be mentioned here that the damping constant, c, must be chosen carefully to obtain the best results.

Figures 21.a and 21.b show the response of the system for sinusoidal Z boom motion with the reduced mass. A comparison of this with the responses shown in Figs. 19.a and 19.b clearly points out the diminished effect of the gravity torque when smaller masses are employed.

IV. CONCLUSIONS

1. For deployment maneuvers during which the inertia symmetry about the spin axis is maintained the stability chart for symmetrical spinning bodies can be used to study the system behavior.
2. For various extension maneuvers the bounds for boom lengths can be determined so that the system does not enter an unstable region.
3. For extension along all three axes with the same end masses and extension rates, if the satellite is initially stable, there is negligible difference in the response of the system with gravity-gradient present or absent.
4. For all the cases where the extension maneuver is performed through an unstable region although the nutation angle does not increase as soon as the system enters the unstable region, there is an exponential type growth in the nutation angle after a certain length of boom has been extended.
5. The analytical solution obtained for the out of plane Euler angles for symmetric extension in torque free space can be used to study the system behavior with gravity torque for a limited time period.
6. For the asymmetric deployment the expression for the gravity torque developed shows that a first order gravity force on the asymmetric mass exerts a torque about the

hub mass center. This torque is an order of magnitude in (r/R) larger than the gravity-gradient torque for the symmetric deployment.

7. For smaller control masses the controlled (asymmetric) offset boom system may be used effectively in the presence of the gravity-torque to reduce nutational motion when there is damping present in the offset boom system. The amount of boom damping required must be carefully selected for best results.
8. For large control masses with gravity torque present the offset (asymmetric) system can be controlled so as to reduce the nutation angle only for the first few seconds, suggesting that the control should be terminated after that.
9. The effect of other perturbations such as due to solar radiation pressure, aerodynamic effects etc., have not been considered here but should be investigated especially for the case of large boom lengths.

REFERENCES

1. Sellappan, R. and Bainum, Peter M., "Dynamics of Spin Stabilized Spacecraft During Deployment of Telescoping Appendages," AIAA - 14th Aerospace sciences Meeting, Washington, D.C., Jan. 26-28, 1976, Paper No. 76-185; also in Journal of Spacecraft and Rockets, Vol. 13, No. 10, Oct. 1976, pp. 605-610.

2. Bainum, P.M. and Sellappan, R., "Spacecraft Detumbling Using Movable Telescoping Appendages," XXVIth International Astronautical Congress, Lisbon, Sept. 21-27, 1975, Paper No. 75-113; also in Acta Astronautica, Vol. 3, No. 11-12, Nov.-Dec. 1976, pp. 953-969.

3. Puri, V. and Bainum, P.M., "Planar Librational Motion of a Gravity-Gradient Satellite During Deployment," Astronautical Research 1971, D. Reidel Publishing Co., Dordrecht, Holland, 1973, pp. 63-80.

4. Thomson, W.T., "Spin Stabilization of Attitude Against Gravity Torque," J. Astronautical Sciences 9, 31-33 (1962) and "Letter to the Editor" from T.R. Kane, et. al., J. Astronautical Sciences 9, 108-109 (1962).

5. Kane, T.R., and Shippy, D.J., "Attitude Stability of a Spinning Unsymmetrical Satellite in a Circular Orbit," J. Astronautical Sciences 10, 114-119 (1963).

6. Edwards, T.L. and Kaplan, M.H., "Automatic Spacecraft Detumbling by Internal Mass Motion," AIAA Journal, Vol. 12, No. 4, 1974, pp. 496-502.

7. Bainum, Peter M., and Sellappan, R., "Optimal Control of Spin Stabilized Spacecraft with Telescoping Appendages," Symposium on Dynamics and Control of Non-Rigid Space Vehicles, European Space Agency, Frascati, Italy, 24-26, May 1976; also in Journal of the Astronautical Sciences, Vol. XXIV, No. 4, October-December 1976, pp. 329-346.

8. Likins, P.W., "Attitude Stability of Space Vehicles," University of California, Los Angeles, Short Course, April 4-15, 1966.

9. IBM 1130 Scientific Subroutine Package Programmer's Manual, IBM Technical Publications Department, White Plains, N.Y.; pp. 92-94.

10. Hughes, P.C., "Dynamics of a Spin-Stabilized Satellite During Extension of Rigid Booms," CASI Trans. Vol. 5, No. 1, March 1972, pp. 11-14.

11. Halfman, R.L., Dynamics Vol. 1 - Particles, Rigid Bodies and Systems, Addison-Wesley Publishing Co., 1962, Chapter 4, pp. 130-134, p. 159.

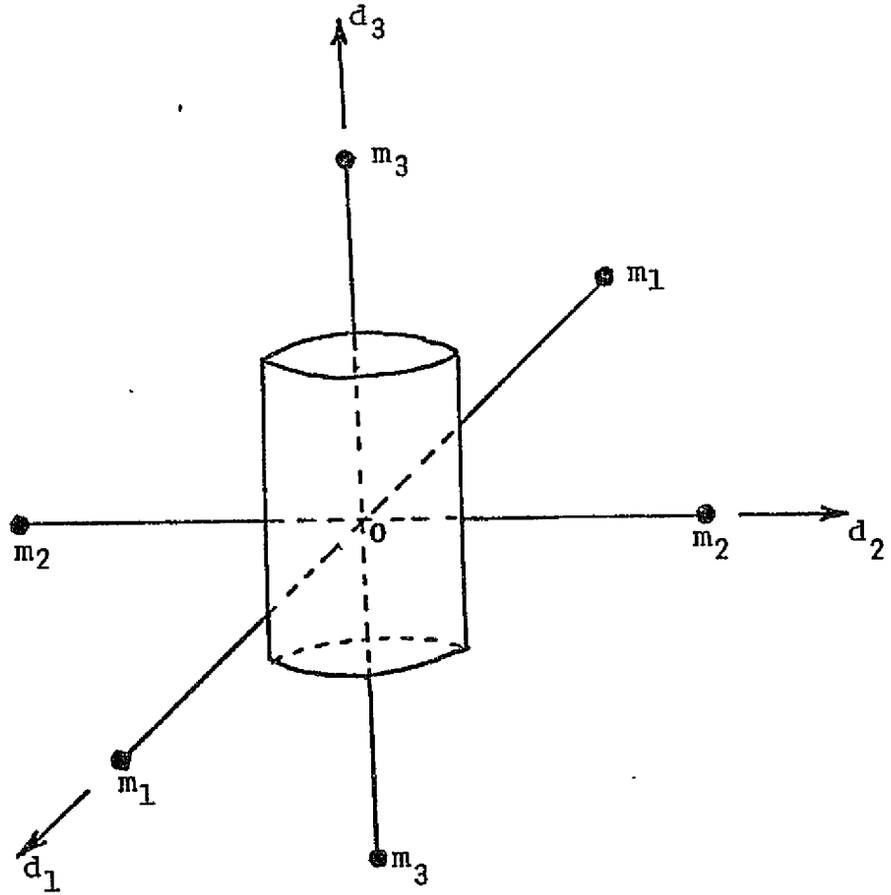

FIG. 1. SYSTEM GEOMETRY FOR SYMMETRIC DEPLOYMENT

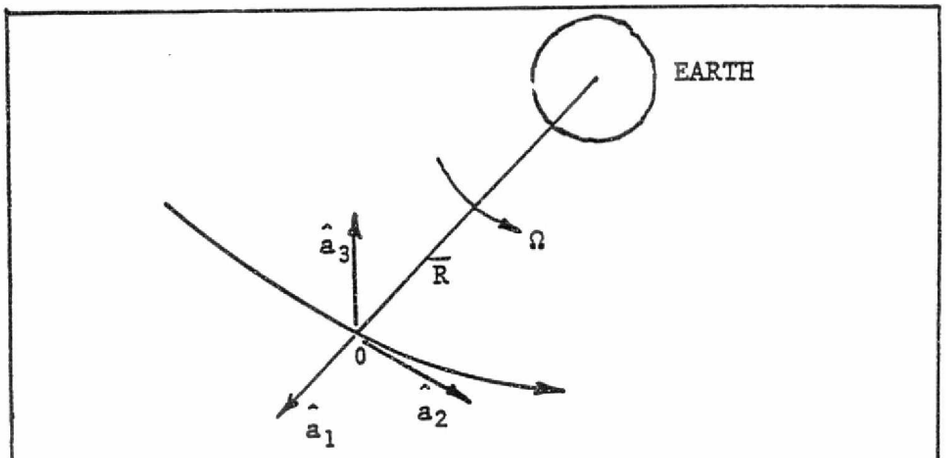

FIG. 2. ORBITING REFERENCE FRAME

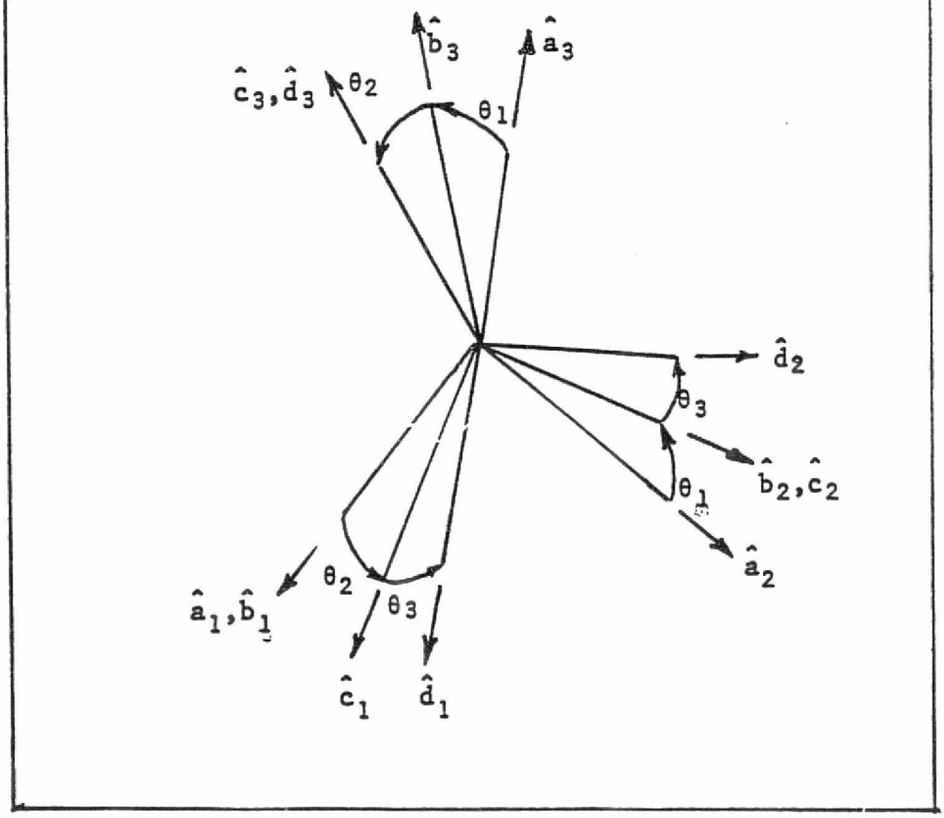

FIG. 3. COORDINATE SYSTEM

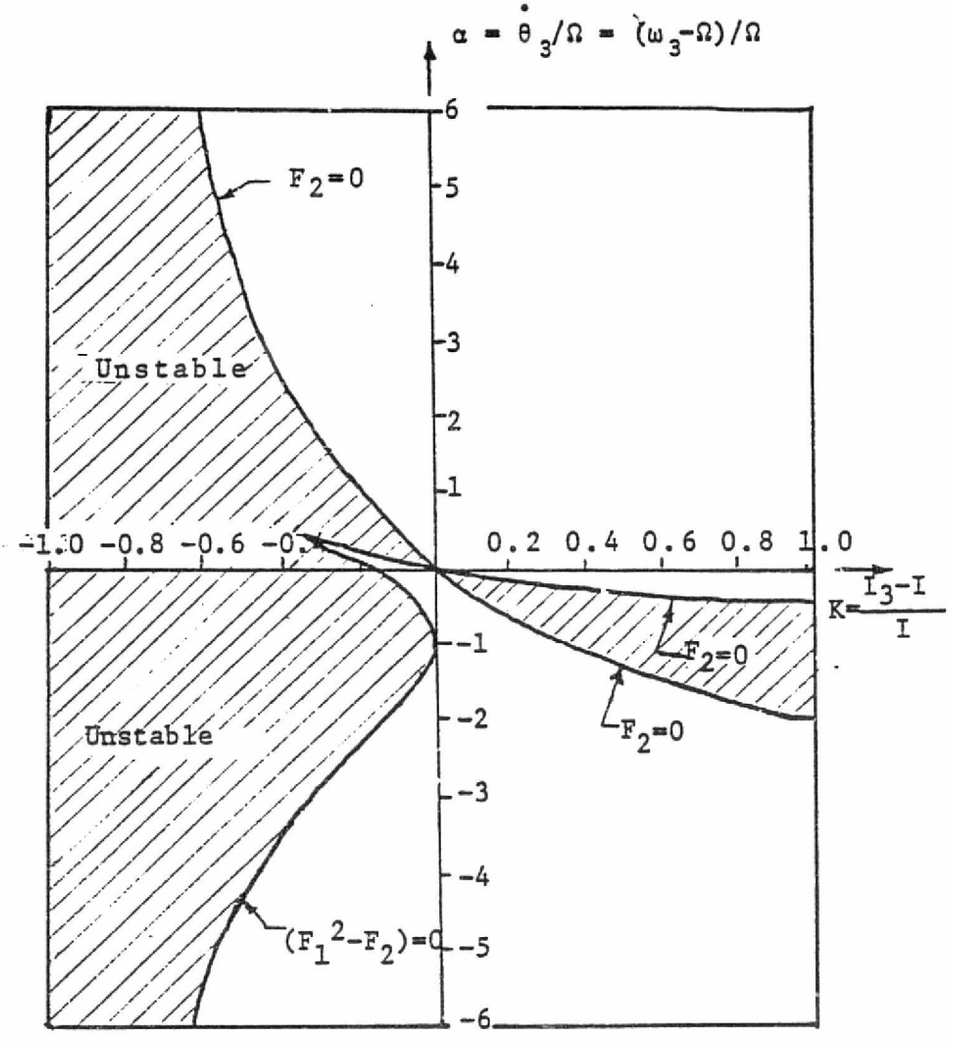

FIG. 4. STABILITY CHART FOR SYMMETRICAL BODIES

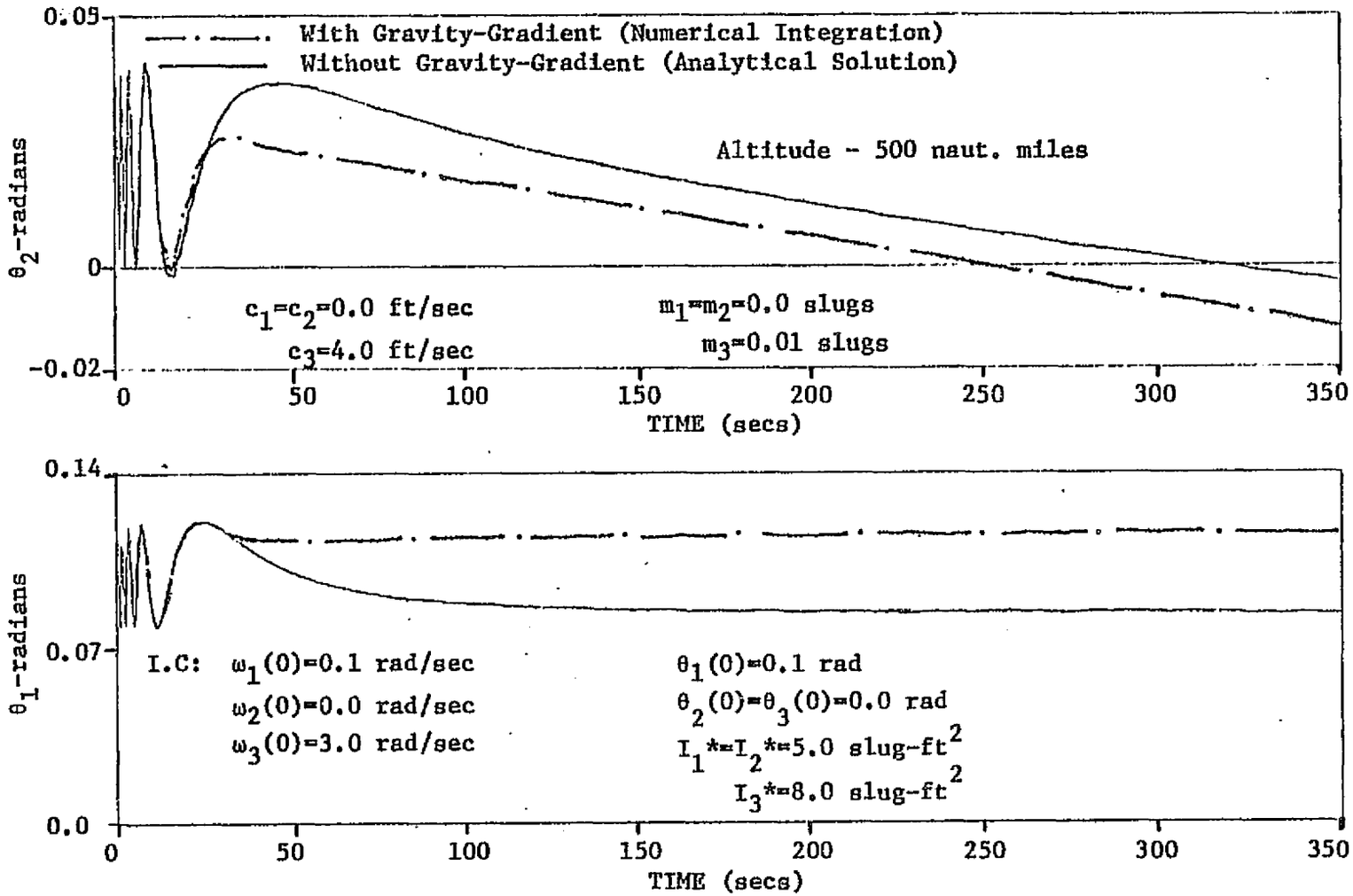

FIG. 5.a. COMPARISON OF RESPONSE OF OUT OF PLANE EULER ANGLES

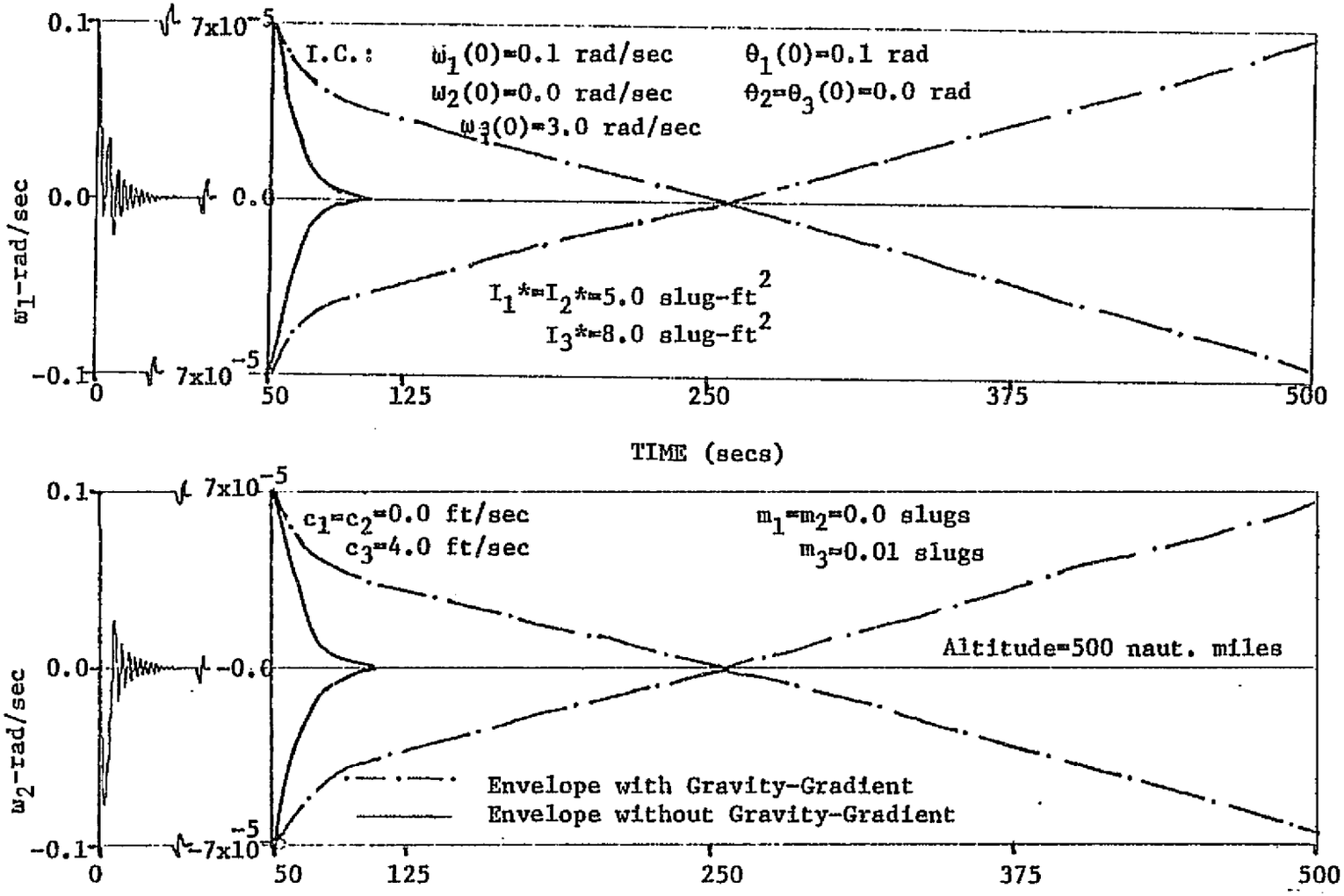

FIG. 5.b. RESPONSE OF TRANSVERSE COMPONENTS OF ANGULAR VELOCITY
EXTENSION ALONG '3' AXIS ONLY. $\alpha=2.9\times10^{3}$, K(0)=0.6

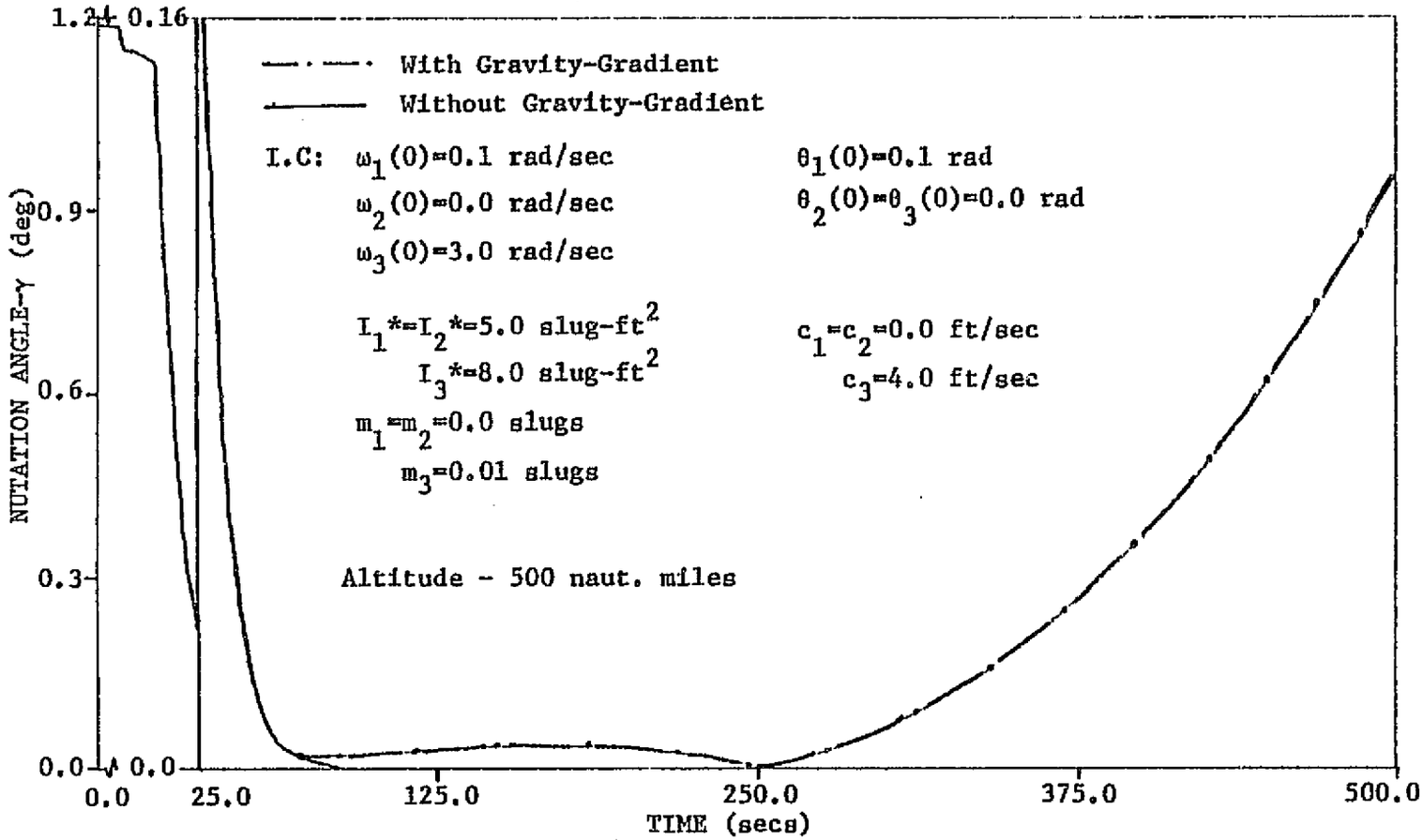

FIG. 5.c. RESPONSE OF NUTATION ANGLE, EXTENSION, ALONG '3' AXIS ONLY
$\alpha=2.9\times10^{-3}$, K(0)=0.6

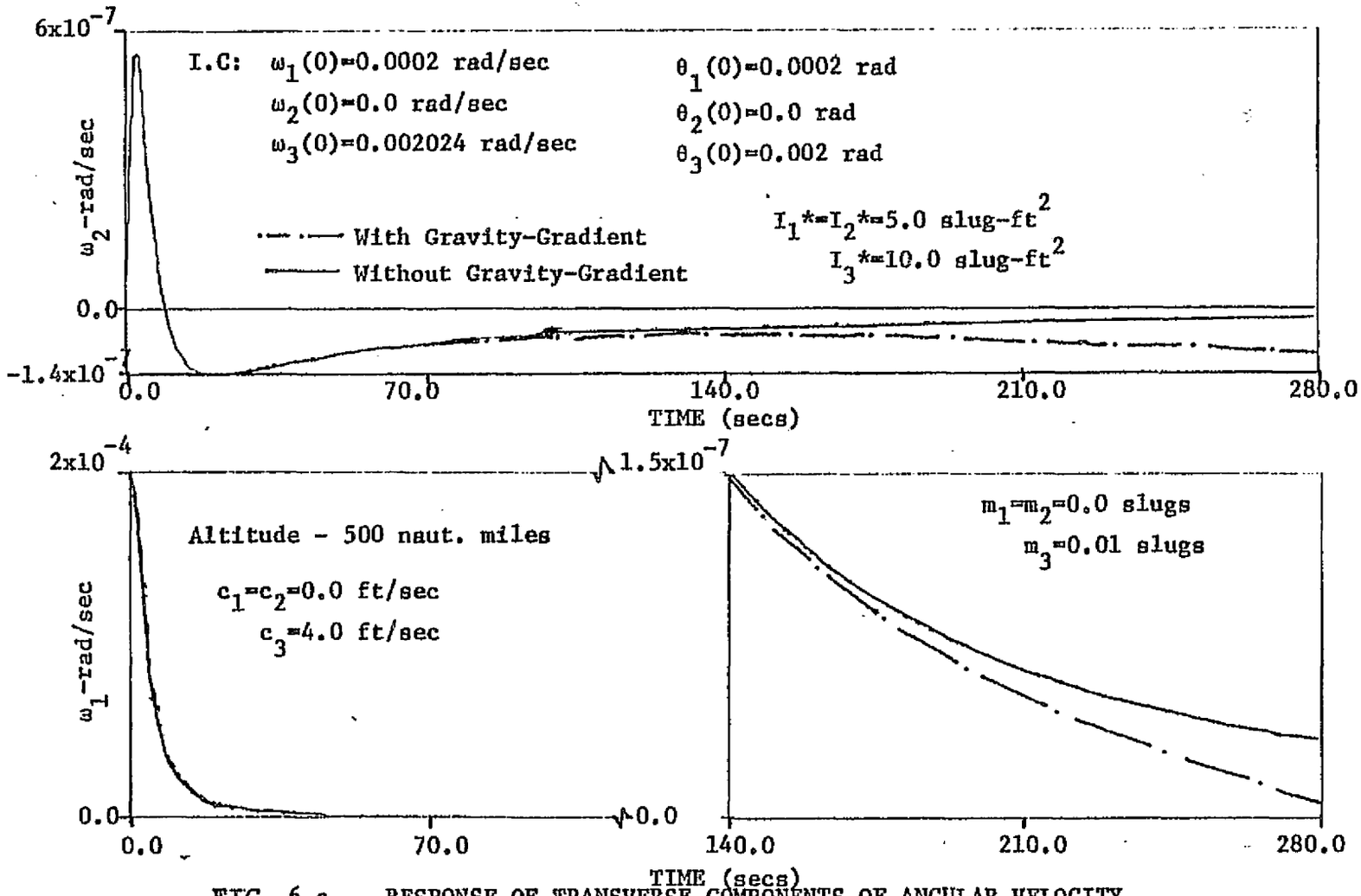

FIG. 6.a. RESPONSE OF TRANSVERSE COMPONENTS OF ANGULAR VELOCITY
EXTENSION ALONG '3' AXIS ONLY . α=1.0, K(0)=1.0

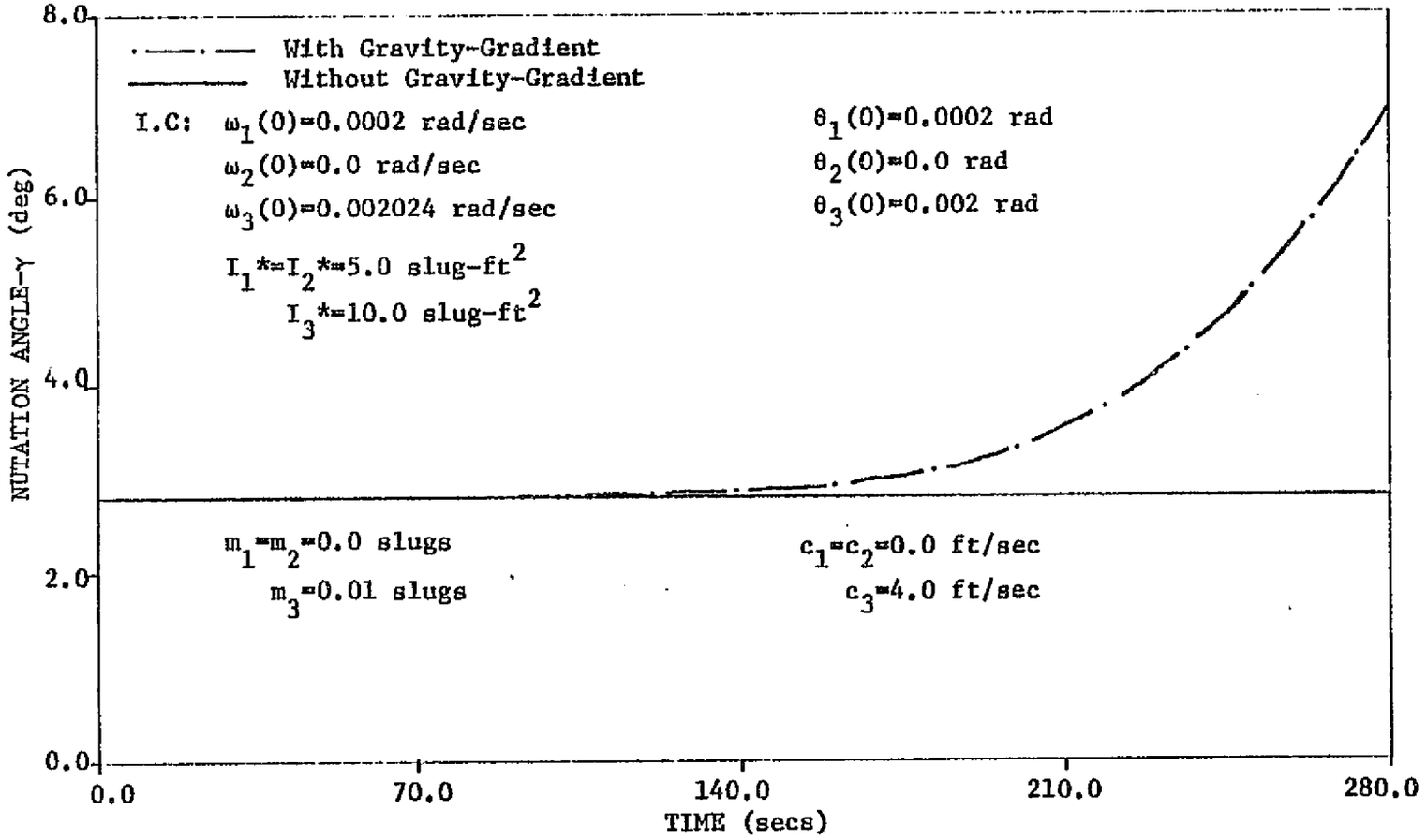

FIG. 6.b. RESPONSE OF NUTATION ANGLE, EXTENSION ALONG '3' AXIS ONLY
α=1.0, K(0)=1.0

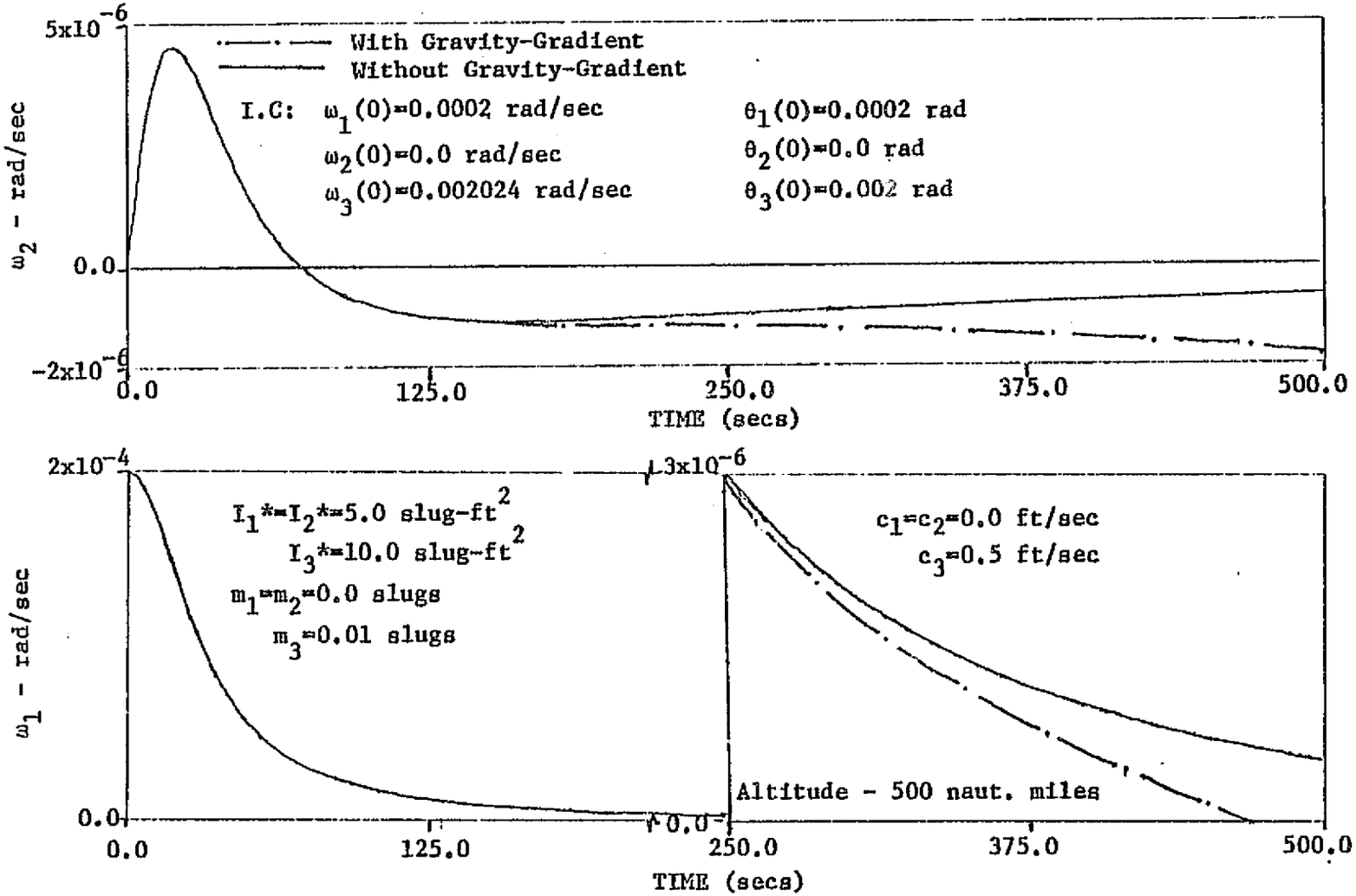

FIG. 7.a. RESPONSE OF TRANSVERSE COMPONENTS OF ANGULAR VELOCITY
EXTENSION ALONG '3' AXIS ONLY, α=1.0, K(0)=1.0

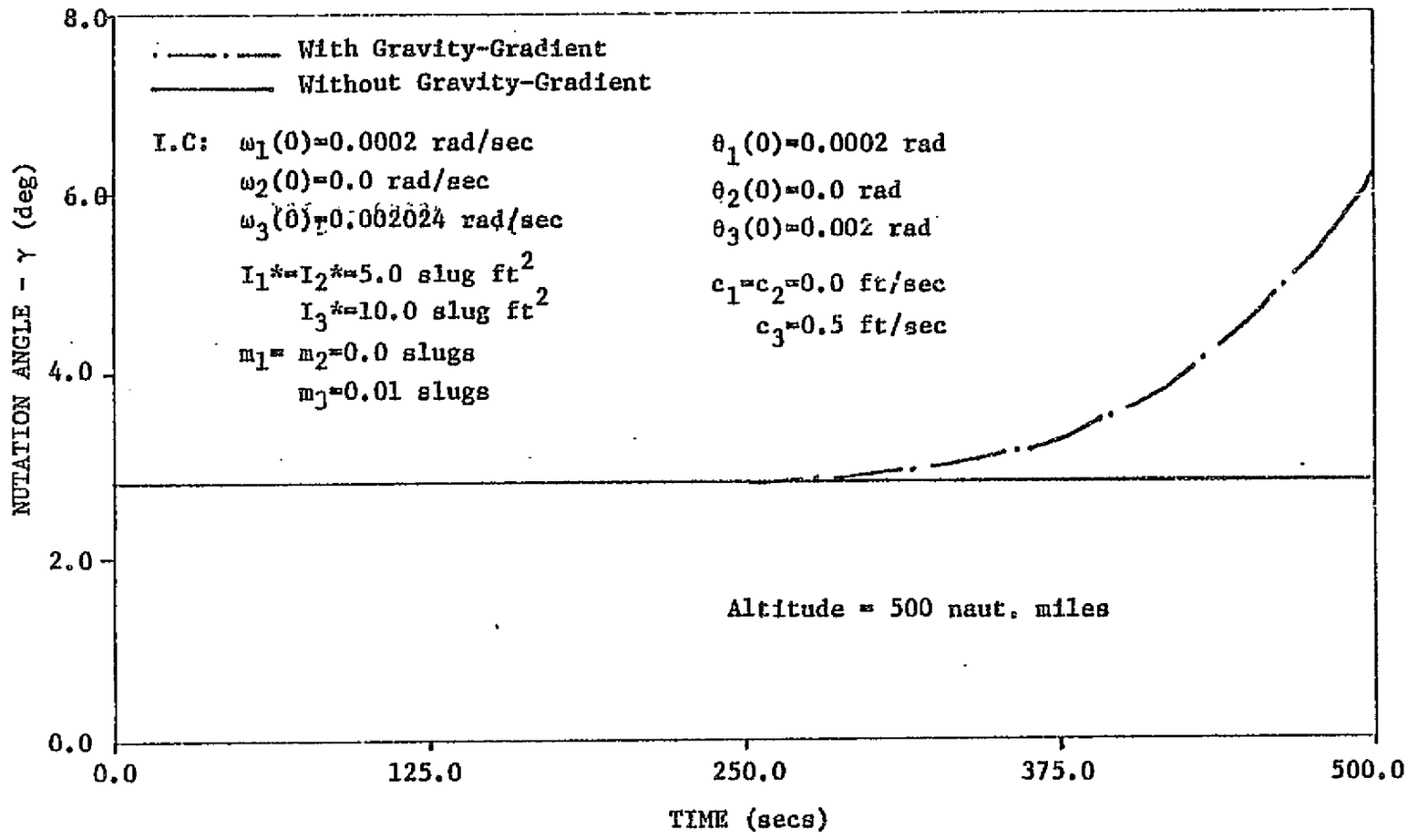

FIG. 7.b. RESPONSE OF NUTATION ANGLE, EXTENSION ALONG '3' AXIS ONLY
$\alpha = 1.0$ $K(0) = 1.0$

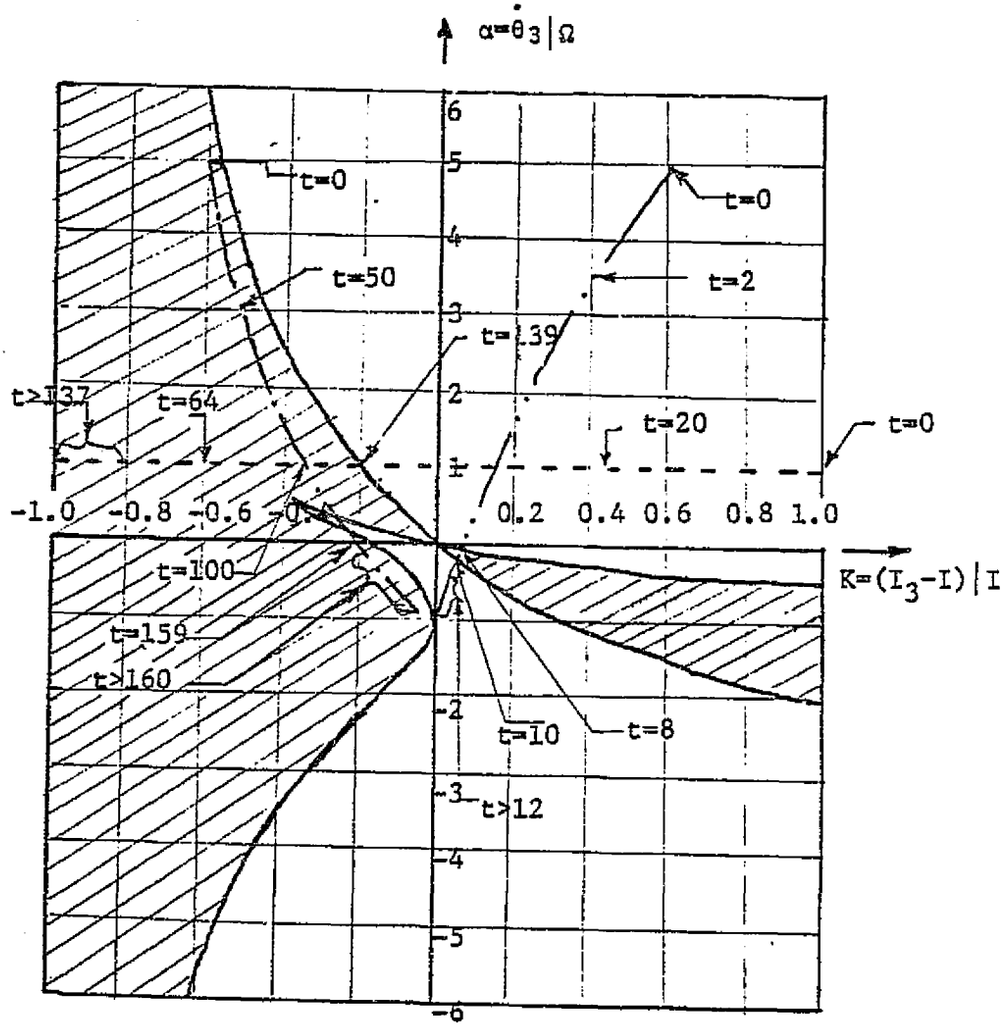

- - - - - EXTENSION ONLY ALONG '3' AXIS (FIG. 7)

·—·· —— EXTENSION ALL THREE AXES BEGINNING IN STABLE REG. (FIG. 11)

·—·—·—·EXTENSION ALL THREE AXES BEGINNING IN UNSTABLE REG. (FIG. 12)

FIG. 8. TIME HISTORIES OF DEPLOYMENT CASES ON THE STABILITY CHART

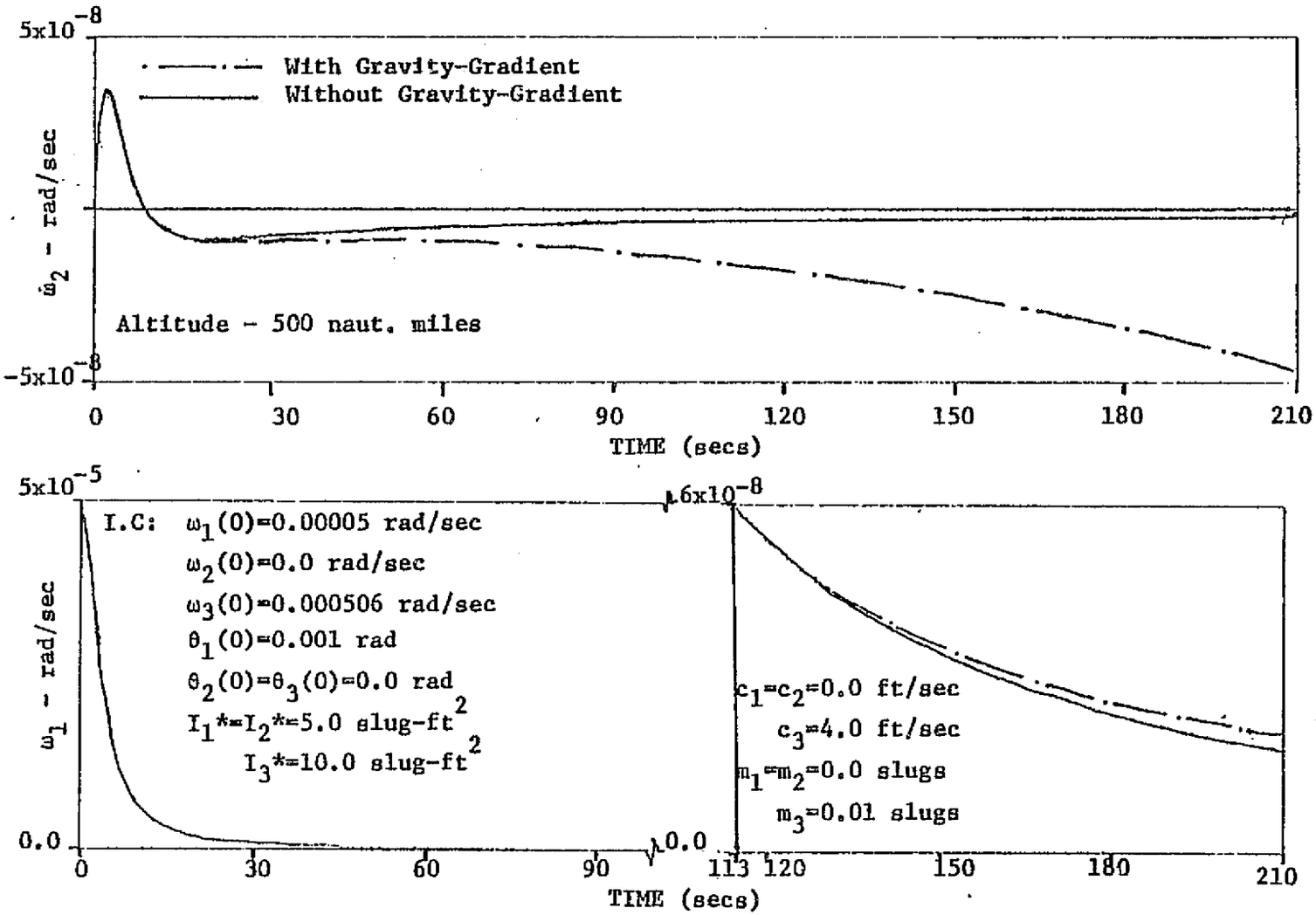

FIG. 9.a. RESPONSE OF TRANSVERSE COMPONENTS OF ANGULAR VELOCITY
EXTENSION ALONG '3' AXIS ONLY, $\alpha=-0.5$, $K(0)=1.0$

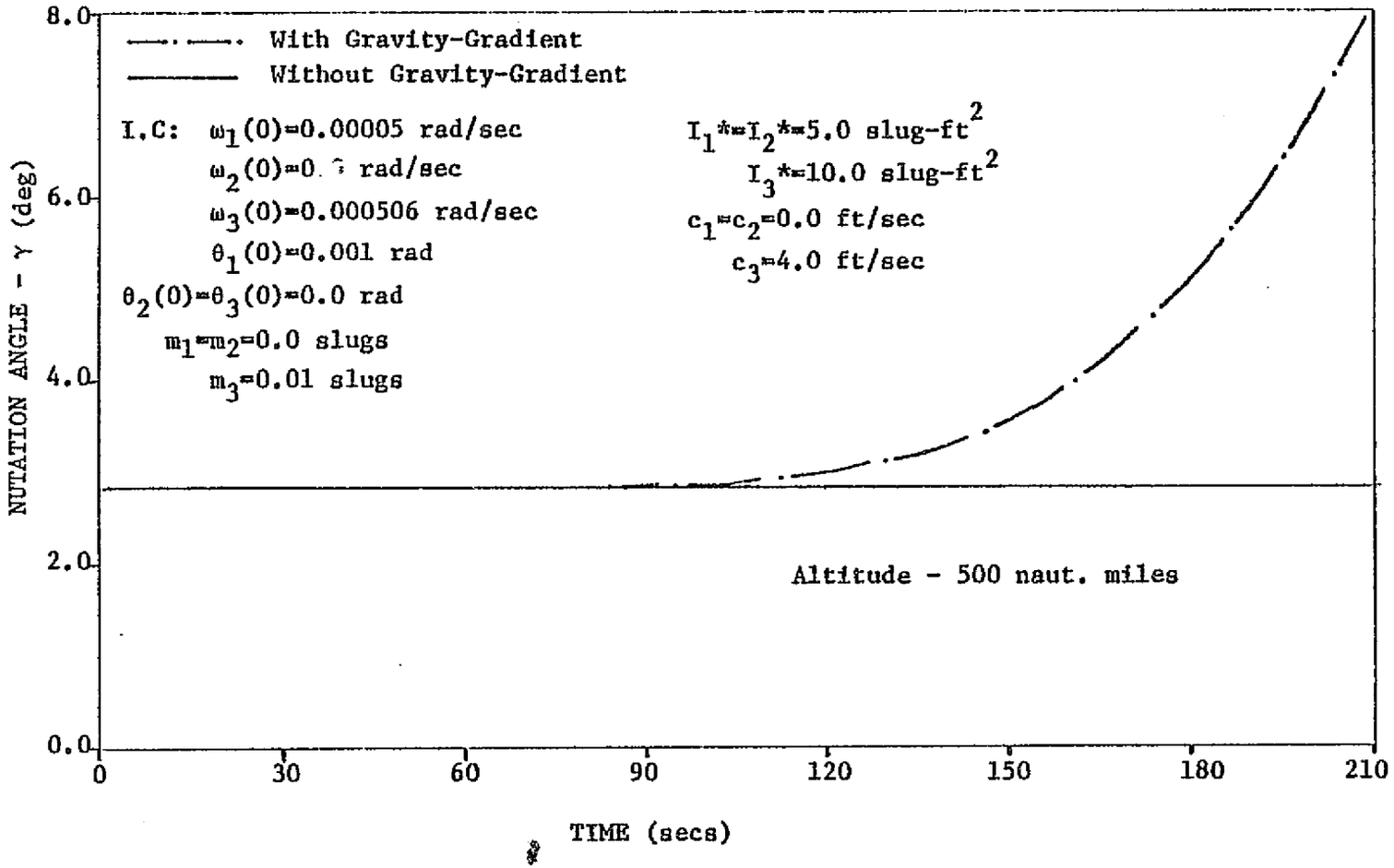

FIG. 9.b. RESPONSE OF NUTATION ANGLE, EXTENSION ALONG '3' AXIS ONLY
$\alpha=-0.5$, $K(0)=1.0$

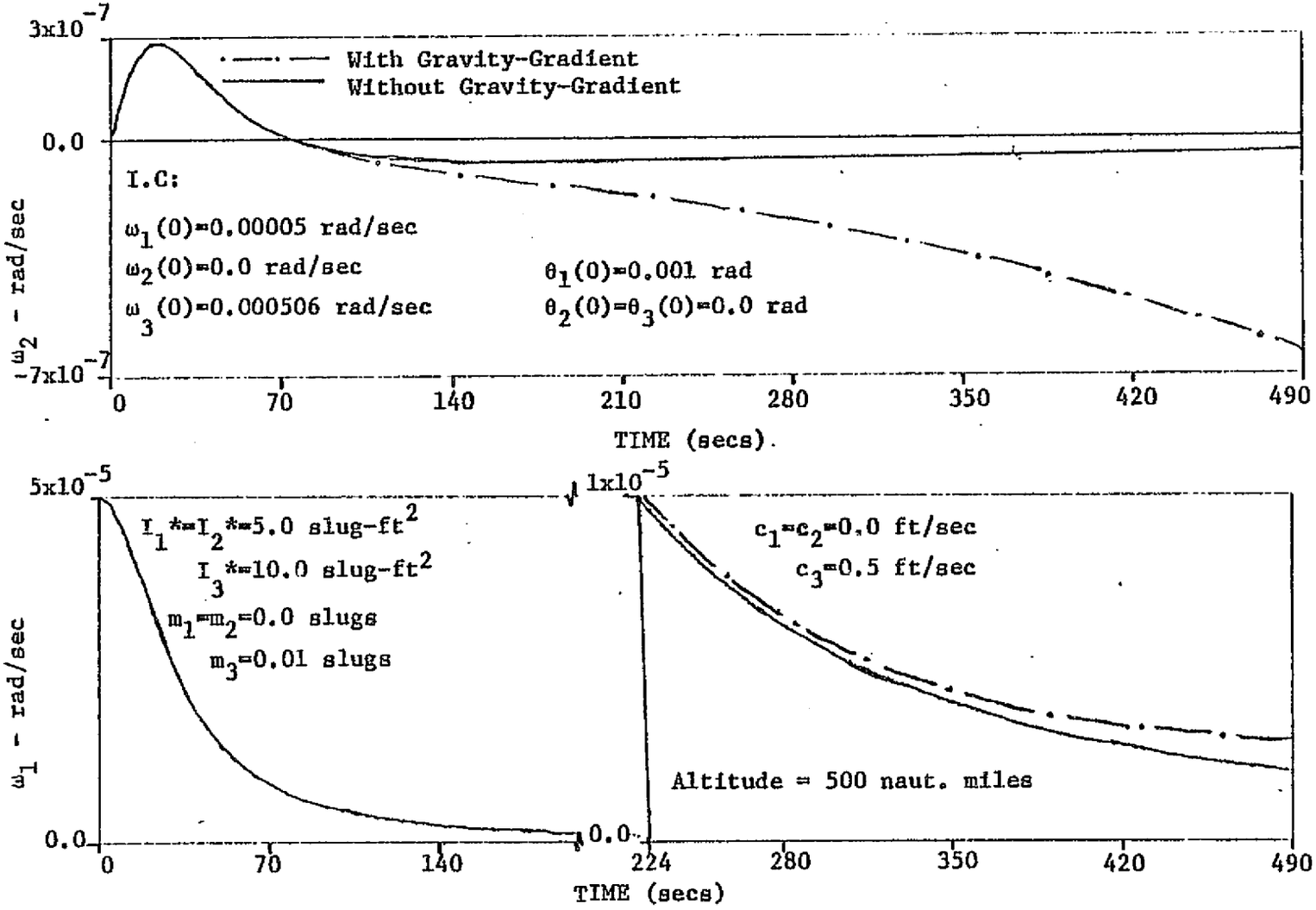

FIG. 10.a. RESPONSE OF TRANSVERSE COMPONENTS OF ANGULAR VELOCITY
EXTENSION ALONG '3' AXIS ONLY, α=-0.5, K(0)=1.0

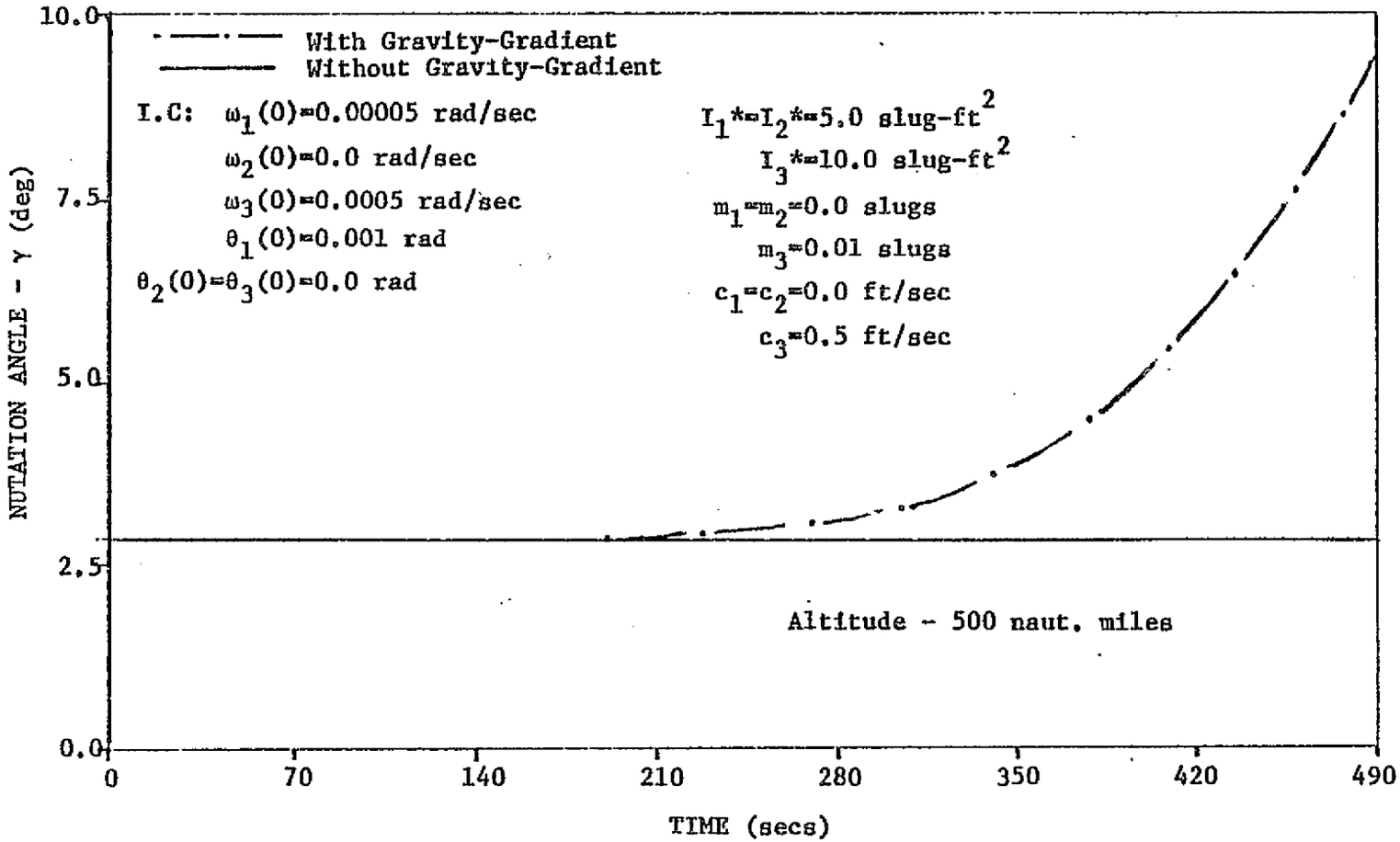

FIG. 10.b. RESPONSE OF NUTATION ANGLE, EXTENSION ALONG '3' AXIS ONLY
$\alpha=-0.5$, $K(0)=1.0$

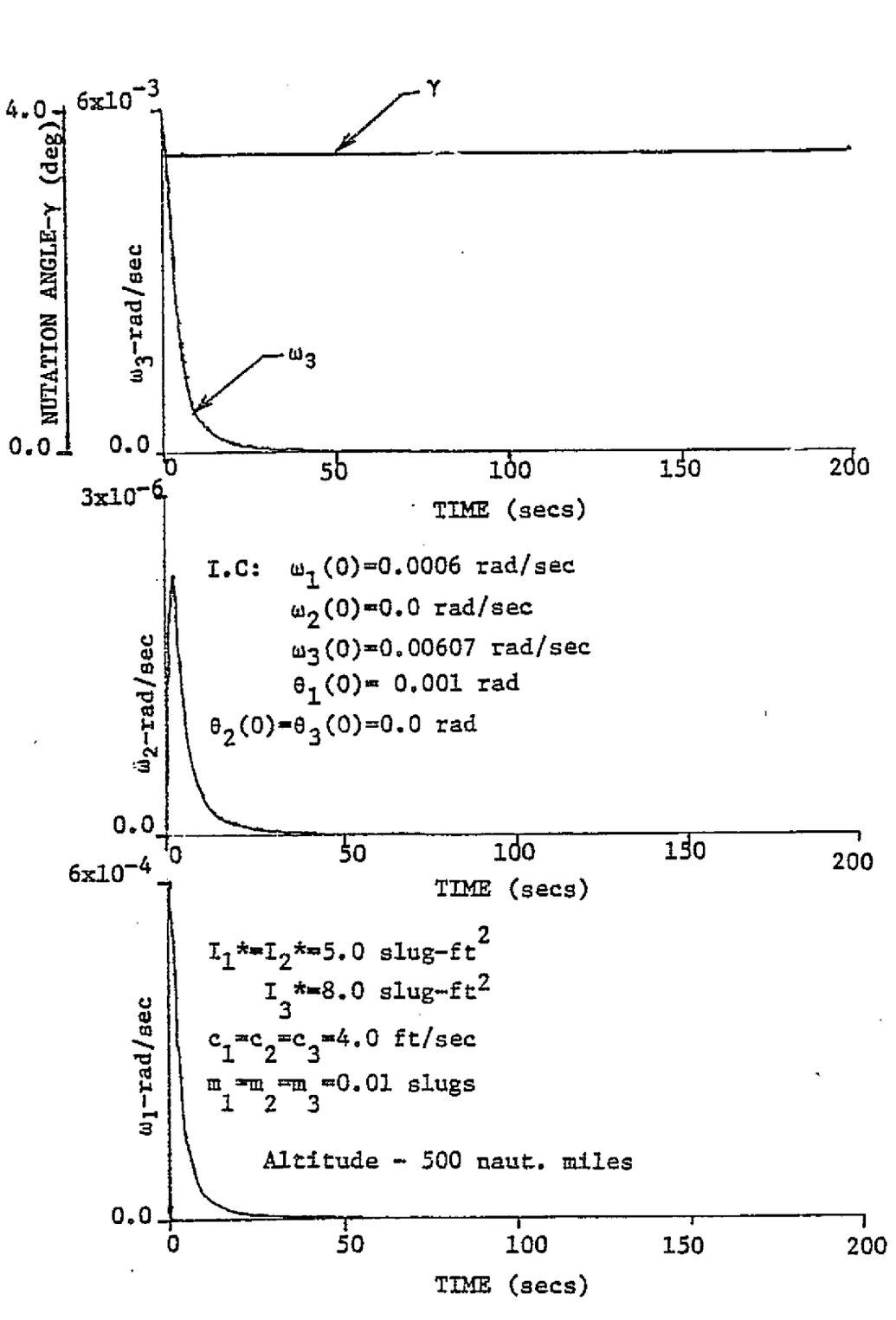

FIG. 11. RESPONSE OF COMPONENTS OF ANGULAR VELOCITY AND NUTATION ANGLE DURING EXTENSION MANEUVER ALONG ALL THREE AXES WITH GRAVITY-GRADIENT, $\alpha(0)=5.0$, $K(0)=0.6$

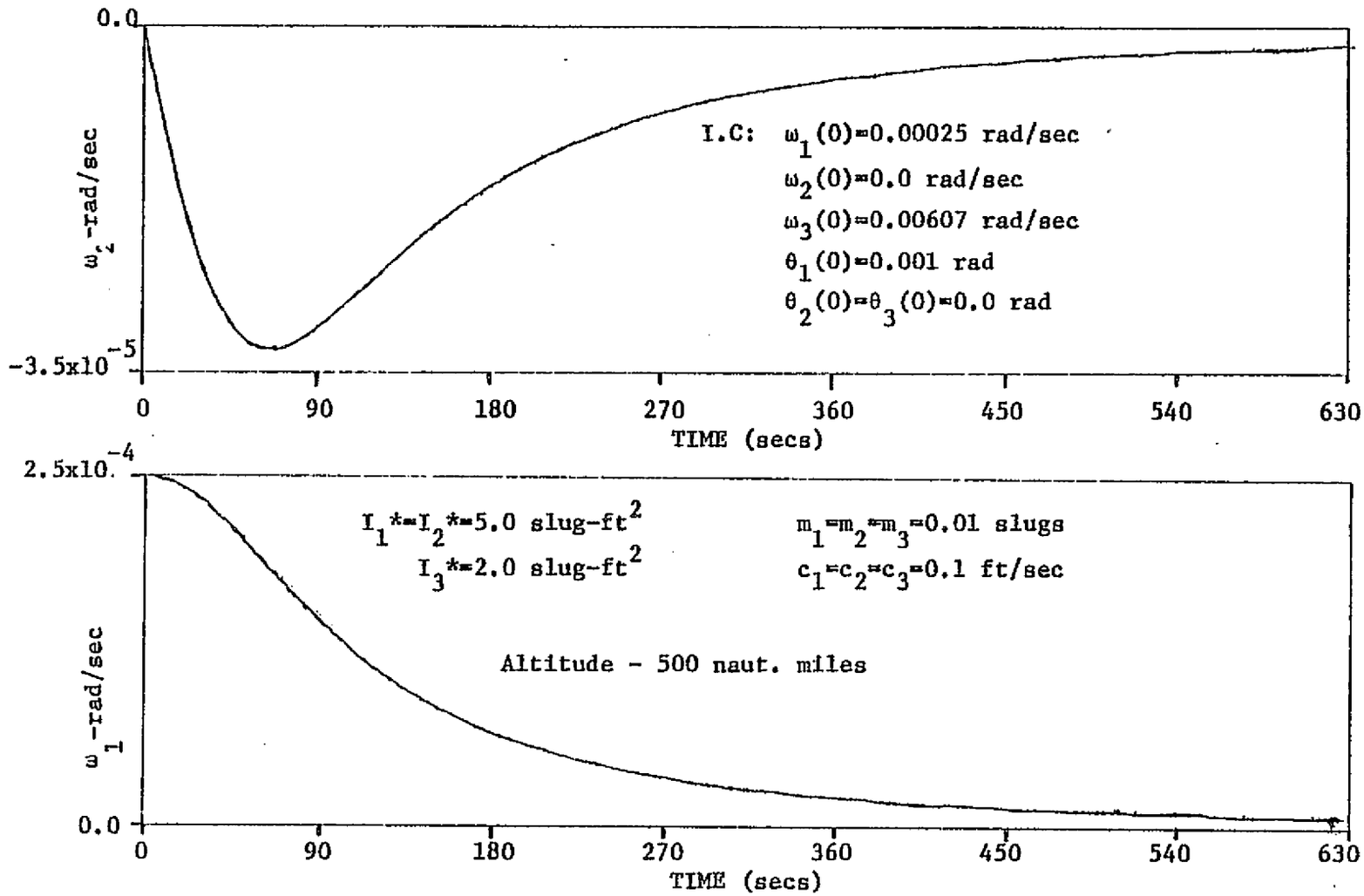

FIG. 12.a. RESPONSE OF TRANSVERSE COMPONENTS OF ANGULAR VELOCITY WITH GRAVITY-GRADIENT EXTENSION ALONG ALL THREE AXES, $\alpha(0)=5.0$, $K(0)=-0.6$

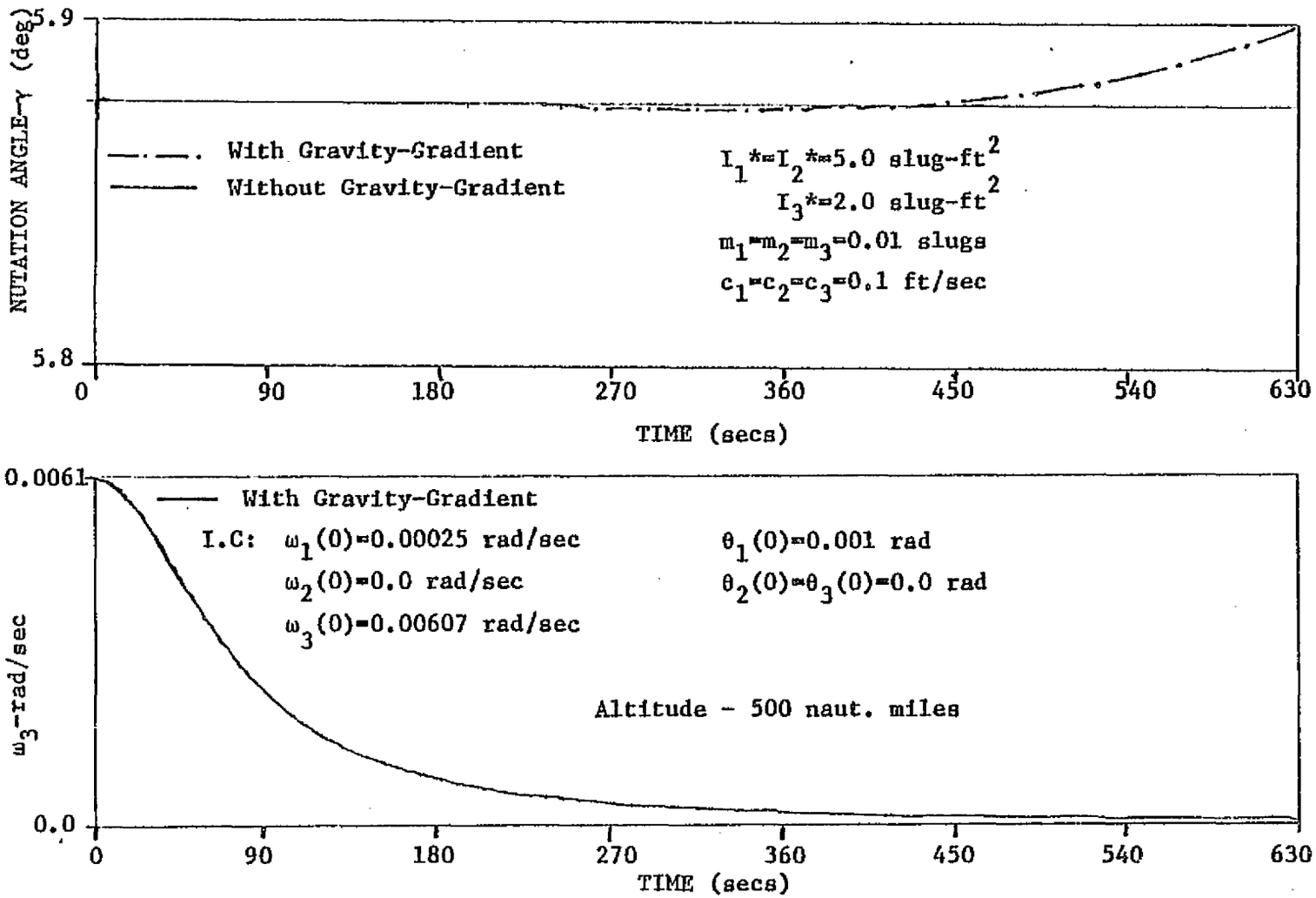

FIG. 12.b. RESPONSE OF SPIN AND NUTATION ANGLE, EXTENSION ALONG ALL THREE AXES
$\alpha(0)=5.0$ $K(0)=-0.6$

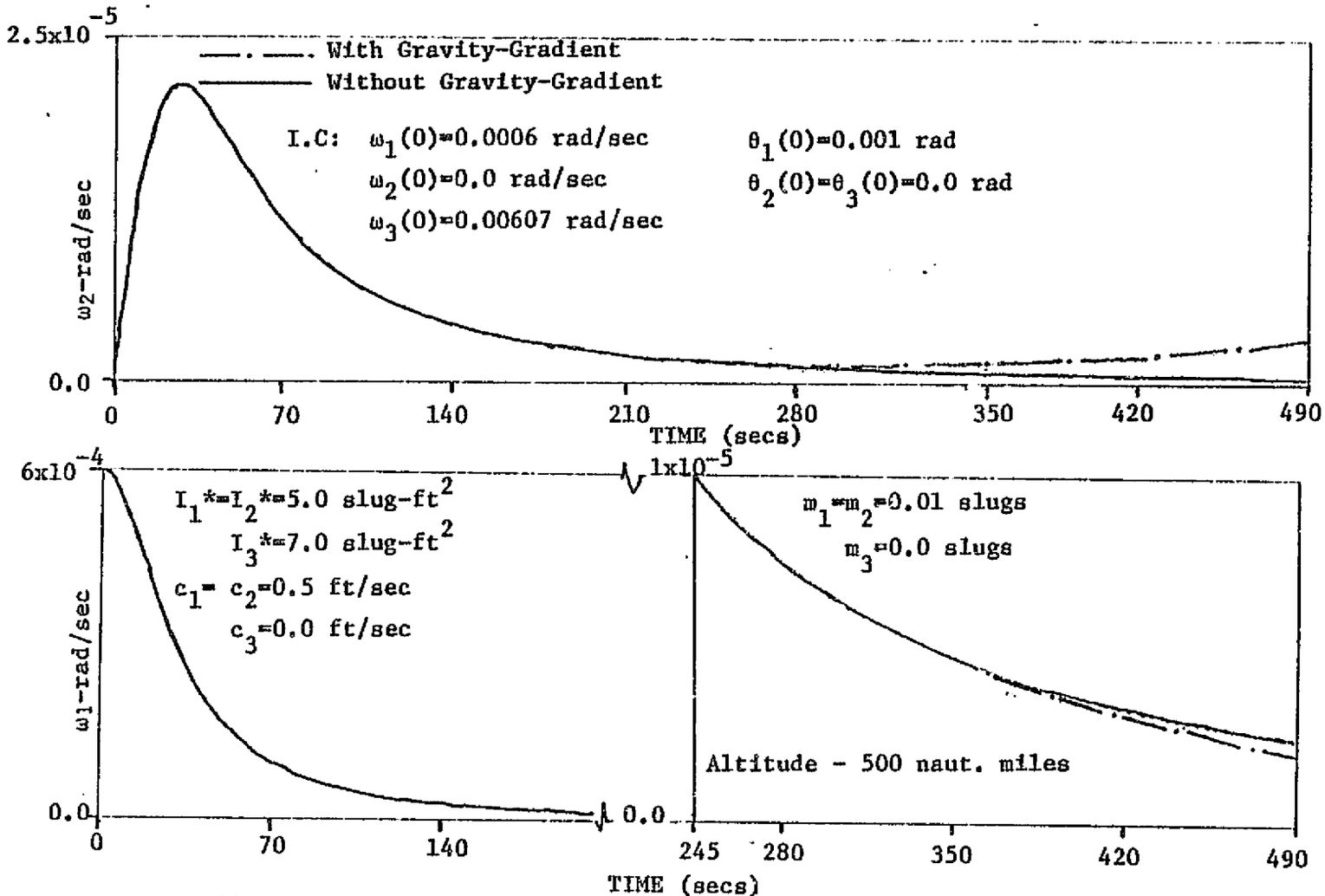

FIG. 13.a. RESPONSE OF TRANSVERSE COMPONENTS OF ANGULAR VELOCITY EXTENSION ALONG '1', '2' AXES ONLY. $\alpha(0)=5.0$, $K(0)=0.4$

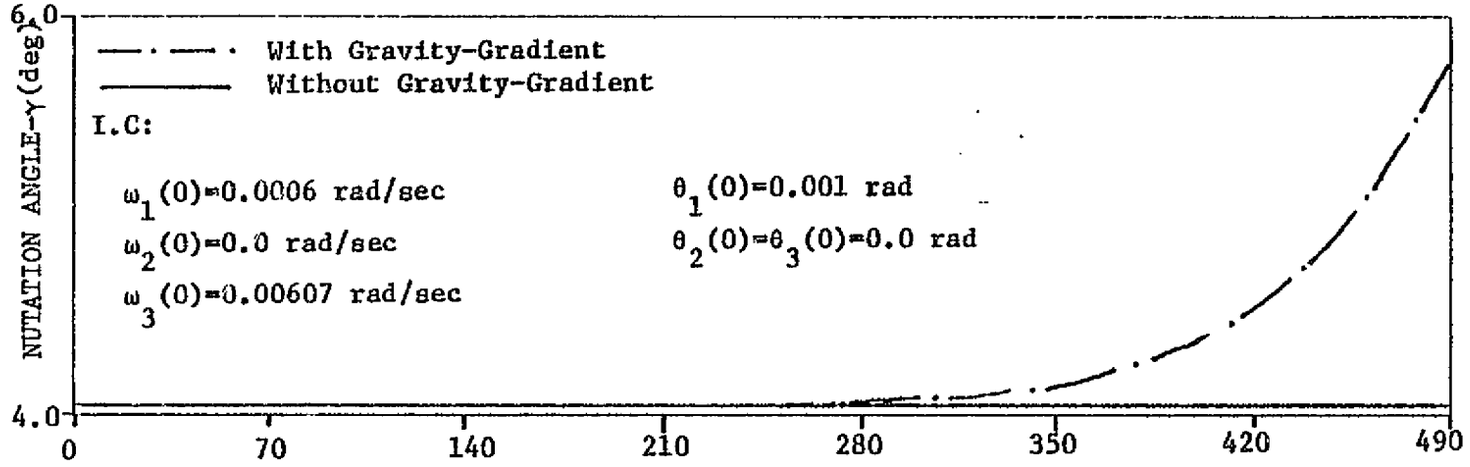

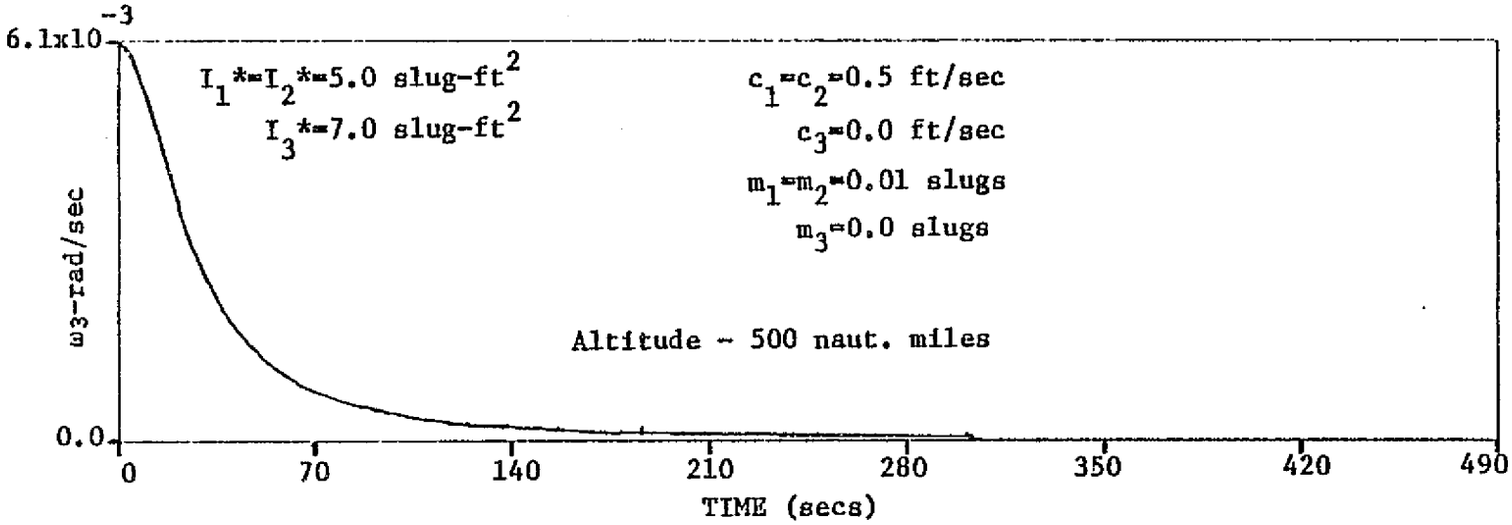

FIG. 13.b. RESPONSE OF SPIN AND NUTATION ANGLE, EXTENSION ALONG '1', '2' AXES ONLY. $\alpha(0)=5.0$ $K(0)=0.4$

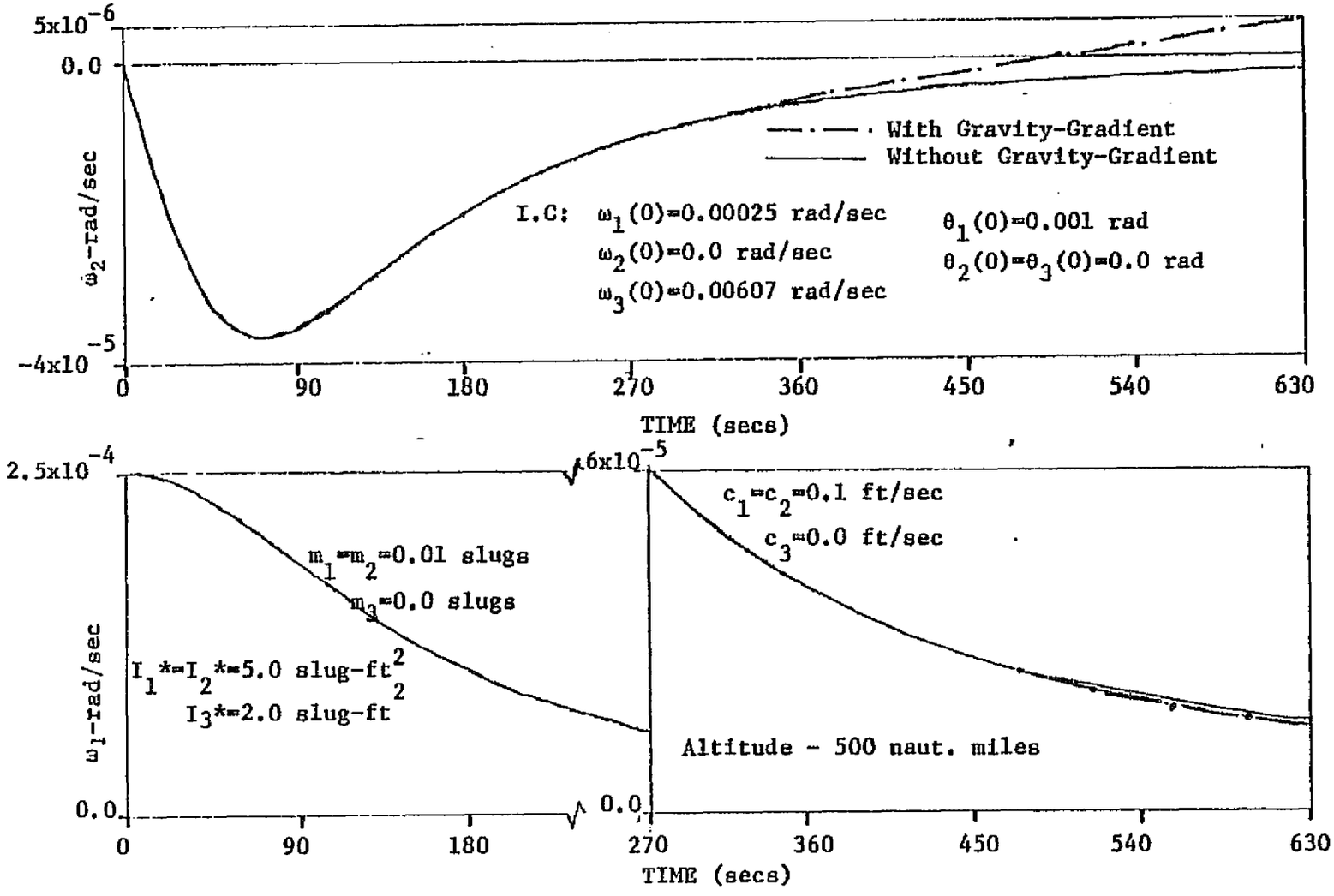

FIG. 14.a. RESPONSE OF TRANSVERSE COMPONENTS OF ANGULAR VELOCITY
EXTENSION ALONG '1', '2' AXES ONLY. $\alpha(0)=5.0$, $K(0)=-0.6$

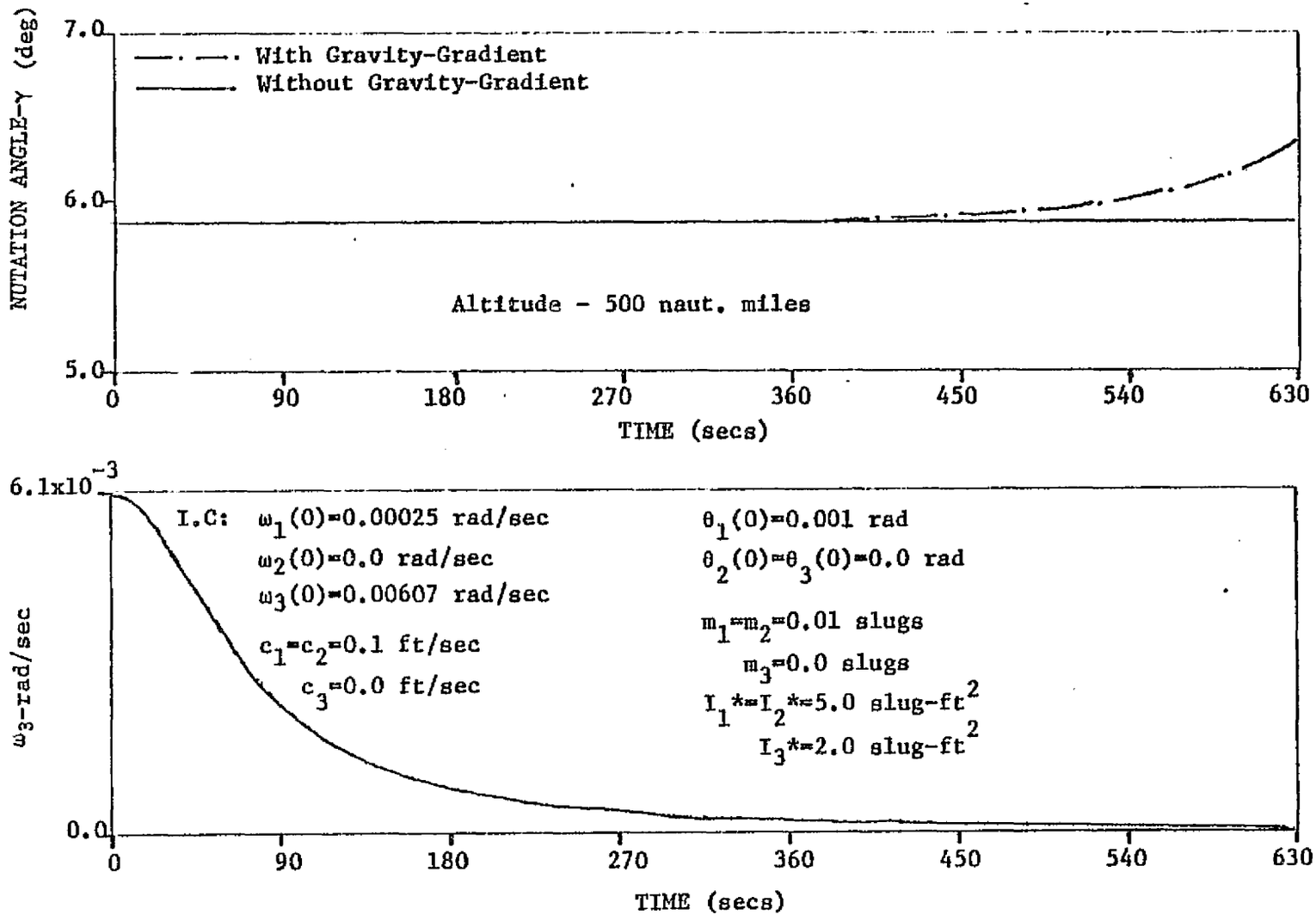

FIG. 14.b. RESPONSE OF SPIN AND NUTATION ANGLE, EXTENSION ALONG '1', '2' AXES ONLY. $\alpha(0)=5.0$, $K(0)=-0.6$

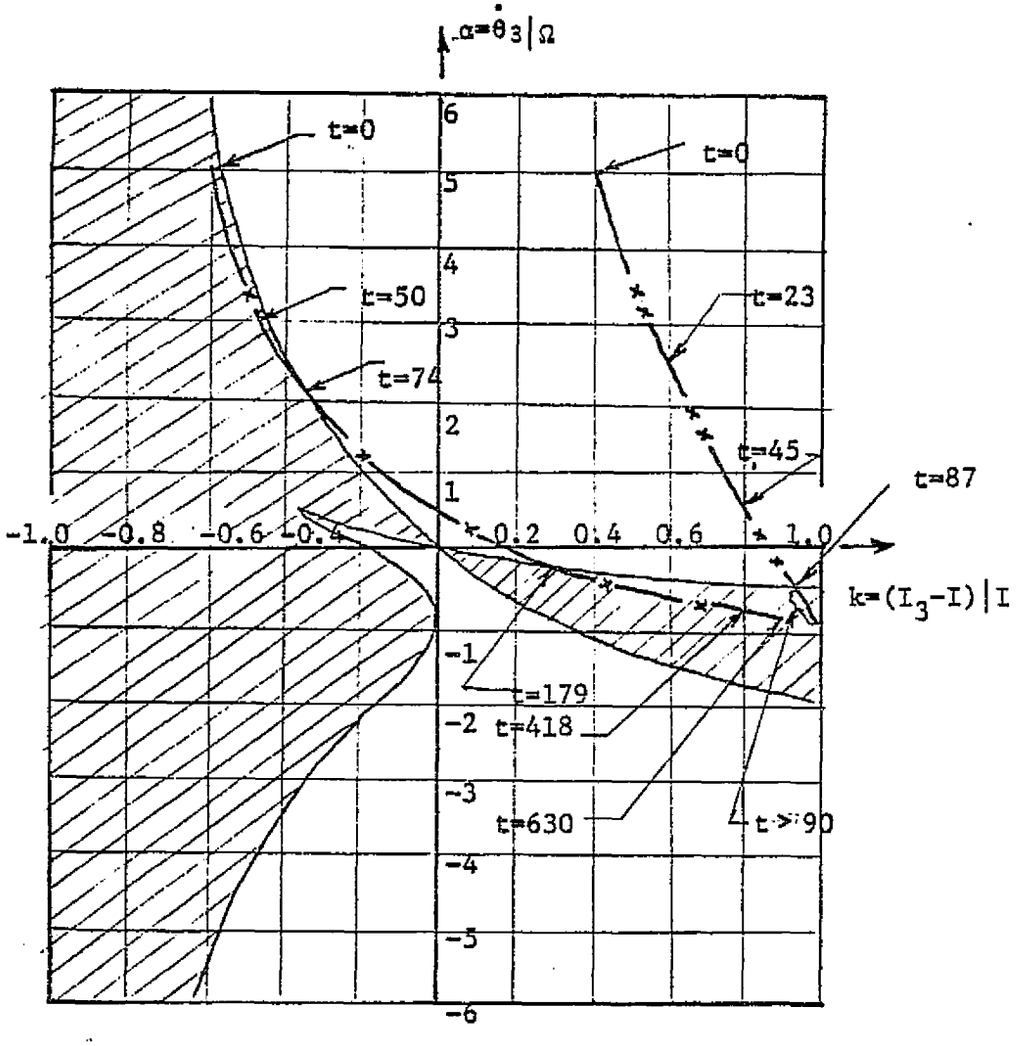

EXTENSION '1', '2' AXES BEGINNING IN STABLE. REG. (FIG 13)

EXTENSION '1', '2' AXES BEGINNING IN UNSTABLE. REG. (FIG. 14)

FIG. 15. TIME HISTORIES OF DEPLOYMENT CASES ON THE STABILITY CHART

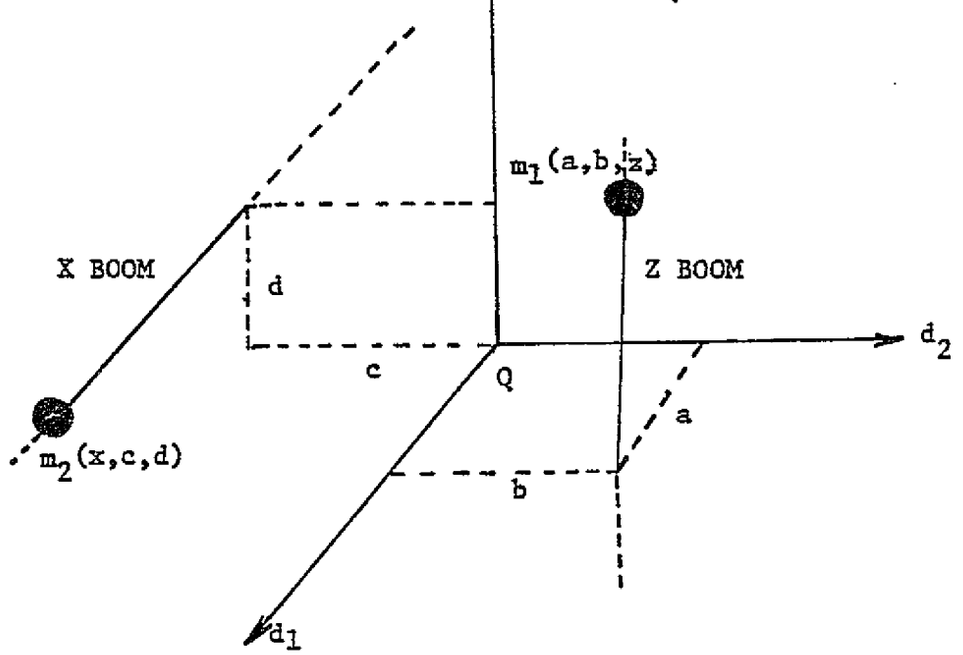

FIG. 16.a. TWO BOOM OFFSET ORIENTATION SYSTEM

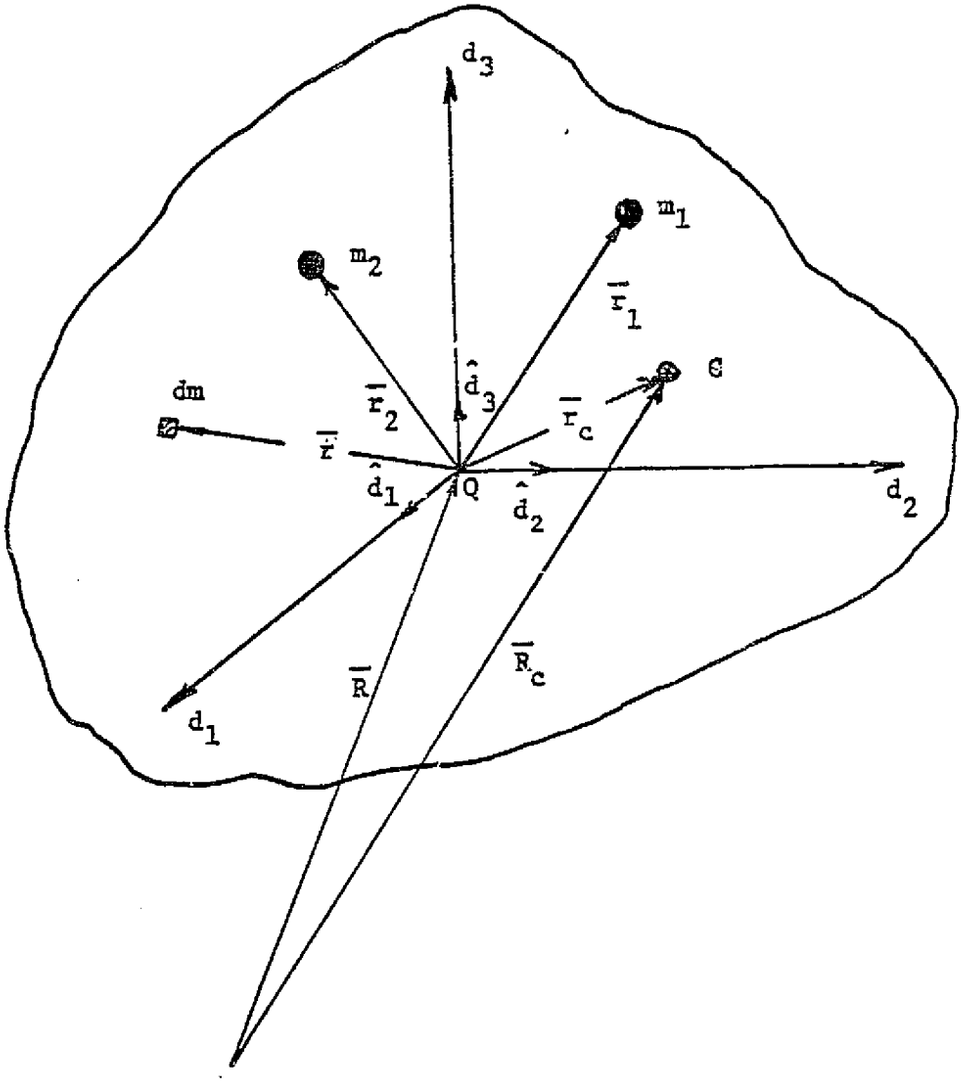

FIG. 16.b. GENERAL CASE OF TWO MASS OFFSET SYSTEM

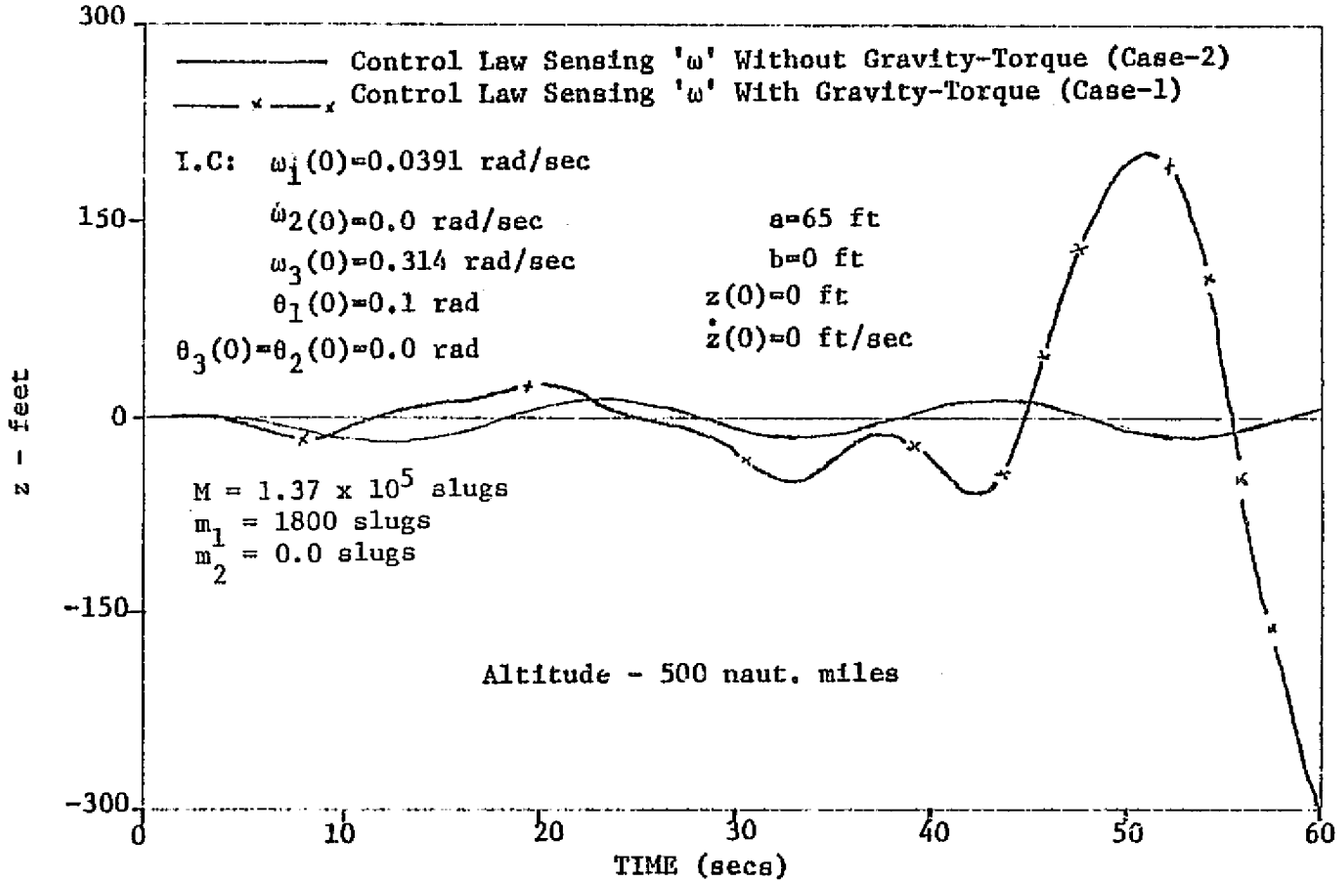

FIG. 17.a. DYNAMIC RESPONSE OF SYSTEM - Z BOOM MOTION

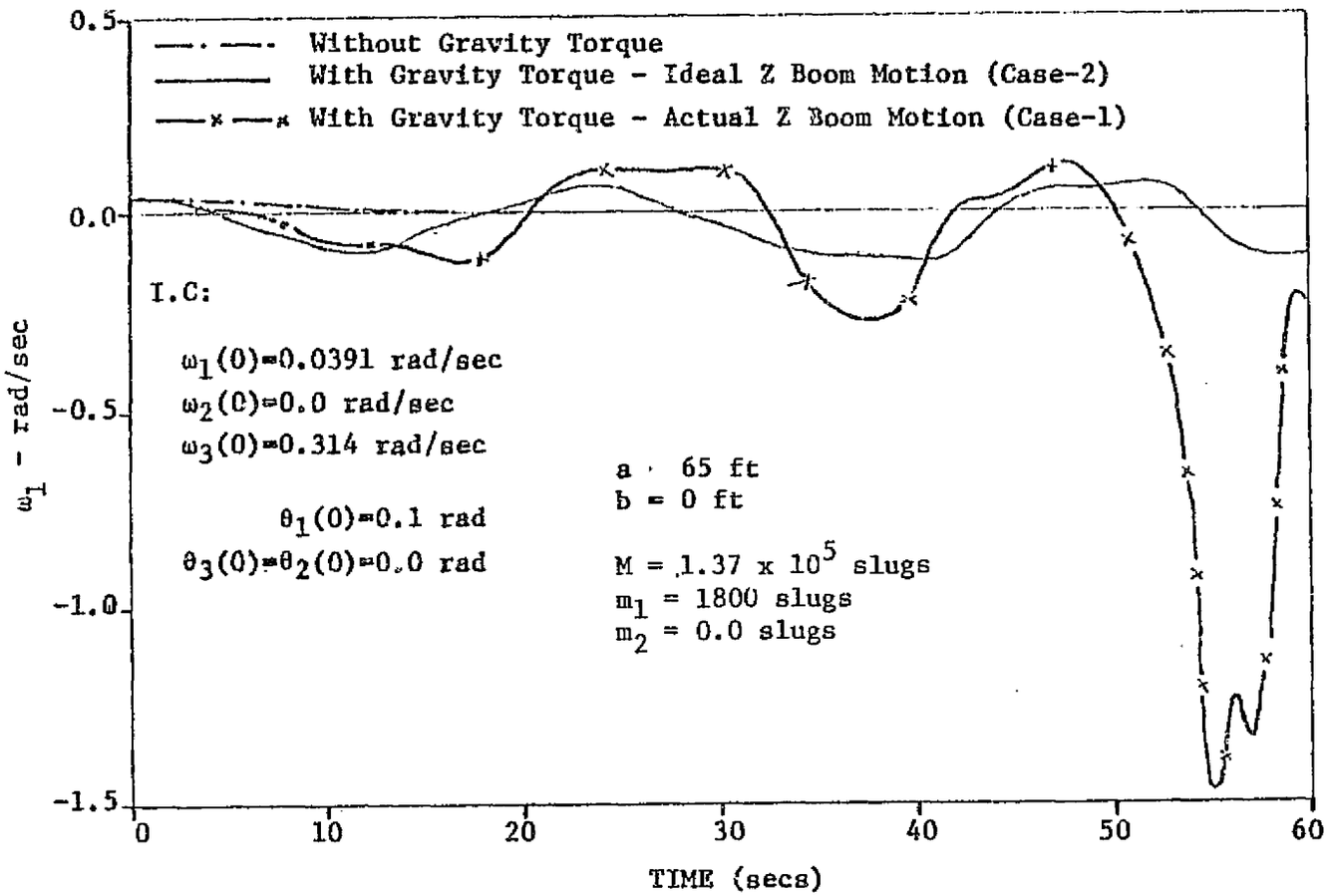

FIG. 17.b. DYNAMIC RESPONSE OF SYSTEM $-\omega_1$ COMPONENT

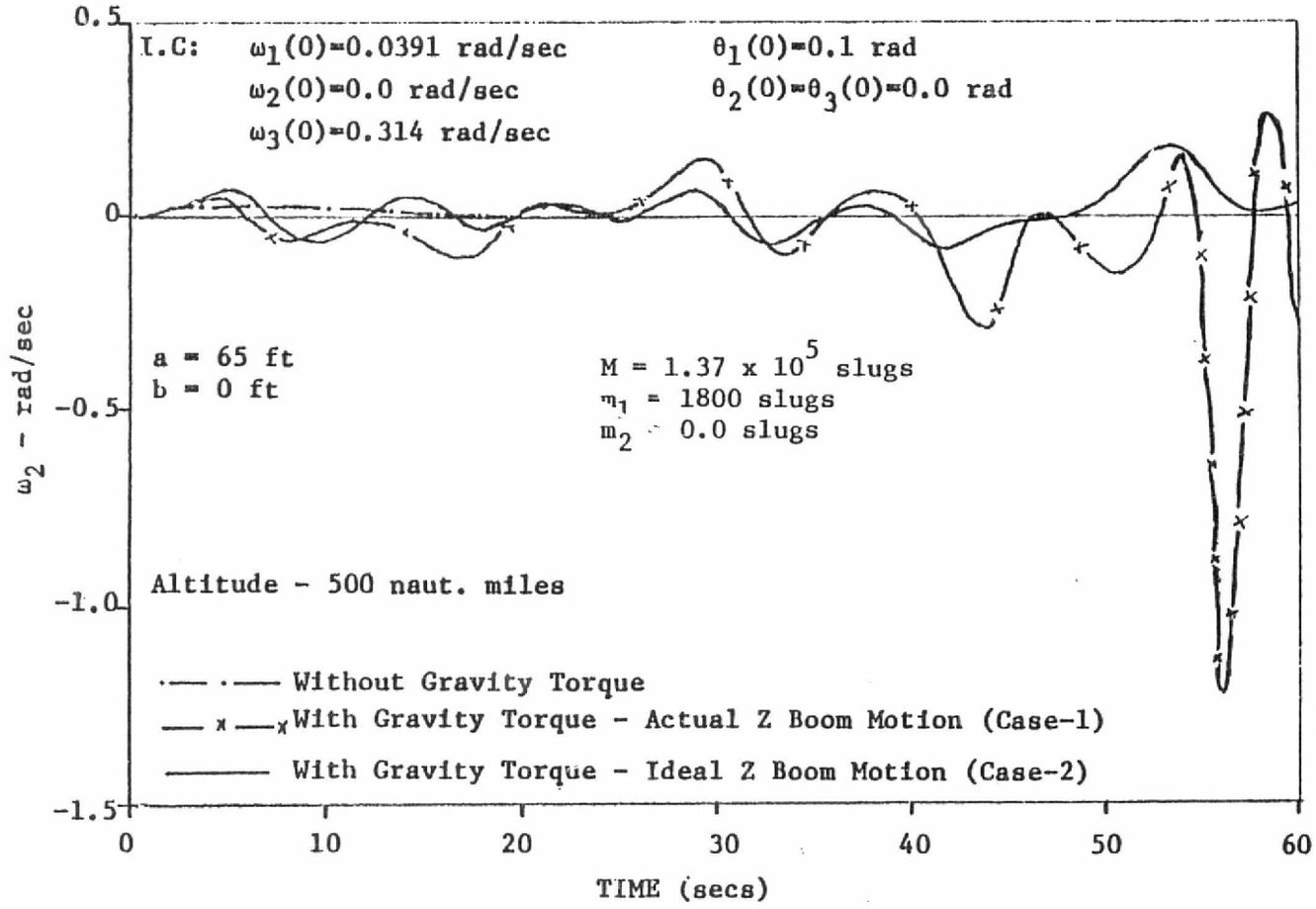

FIG. 17.c. DYNAMIC RESPONSE OF SYSTEM $-\omega_2$ COMPONENT

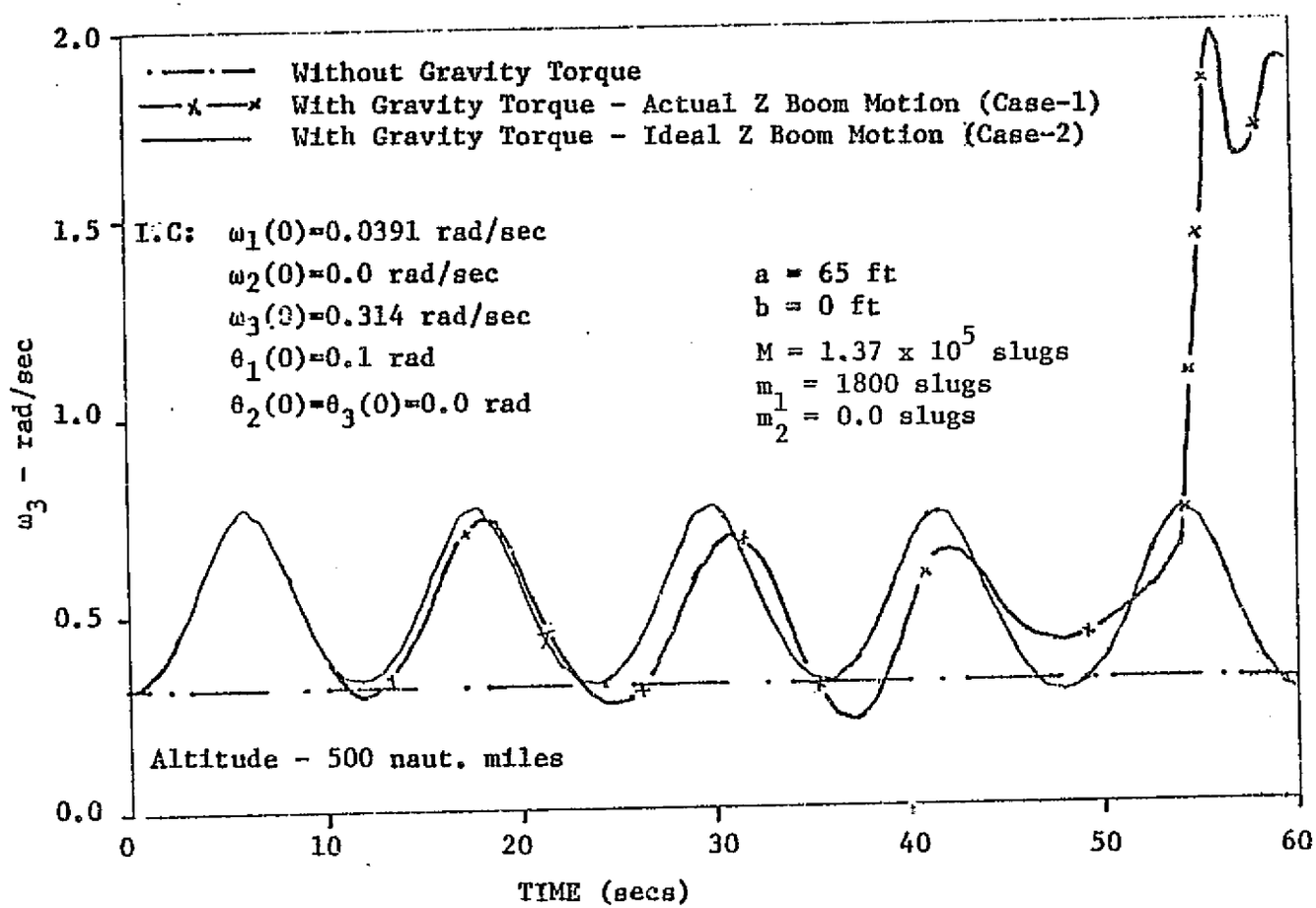

FIG. 17.d. DYNAMIC RESPONSE OF SYSTEM -ω_3 COMPONENT

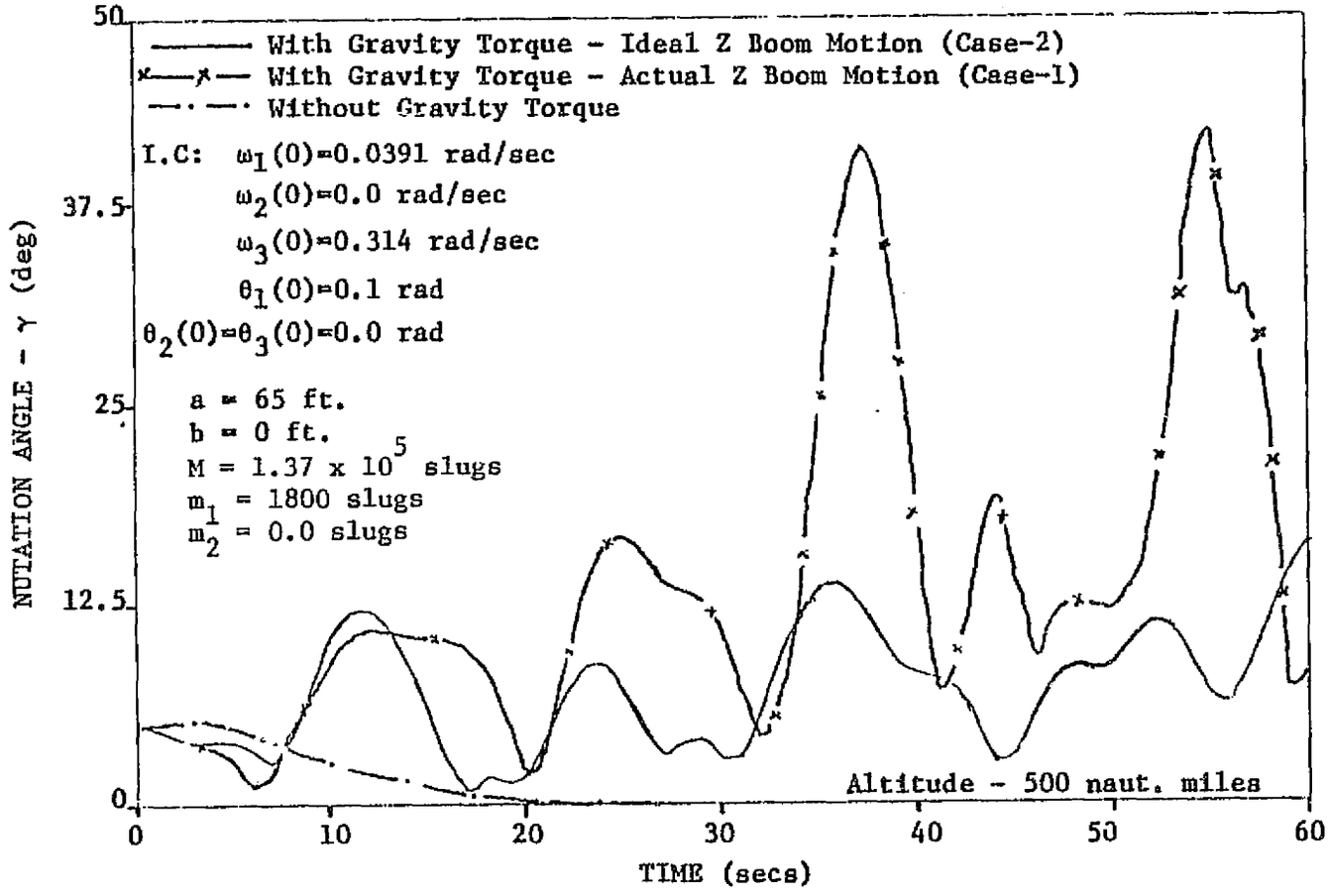

FIG. 17.e. DYNAMIC RESPONSE OF NUTATION ANGLE

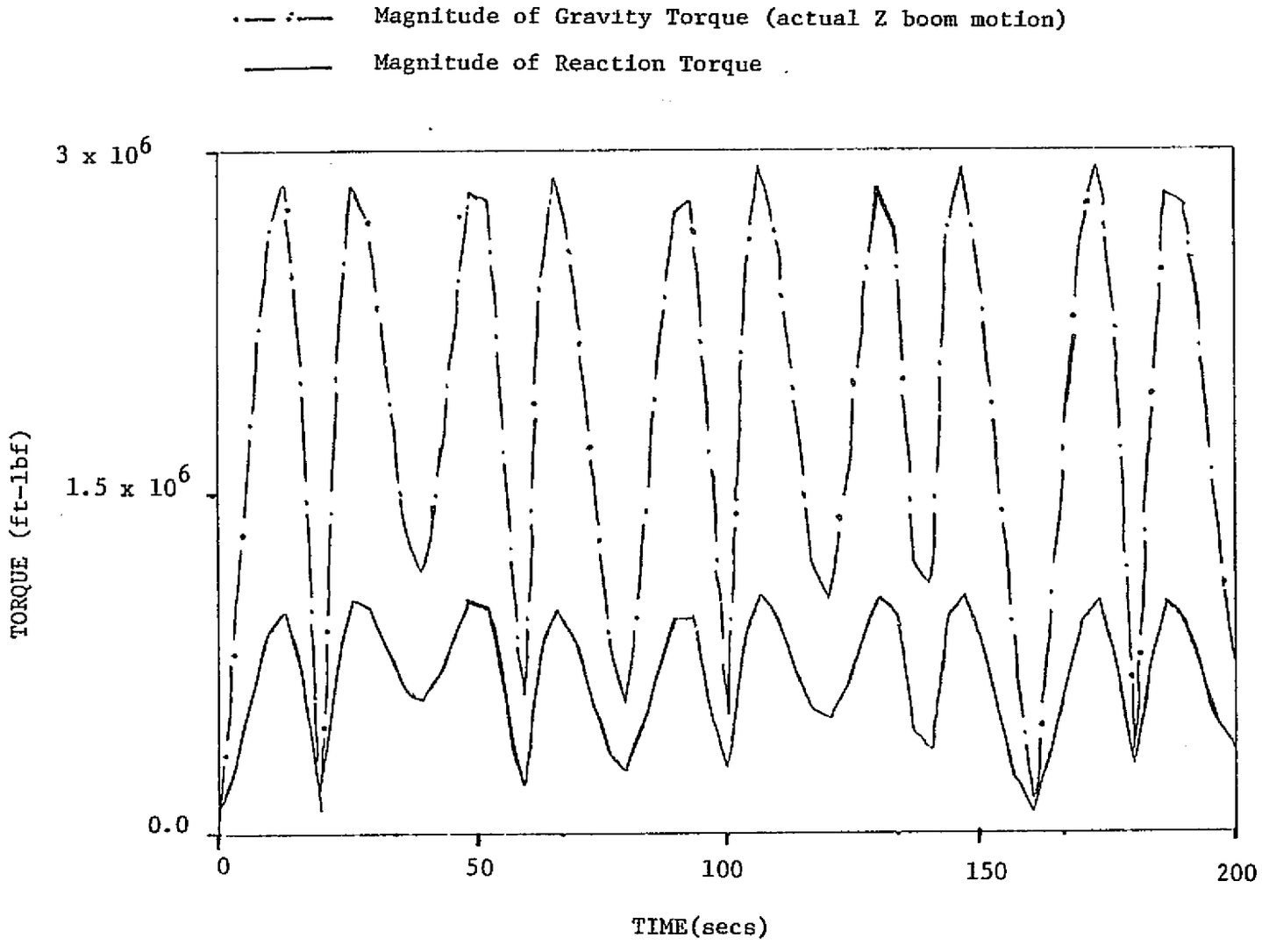

FIG. 17.f. COMPARISON OF GRAVITY TORQUE AND REACTION TORQUE MAGNITUDES

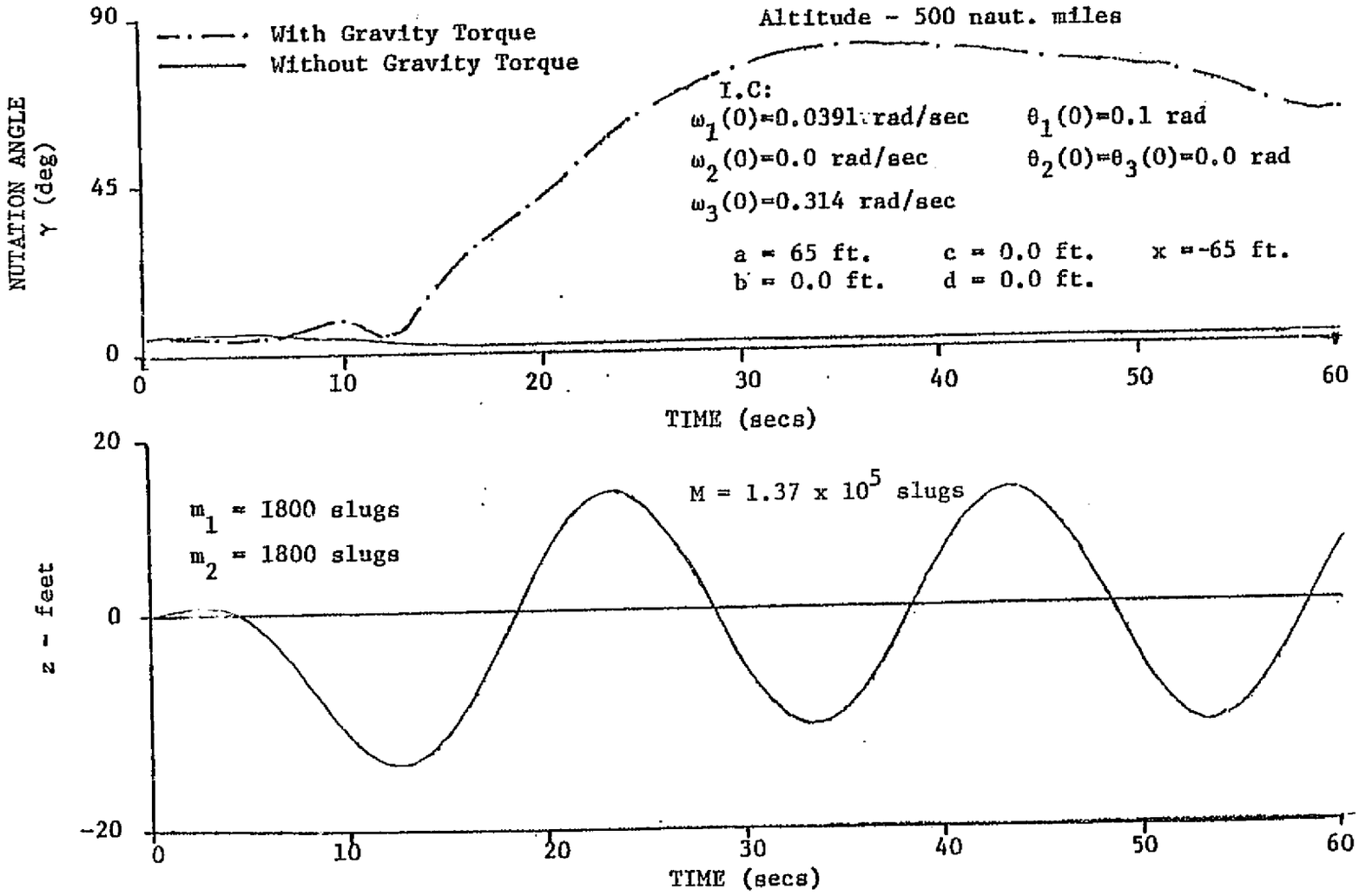

FIG. 18.a. DYNAMIC RESPONSE OF SYSTEM WITH COUNTER MASS
RESPONSE OF NUTATION ANGLE FOR SHOWN Z BOOM MOTION

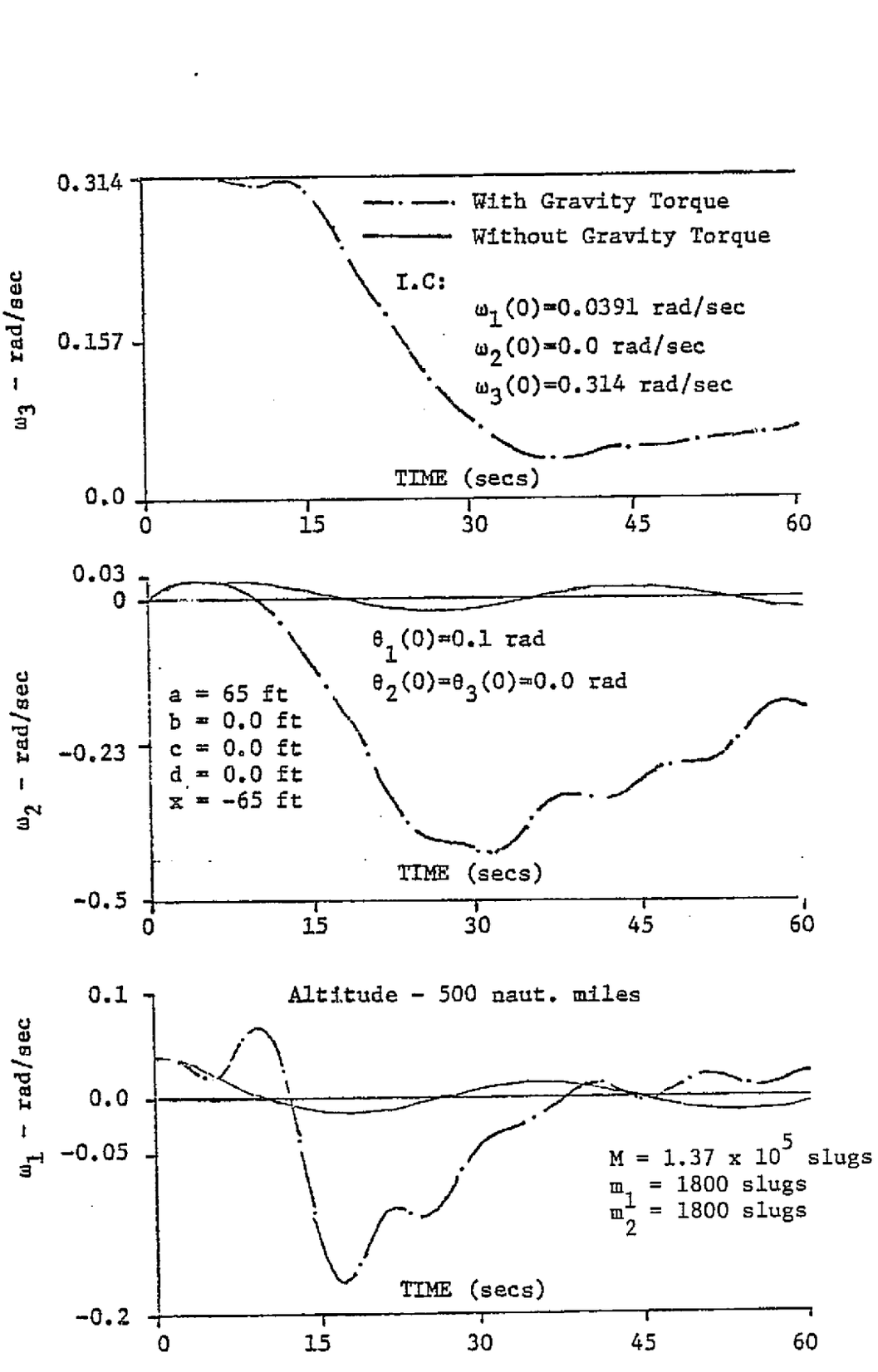

FIG. 18.b. DYNAMIC RESPONSE OF ANGULAR VELOCITY COMPONENTS WITH COUNTER MASS

——— Without Gravity-Torque

—·—· With Gravity-Torque

I.C: $\omega_1(0)=0.0391$ rad/sec $\quad \theta_1(0)=0.1$ rad

$\omega_2(0)=0.0$ rad/sec $\quad \theta_2(0)=\theta_3(0)=0.0$ rad

$\omega_3(0)=0.314$ rad/sec $\quad M = 1.37 \times 10^5$ slugs

Altitude - 500 naut. miles $\quad m_1 = 1800$ slugs

a = 65 ft. $\quad m_2 = 0.0$ slugs

b = 0 ft.

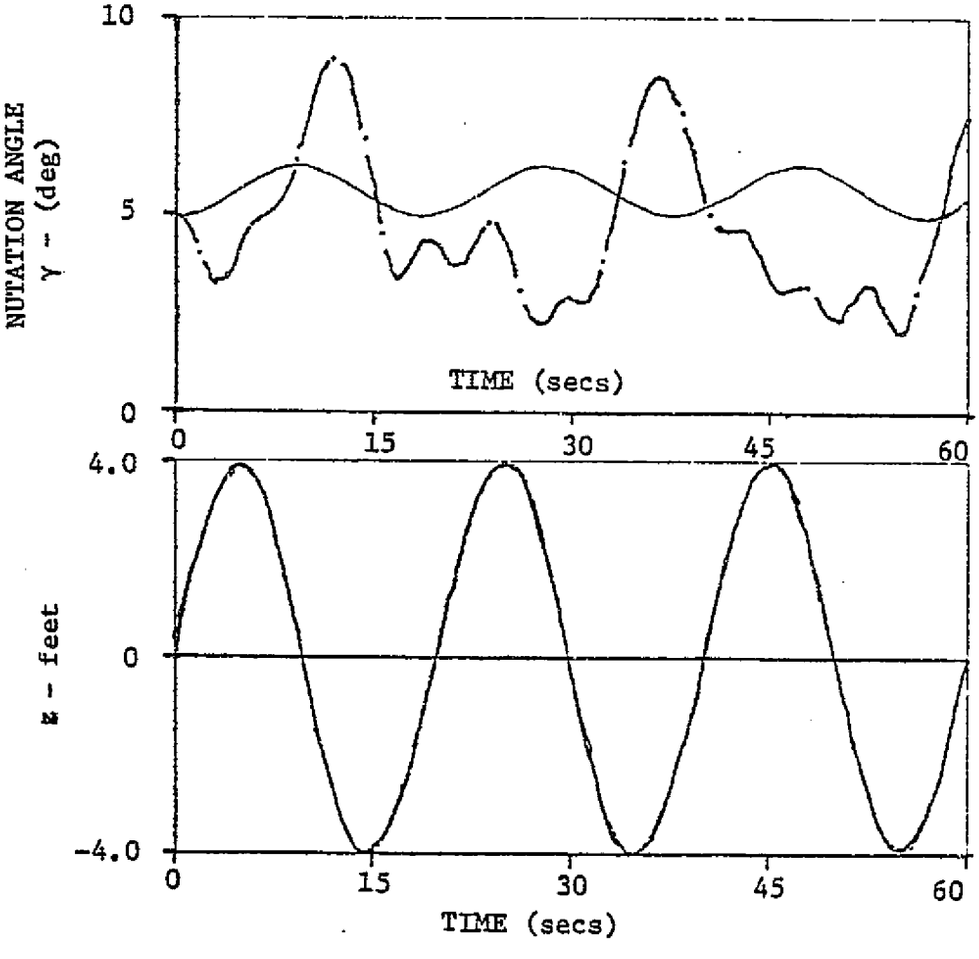

FIG. 19.a. DYNAMIC RESPONSE OF SYSTEM WITH SINUSOIDAL Z-BOOM MOTION. $\ddot{z} = 4 \sin 0.314\ t$

$M = 1.37 \times 10^5$ slugs
$m_1 = 1800$ slugs
$m_2 = 0.0$ slugs

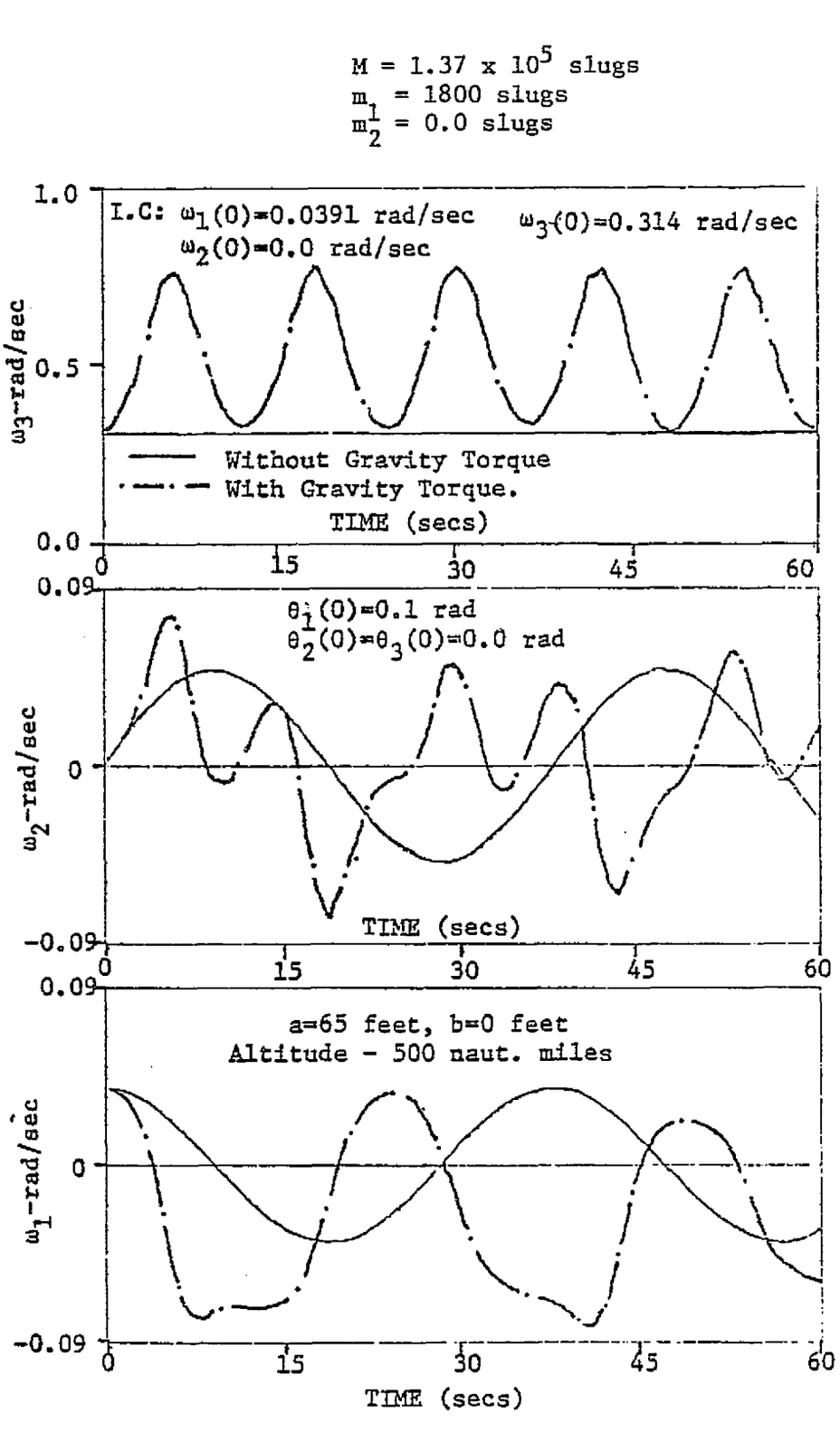

FIG. 19.b. DYNAMIC RESPONSE OF ANGULAR VELOCITY COMPONENTS WITH SINUSOIDAL Z-BOOM MOTION

I.C: $\omega_1(0) = 0.0391$ rad/sec
$\omega_2(0) = 0.0$ rad/sec
$\omega_3(0) = 0.314$ rad/sec

$\theta_1(0) = 0.1$ rad
$\theta_2(0) = \theta_3(0) = 0.0$ rad
a = 65 ft
b = 0 ft

$\dot{z}(0) = 0$ ft
$\dot{z}(0) = 0$ ft/sec
M = 4258 slugs
$m_1 = 55.95$ slugs
$m_2 = 0.0$ slugs

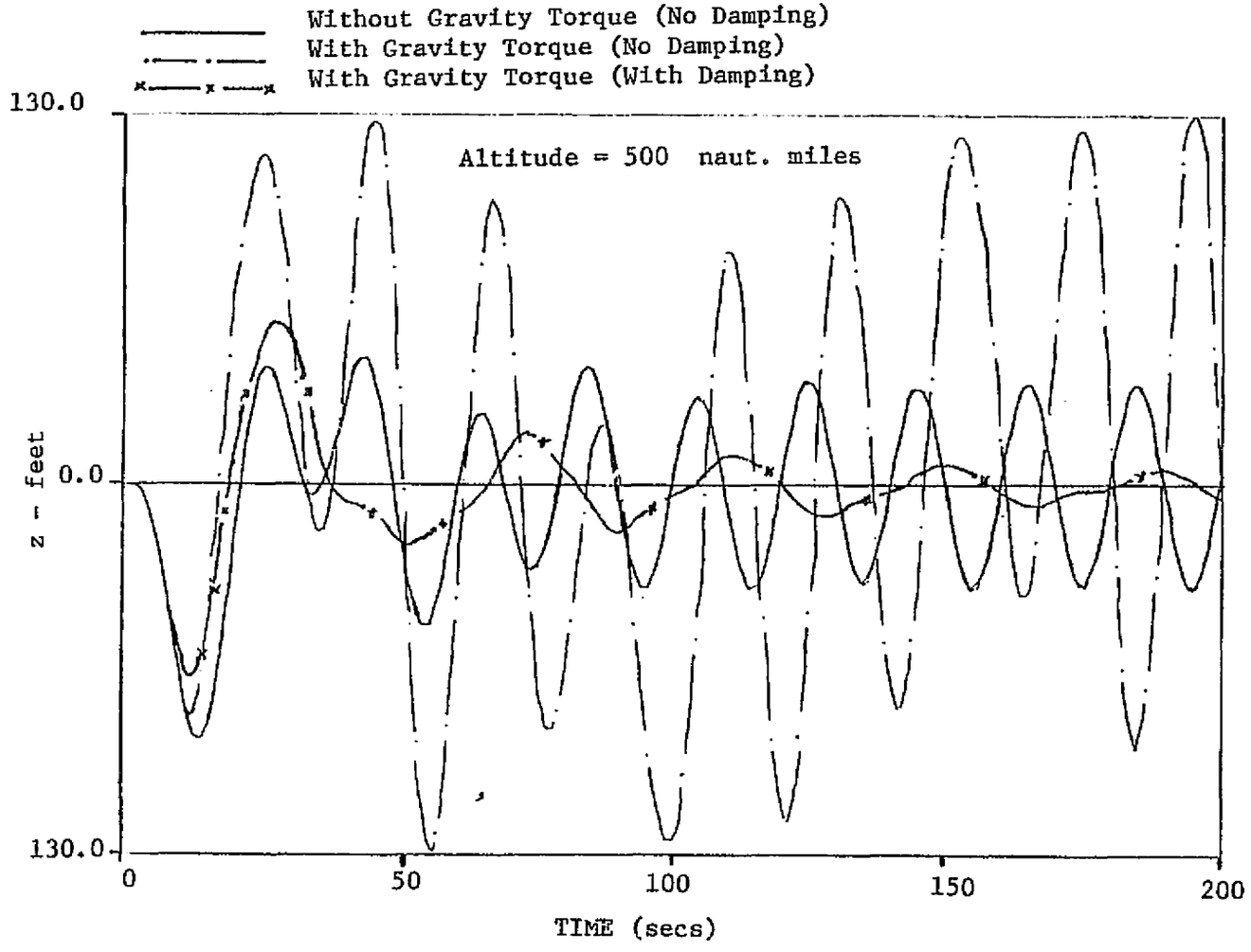

FIG. 20.a. DYNAMIC RESPONSE OF SYSTEM -Z BOOM MOTION

I.C: $\omega_1(0) = 0.0391$ rad/sec
$\omega_2(0) = 0.0$ rad/sec
$\omega_3(0) = 0.314$ rad/sec

$\theta_1(0) = 0.1$ rad
$\theta_2(0) = \theta_3(0) = 0.0$ rad
$a = 65$ ft
$b = 0$ ft

$z(0) = 0$ ft
$\dot{z}(0) = 0$ ft/sec
$M = 4258$ slugs
$m_1 = 55.95$ slugs
$m_2 = 0.0$ slugs

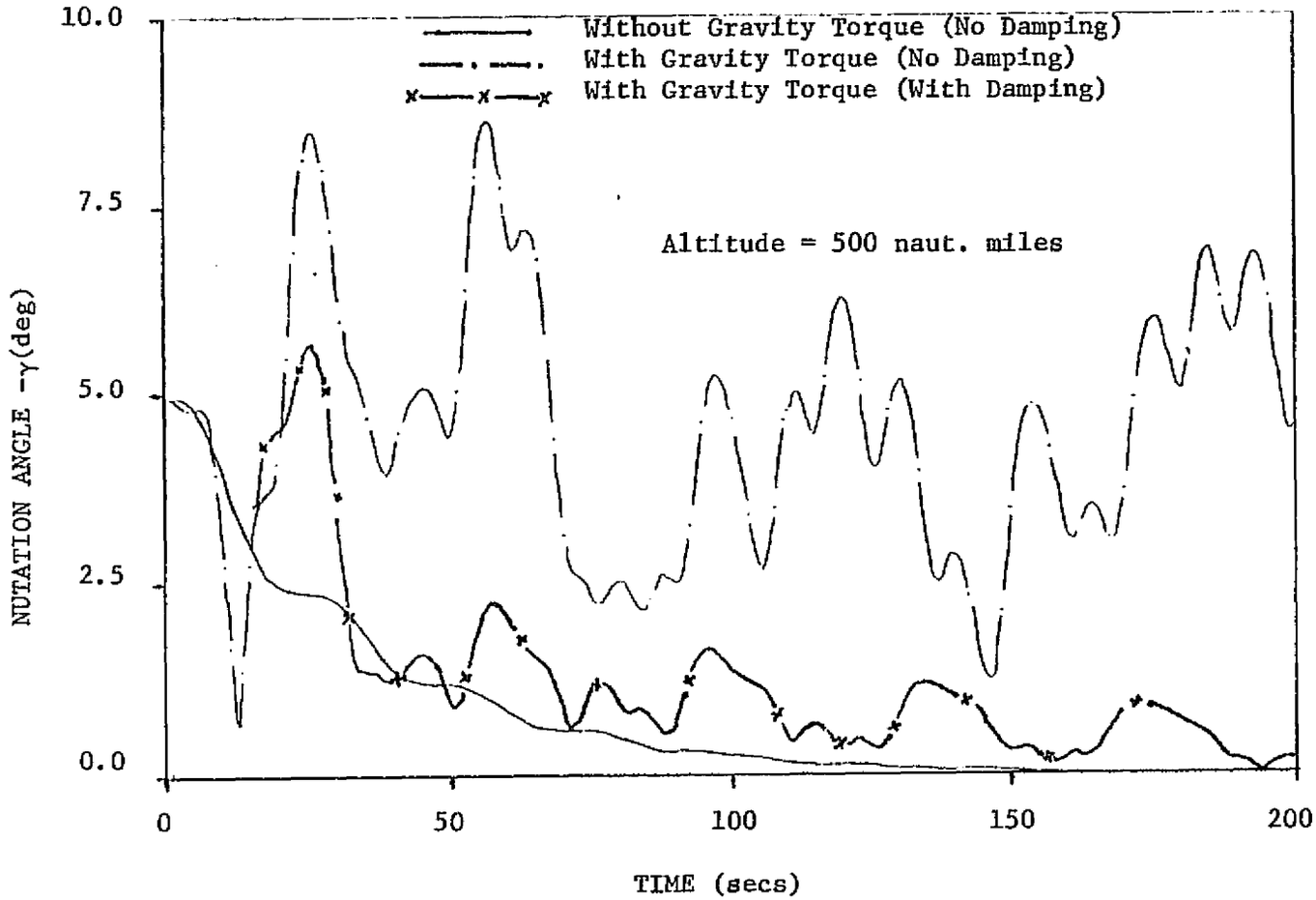

FIG. 20.b. DYNAMIC RESPONSE OF NUTATION ANGLE

—·—·— With Gravity-Torque
——— Without Gravity-Torque

I.C: $\omega_1(0) = 0.0391$ rad/sec
$\omega_2(0) = 0.0$ rad/sec
$\omega_3(0) = 0.314$ rad/sec
$\theta_1(0) = 0.1$ rad
$\theta_2(0) = \theta_3(0) = 0.0$ rad
$a = 65$ ft $b = 0$ ft

$M = 4258$ slugs
$m_1 = 55.95$ slugs
$m_2 = 0.0$ slugs

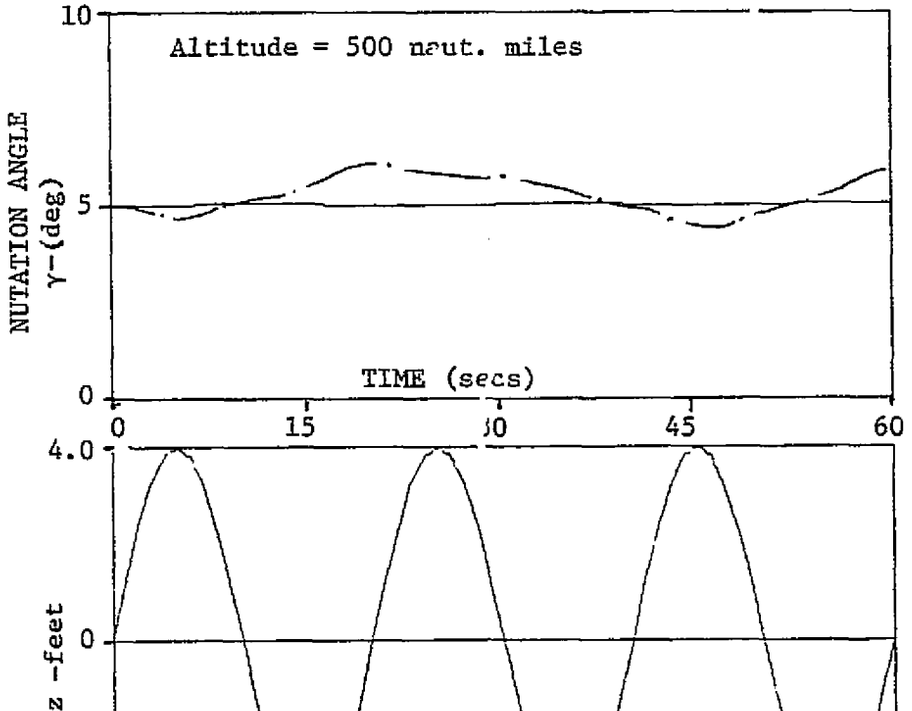

FIG. 21.a. DYNAMIC RESPONSE OF SYSTEM WITH SINUSOIDAL Z BOOM MOTION: $z = 4 \sin 0.314t$

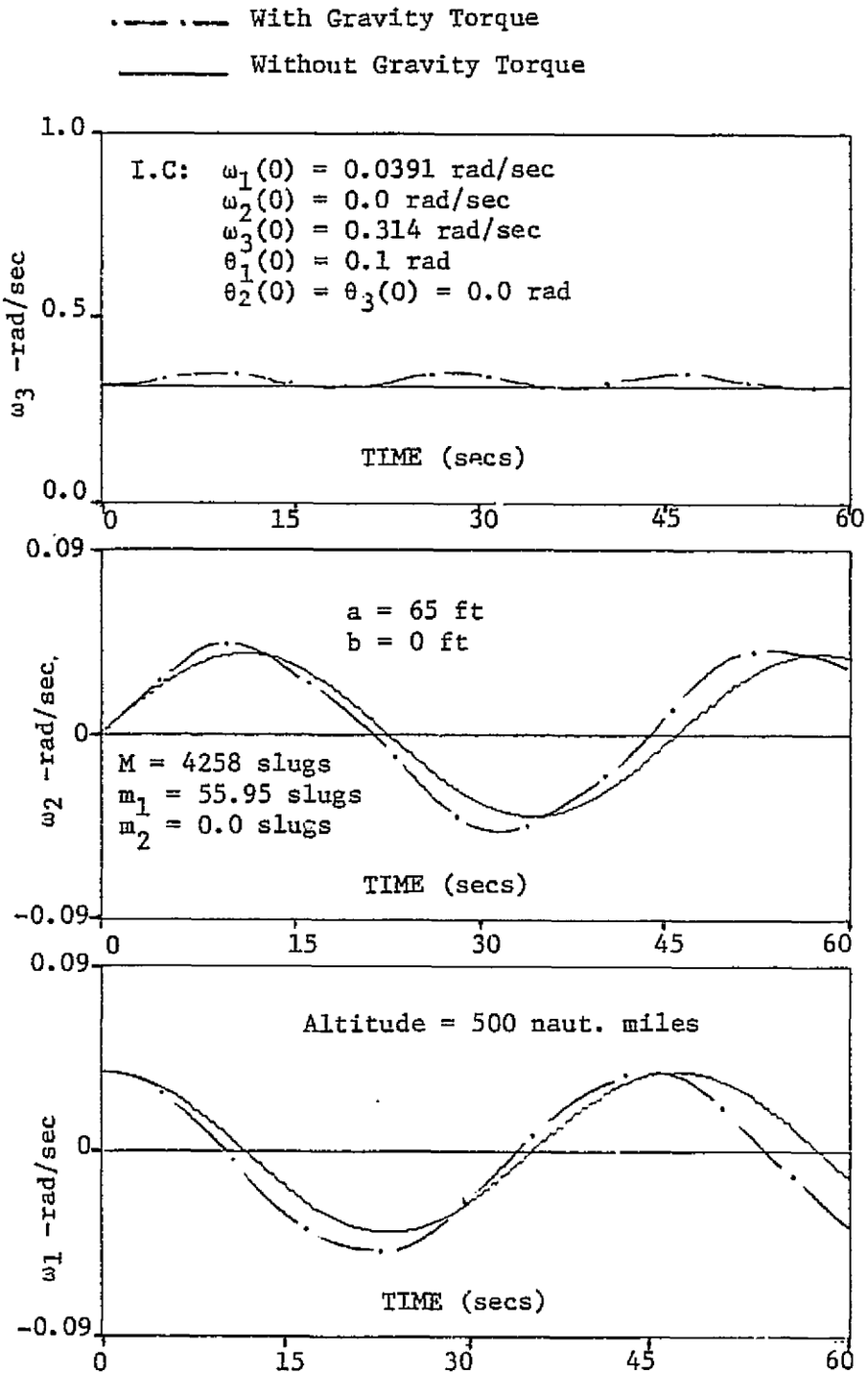

FIG. 21.b. DYNAMIC RESPONSE OF ANGULAR VELOCITY COMPONENTS WITH SINUSOIDAL Z BOOM MOTION
z = 4 Sin 0.314t

COMPUTER PROGRAM
SYMMETRIC DEPLOYMENT

```
2/10/77   21:27:41
!JOB [READ IN AT 21:23:25]     MAHESH RAJAN
!FORT/A/B/E/P/S FORT.LS/L
!LISTING
; C      CASE-3    ALFA=-0.5       FAST EXT
; C      DYNAMICS OF SYSTEM DURING NOMINAL DEPLOYMENT
; C      FOR SPIN PRINCIPALLY ABOUT 3-AXIS AND SYMMETRIC EXTENSION
; C      INCLUDING GRAVITY GRADIENT EFFECTS       BB=1.0
; C      ALTIUDE =500 NAUTICAL MILES.
;        EXTERNAL RGS01,RGS02
;        DIMENSION PARM(5),Y(6),DY(6),WORK(8,6),SIZE(6)
;        REAL I10,I20,I30,M1,M2,M3,I1,I2,I3
;        COMMON Y,ALFA
;        COMMON I10,I20,I30,I1,I2,I3,M1,M2,M3,C1,C2,C3
;        EQUIVALENCE(Y(1),W1),(Y(2),W2),(Y(3),W3),(Y(4),A1),(Y(5),A2),
;       3(Y(6),A3)
;        CALL INOUT(2,5)
;        CALL OPEN(1,'RAJAN',3,IER)
;        IF(IER.NE.1)STOP UNABLE TO OPEN FILE
; C
;        TMAX=490.0
;        STEP=2.0
;        TOL=0.01
;        READ(2,91)M1,M2,M3
;        READ(2,91)I10,I20,I30
;        READ(2,91)C1,C2,C3
;        READ(2,92)Y
;        READ(2,92)SIZE
;        WRITE(5,93)M1,M2,M3
;        WRITE(5,94)I10,I20,I30
;        WRITE(5,95)C1,C2,C3
;        WRITE(5,96)Y
;        WRITE(5,97)SIZE
;        WRITE(5,98)
;        PARM(1)=0.0
;        PARM(2)=TMAX
;        N=6
;        PARM(3)=STEP
;        CALL RKSCL(N,SIZE,DY,TOL,PARM)
;        CALL RKGS(PARM,Y,DY,N,IHLF,RGS01,RGS02,WORK)
;        WRITE (5,99)IHLF
; C
;   91   FORMAT(3F10.0)
;   92   FORMAT(6F10.0)
;   93   FORMAT(1X,'M1=',F10.6,5X,'M2=',F10.6,5X,'M3=',F10.6)
;   94   FORMAT(1X,'I10=',F10.6,5X,'I20=',F10.6,5X,'I30=',F10.6)
;   95   FORMAT(1X,'C1=',F10.6,5X,'C2=',F10.6,5X,'C3=',F10.6)
;   96   FORMAT(3X,'Y',3X,6F14.9)
;   97   FORMAT(3X,'SIZE',6F14.9)
;   98   FORMAT('1',T8,'T',T17,'W1',T30,'W2',T43,'W3',T55,'THETA-1',
;       2169,'THETA-2',T81,'THETA-3',T96,'ALFA',T110,'IHLF',/)
;   99   FORMAT('0IHLF=',I3)
; C
;        CALL EXIT
;        END
```

ORIGINAL PAGE IS
OF POOR QUALITY

```
PROGRAM IS RELOCATABLE
                              .TITL   .MAIN
!FORT/A/B/E/P/S FORT.LS/L
!LISTING
;       SUBROUTINE RGS01(T,Y,DY)
;       DIMENSION Y(6),DY(6)
;       REAL I10,I20,I30,L1,L2,L3,M1,M2,M3,I1,I2,I3,K,KB
;       COMMON W1,W2,W3,A1,A2,A3,ALFA
;       COMMON I10,I20,I30,I1,I2,I3,M1,M2,M3,C1,C2,C3
; C
;       L1=C1*T
;       L2=C2*T
;       L3=C3*T
;       E1=M1*L1*L1
;       E2=M2*L2*L2
;       E3=M3*L3*L3
;       I1=I10+2.0*(E2+E3)
;       I2=I20+2.0*(E3+E1)
;       I3=I30+2.0*(E1+E2)
;       DI1=4.0*(M2*L2*C2+M3*L3*C3)
;       DI2=4.0*(M1*L1*C1+M3*L3*C3)
;       DI3=4.0*(M2*L2*C2+M1*L1*C1)
;       K=1.407528*(10.0**16)
;       R=2.39506*(10.0**7)
;       BB=1.0
;       KB=3.0*K*BB/(R**3)
;       C01=COS(A1)
;       C02=COS(A2)
;       C03=COS(A3)
;       S01=SIN(A1)
;       S02=SIN(A2)
;       S03=SIN(A3)
;       Z=SQRT(K/(R**3))
;       DY(1)=(W3*W2*(I2-I3)-DI1*W1+KB*(I2-I3)*C02*S02*S03)/I1
;       DY(2)=(W1*W3*(I3-I1)-DI2*W2+KB*(I1-I3)*C02*S02*C03)/I2
;       DY(3)=(W2*W1*(I1-I2)-DI3*W3+KB*(I1-I2)*C02*C02*C03*S03)/I3
;       DY(4)=(W1*C03-W2*S03+Z*C01*S02)/C02
;       DY(5)=(W1*S03+W2*C03-Z*S01)
;       DY(6)=(W3*C02-W1*C03*S02+W2*S02*S03-Z*C01)/C02
;       ZZ=SQRT((I1*W1)**2+(I2*W2)**2)
;       ZY=I3*W3
;       ALFA=ATAN2(ZZ,ZY)*57.2958
;       RETURN
;       END


PROGRAM IS RELOCATABLE
                              .TITL   RGS01
!FORT/A/B/E/P/S FORT.LS/L
!LISTING
;       SUBROUTINE RGS02(T,Y,DY,IHLF,N,P)
;       LOGICAL RKNXT
;       COMMON W1,W2,W3,A1,A2,A3,ALFA
;       COMMON I10,I20,I30,I1,I2,I3,M1,M2,M3,C1,C2,C3
;       DIMENSION Y(6),DY(6),DUMMY(6)
; C
;       CALL RGS01(T,Y,DUMMY)
;       TP=T
;       IF(.NOT.RKNXT(IHLF)) GO TO 8
;       WRITE(5,1)TP,Y(1),Y(2),Y(3),Y(4),Y(5),Y(6),ALFA,IHLF
;   1   FORMAT(1X,F7.3,6(1X,E15.8),1X,F10.7,1X,I3)
;       WRITE BINARY (1) T,Y(1),Y(2),ALFA
;   8   CONTINUE
```

```
;       RETURN
;       END

PROGRAM IS RELOCATABLE
                              .TITL   RGS02
!RLDR/M TMP/S 001 002 003 DP0:SSP.LB FORT.LB
!EXEC
M1=  0.000000      M2=  0.000000      M3=  0.010000
I10=  5.000000      I20=  5.000000      I30= 10.000000
C1=  0.000000      C2=  0.000000      C3=  4.000000
  Y       0.000050000   0.000000000   0.000506080   0.001000000   0.000000000
  SIZE    0.000050000   0.000050000   0.000510000   0.050000000   0.050000000

   Y      0.000000000
   SIZE   1.000000000
```

COMPUTER PROGRAM
ASYMMETRIC DEPLOYMENT

```
2/26/77   16:54:22
!JOB (READ IN AT 16:53:58)     MAHESH RAJAN
!FORT/A/B/E/P/S FORT.LS/L
!LISTING
; C      EFFECT OF GRAVITY TORQUE     ASYMMETRIC APPENDAGES
; C      ALTIUDE =500 NAUTICAL MILES.
; C      INCLUDING GRAVITY-GRADIENT EFFECTS        GG=1.0
;        EXTERNAL RGS01,RGS02
;        DIMENSION PARM(5),Y(6),DY(6),WORK(8,6),SIZE(6)
;        REAL I1,I2,I3,MB,M1,M2,K
;        COMMON Y
;        COMMON I1,I2,I3,MB,M1,M2
;        COMMON AA,BB,CC,DD
;        COMMON Z,DZ,DDZ
;        COMMON N,M
;        COMMON C(3,3)
;        EQUIVALENCE(Y(1),W1),(Y(2),W2),(Y(3),W3),(Y(4),A1),(Y(5),A2),
;       3(Y(6),A3)
;        CALL INOUT(2,5)
;        CALL OPEN(1,'RAJAN',3,IER)
;        IF(IER.NE.1)STOP UNABLE TO OPEN FILE
;        READ(2,91)TMAX,STEP,TOL
;   91   FORMAT(8F10.0)
;        PARM(1)=0.0
;        PARM(2)=TMAX
;        PARM(3)=STEP
; C      INITIAL VALUES
;        READ(2,91)Y
;        READ(2,91)SIZE
;        READ(2,911)I1,I2,I3
;        READ(2,911)MB,M1,M2
;        READ(2,911)AA,BB,CC,DD
;  911   FORMAT(4F20.4)
;        N=6
;        M=3
;        WRITE(5,92)TMAX,STEP,TOL
;        WRITE(5,93)I1,I2,I3
;        WRITE(5,94)MB,M1,M2
;        WRITE(5,95)AA,BB,CC,DD
;        WRITE(5,96)Y
;        WRITE(5,97)SIZE
;        WRITE(5,98)
;   92   FORMAT(1X,'TMAX=',F10.6,5X,'STEP=',F10.6,5X,'TOL=',F10.6)
;   93   FORMAT(1X,'I1=',E15.4,5X,'I2=',E15.4,5X,'I3=',E15.4)
;   94   FORMAT(1X,'MB=',E15.4,5X,'M1=',E15.4,5X,'M2=',E15.4)
;   95   FORMAT(1X,'AA=',F10.6,2X,'BB=',F10.6,2X,'CC=',F10.6,2X,'DD=',
;       @F10.6)
;    96  FORMAT(3X,'Y',3X,6F15.6)
;    97  FORMAT(3X,'SIZE',6F15.6)
;    98  FORMAT('1',T8,'I',T17,'W1',T30,'W2',T43,'W3',T55,'THETA-1',
;       2T69,'THETA-2',T81,'THETA-3',T96,'ALFA',T110,'IHLF',/)
; C
;        CALL RKSCL(N,SIZE,DY,TOL,PARM)
;        CALL RKGS(PARM,Y,DY,N,IHLF,RGS01,RGS02,WORK)
;        WRITE(5,99)IHLF
;   99   FORMAT('0IHLF=',I3)
;        CALL EXIT
```

```
;       END

PROGRAM IS RELOCATABLE
                              .TITL    .MAIN
!FORT/A/R/E/P/S FORT.LS/L
!LISTING
;       SUBROUTINE RGS01(T,Y,DY)
;       DIMENSION Y(6),DY(6),C(3,3)
;       REAL I1,I2,I3,MB,M1,M2,K
;       COMMON A1,A2,A3,A1,A2,A3
;       COMMON I1,I2,I3,MB,M1,M2
;       COMMON AA,BB,CC,DD
;       COMMON Z,DZ,DDZ
;       COMMON N,M
;       COMMON C
; C     CAL. OF COEFF. OF L.H.S. OF MATRIX EQN.
;       U1=M1*(MB+M2)/(MB+M1+M2)
;       U2=M2*(MB+M1)/(MB+M1+M2)
;       U3=-M1*M2/(MB+M1+M2)
;       X=0.0
;       DX=0.0
;       DDX=0.0
;       TT=0.314*T
;       SQ1=SIN(TT)
;       CQ1=COS(TT)
;       ET=EXP(-0.54*TT)
;       CQ2=COS(0.428*TT)
;       SQ2=SIN(0.428*TT)
;       Q1=0.655*SQ1+0.417*CQ1
;       Q2=ET*(0.417*CQ2+2.056*SQ2)
;       Q3=ET*(-0.417*0.428*SQ2+2.056*0.428*CQ2)
;       QZ=Q1-Q2
;       Z=17.72*QZ
;       QDZ=0.655*CQ1-0.417*SQ1-Q3+0.54*Q2
;       DZ=0.314*17.72*QDZ
;       QDDZ=-Q1-ET*(-0.417*0.428*0.428*CQ2-2.056*0.428*0.428*SQ2)+2.0*
;      @0.54*Q3-0.54*0.54*Q2
;       DDZ=0.314*0.314*17.72*QDDZ
;       C(1,1)=I1+U1*(BB**2+Z**2)+U2*(CC**2+DD**2)+2.*U3*(BB*CC+DD*Z)
;       C(1,2)=-U1*AA*BB-U2*CC*X-U3*(AA*CC+BB*X)
;       C(1,3)=-U1*AA*Z-U2*DD*X-U3*(AA*DD+X*Z)
;       C(2,1)=C(1,2)
;       C(2,2)=I2+U1*(AA**2+Z**2)+U2*(DD**2+X**2)+2.0*U3*(AA*X+DD*Z)
;       C(2,3)=-U1*BB*Z-U2*CC*DD-U3*(BB*DD+CC*Z)
;       C(3,1)=C(1,3)
;       C(3,2)=C(2,3)
;       C(3,3)=I3+U1*(AA**2+BB**2)+U2*(CC**2+X**2)+2.0*U3*(BB*CC+AA*X)
; C     CAL. OF R.H.S OF MATRIX EQUATION
;       GT=1.407528*(10.0**16)
;       R=2.39506*(10.0**7)
;       GG=1.0
;       K=GT*GG
;       OM=SQRT(GT/(R**3))
;       CO1=COS(A1)
;       CO2=COS(A2)
;       CO3=COS(A3)
;       SO1=SIN(A1)
;       SO2=SIN(A2)
;       SO3=SIN(A3)
;       RK=3.0*K/P**3
;       R1K=RK*M1*(AA*CO2*CO3-BB*CO2*SO3+Z*SO2)
;       R2K=RK*M2*(X*CO2*CO3-CC*CO2*SO3+DD*SO2)
```

```
;       ZDM=Z*M1+DD*M2
;       AXM=AA*M1+X*M2
;       BCM=BB*M1+CC*M2
;       A10=(I3-I2)*W2*W3
;       A11=U1*(-AA*Z*W1*W2+(BB**2-Z**2)*W2*W3+AA*BB*W1*W3+2.*Z*DZ*W1+
;      *BB*Z*(W3**2-W2**2)+BB*DDZ)
;       A12=U2*(-DD*X*W1*W2+(CC**2-DD**2)*W2*W3+CC*X*W1*W3-2.*CC*DX*W2
;      @-2.*DD*DX*W3+CC*DD*(W3**2-W2**2))
;       A13=U3*((-AA*DD-Z*X)*W1*W2+2.*(BB*CC-DD*Z)*W2*W3+(AA*CC+BB*X)
;      @*W1*W3+2.*DD*DZ*W1-2.*BB*DX*W2-2.*DX*Z*W3+(BB*DD+CC*Z)*(W3**2
;      @-W2**2)+CC*DDZ)
;       A14=RK*(I2-I3)*C02*S02*S03
;       A15=(K/R**2)*(-C02*S03*ZDM-S02*BCM)
;       A16=R1K*(Z*C02*S03+BB*S02)
;       A17=R2K*(DD*C02*S03+CC*S02)
;       DY(1)=-(A10+A11+A12+A13-A14-A15-A16-A17)
;       B10=(I1-I3)*W3*W1
;       B11=U1*(-BB*Z*W1*W2+AA*BB*W2*W3+(AA**2-Z**2)*W3*W1-2.*Z*DZ*W2
;      @+AA*Z*(W3**2-W1**2)+AA*DDZ)
;       B12=U2*(-CC*DD*W1*W2+CC*X*W2*W3+(X**2-DD**2)*W3*W1-2.*X*DX*W2
;      @+DX*(W3**2-W1**2)-DD*DDX)
;       B13=U3*(-(BB*DD+CC*Z)*W1*W2+(AA*CC+BB*X)*W2*W3+2.*(AA*X-DD*Z)
;      @*W3*W1-2.*(AA*DX+DD*DZ)*W2+(AA*DD+X*Z)*(W3**2-W1**2)+X*DDZ-Z*DDX)
;       B14=RK*(I1-I3)*S02*C02*C03
;       B15=(K/R**2)*(-C02*C03*ZDM+S02*AXM)
;       B16=R1K*(Z*C02*C03-AA*S02)
;       B17=R2K*(DD*C02*C03-X*C02)
;       DY(2)=-(B10-B11-B12-B13-B14-B15-B16-B17)
;       C10=(I2-I1)*W1*W2
;       C11=U1*((BB**2-AA**2)*W1*W2-AA*Z*W2*W3+BB*Z*W3*W1+2.*AA*DZ*W1+
;      @2.*BB*DZ*W2+AA*BB*(W1**2-W2**2))
;       C12=U2*((CC**2-X**2)*W1*W2-DD*X*W2*W3+CC*DD*W3*W1-2.*X*DX*W3
;      @+CC*X*(W1**2-W2**2)+CC*DDX)
;       C13=U3*(2.*(BB*CC-AA*X)*W1*W2-(AA*DD+X*Z)*W2*W3+(BB*DD+CC*Z)*W3*W1
;      @+2.*(X*DZ*W1+CC*DZ*W2-AA*DX*W3)+(AA*CC+BB*X)*(W1**2-W2**2)+BB*
;      @DDX)
;       C14=RK*(I1-I2)*C02*C02*C03*S03
;       C15=(K/R**2)*(C02*S03*AXM+C02*C03*BCM)
;       C16=R1K*(AA*C02*S03+BB*C02*C03)
;       C17=R2K*(CC*C02*C03+X*C02*S03)
;       DY(3)=-(C10-C11-C12-C13-C14-C15+C16+C17)
;       DY(4)=(W1*C03-W2*S03+OM*C01*S02)/C02
;       DY(5)=(W1*S03+W2*C03-OM*S01)
;       DY(6)=(W3*C02-W1*C03*S02+W2*S02*S03-OM*C01)/C02
;       CALL SIMQ(C,DY,M,KS)
;       IF(KS)3,2,3
;   2   RETURN
;   3   WRITE(5,4)
;   4   FORMAT(//'SINGULAR EQUATIONS')
;       RETURN
;       END

PROGRAM IS RELOCATABLE
                        .TITL   RGS01
!FORT/A/R/E/P/S FORT.LS/L
!LISTING
;       SUBROUTINE RGS02(T,Y,DY,IHLF,N,P)
;       LOGICAL RKNXT
;       DIMENSION Y(6),DY(6),DUMMY(6)
;       REAL I1,I2,I3,MB,M1,M2,K
;       COMMON W1,W2,W3,A1,A2,A3
;       COMMON I1,I2,I3,MB,M1,M2
```

```
;       COMMON AA,BB,CC,DD
;       COMMON Z,DZ,DDZ
; C
;       CALL RGS01(T,Y,DUMMY)
;       H1=I1*N1
;       H2=I2*N2
;       H3=I3*N3
;       ALFA=ATAN2(SQRT(H1*H1+H2*H2),H3)*57.2958
;       TP=T
;       IF(.NOT.RKNXT(IHLF)) GO TO 8
;       WRITE(5,1)TP,Y,Z,DZ,ALFA,IHLF
;   1   FORMAT(1X,F5.1,8(1X,E12.5),1X,F7.4,1X,I2)
;       WRITE BINARY (1) T,Z
;   8   CONTINUE
;       RETURN
;       END
```

```
PROGRAM IS RELOCATABLE
                                .TITL   RGS02
!RLDR/M TMP/S 001 002 003 DP0:SSP.LB FORT.LB
!EXEC
TMAX= 60.000000     STEP=  1.000000     TOL=  0.010000
I1=     0.1050E  8      I2=     0.1050E  8      I3=     0.1500E  8
MB=     0.1370E  6      M1=     0.1800E  4      M2=     0.0000E  0
AA= 65.000000  BB=  0.000000  CC=  0.000000  DD=  0.000000
  Y          0.039100        0.000000        0.314000        0.100000
  SIZE       1.500000        1.500000        2.000000        2.200001

  Y          0.000000        0.000000
  SIZE       1.000000       42.000000
```